IJEST

ISSN: 0973-6255
Vol. 2 No. 1
January - June 2008

Indian Journal of Engineering, Science, and Technology

A Refereed Research Journal









BANNARI AMMAN
INSTITUTE OF TECHNOLOGY
Stay Ahead

BANNARI AMMAN INSTITUTE OF TECHNOLOGY
Sathyamangalam - 638 401 Erode District Tamil Nadu India

ABOUT BANNARI AMMAN INSTITUTE OF TECHNOLOGY

The Bannari Amman Institute of Technology (BIT) is a vibrant institute of higher education promoted by the Bannari Amman Group, a leading corporate house in the Southern part of India, under the aegis of the Bannariamman Educational Trust in 1996 in the town of Sathyamangalam in Erode District of Tamil Nadu.

It is an impressive campus situated in a serene surrounding at the foothills of the Nilgiris Mountains encompassing a sprawling area of 165 acres with a built-up area of more than 12 lakh square feet and presents an exemplary illustration of corporate contribution to society. BIT is a modern campus with up-to-date teaching facilities. It is an ideal, conducive, educational retreat where one can fully focus on studies and attain academic excellence.

With an overall strength of 4000 students on roll, the Institute offers 12 undergraduate programmes, and 12 postgraduate programmes in engineering, technology, management, & applied sciences, and 6 Ph.D./ M.S. (By Research) in engineering and technology under affiliation to Anna University, Coimbatore and approved by the All India Council for Technical Education, New Delhi. Six of the BE/BTech programmes have been accredited by NBA. The college is an ISO 9001:2000 certified institution. The zeal and dedication with which BIT pursues its motto 'Stay Ahead' makes it different from other institutions.

There are 30 doctorates among 285 members of faculty to provide personalised care for the students. The zeal and dedication with which BIT pursues its motto 'Stay Ahead' makes it different from other institutions.

Indian Journal of Engineering, Science, and Technology

IJEST is a refereed research journal published half-yearly by Bannari Amman Institute of Technology. Responsibility for the contents rests upon the authors and not upon the IJEST. For copying or reprint permission, write to Copyright Department, IJEST, Bannari Amman Institute of Technology, Sathyamanagalam, Erode District - 638 401, Tamil Nadu, India.

Editor-in-Chief

Dr.A.Shanmugam
Principal
Bannari Amman Institute of Technology

Associate Editor

Dr.R.V.Mahendra Gowda
Professor & Head
Department of Textile - Fashion Technology
Bannari Amman Institute of Technology

Editorial Board

Dr.Dinesh K Sukumaran
Director, Magnetic Resonance Centre
Department of Chemistry
The State University of New York Buffalo
USA – 141 214

Dr.Jagannathan Sankar
Distinguished University Professor
Department of Mechanical and Chemical Engineering
North Carolina A&T State University
NC 27411, USA

Dr.Ravi Sankar
Professor
Department of Electrical Engineering
University of South Florida
Sarasota, FL 34243, USA

Dr.H.S.Jamadagni
Chairman CEDT
Indian Institute of Science
Bangalore – 560 012

Dr.A.K.Sarje
Professor
Department of Electronics & Computer Engineering
Indian Institute of Technology, Roorkee - 247 667

Dr.Talabatulla Srinivas
Assistant Professor
Department of Electrical & Communication Engineering
Indian Institute of Science
Bangalore - 560 012

Dr.V.K.Kothari
Professor
Department of Textile Technology
Indian Institute of Technology – Delhi
New Delhi – 110 016

Dr.S.Mohan
Professor & Head
Department of Civil Engineering
Indian Institute of Technology – Madras
Chennai – 600 036

Dr.R.Sreeramkumar
Professor
Department of Electrical Engineering
National Institute of Technology - Calicut
Calicut – 673 601

Dr.P.Nagabhushan
Professor
Department of Studies in Computer Science
University of Mysore, Mysore - 570 006

Dr.E.G.Rajan
Director
Pentagram Research Centre Pvt. Ltd.
Hyderabad – 500 028

Mr.S.Sivaraj
Head
Learning Resource Centre
Bannari Amman Institute of Technology
Sathyamangalam - 638 401

Indian Journal of Engineering, Science, and Technology

Volume 2 Number 1 **January - June 2008**

CONTENTS

ENERGY CONSERVATION IN AGRICULTURAL PUMP-SETS

T.Tamizharasan
Department of Mechanical Engineering, Anjalai Ammal Mahalingam Engineering College,
Kovilvenni - 614 403, Thiruvarur District, Tamil Nadu
E-mail: t_thamil2k2@yahoo.co.in
(Received on 22 March 2007 and accepted on 12 September 2007)

Abstract

Agriculture is the largest sector of economic activity in our country. The progress in agriculture is attributed to improvement and utilization of input and output powers of agricultural equipment such as centrifugal pump. Energy is the primary resource and is essential for all kinds of technical developments. Innovation of different technologies for the utilization of energy play a crucial role in the development of a nation. In this work, it is claimed that a definite amount of energy is conserved from the water being discharged out from the delivery pipe of the agricultural pump-sets without affecting the normal performance of the pump. In this analysis, approximately 25% of operating electrical energy is conserved from the kinetic energy of pumped water by sacrificing only a small percentage of input electrical energy, which is almost negligible in actual practice. It is estimated that the maximum pay-back period for this additional financial investment is around 3 years.

Keywords: *Agricultural Pumpset, Alternator, Energy Conservation, Pelton Turbine*

1. INTRODUCTION

In the pump sets used for irrigation purposes, the electric motors are coupled with centrifugal pumps. From the survey taken in ten villages of south Tamil Nadu, it is learnt that the motors run approximately at 70% of full load [1]. But in the present research work, the above problem is not considered and the energy which is carried away by the water coming out from the pump [2] is partially conserved and utilized for pumping water [3] or for some other lighting purposes.

The kinetic energy of the discharging water is utilized to generate a considerable amount of electric power [4]. This electric power generated is utilized to operate a secondary motor [5], which is coupled with the primary electric motor as shown in Figure 1. Since the total load of the pump is shared by two motors one of which is run by the conserved energy, the total energy input to the pump-set is reduced to a considerable extent. After conducting enough number of experiments by varying the parameters, it is understood that a considerable amount of energy is conserved from the discharge side of the agricultural pump sets used for irrigation purposes [6].

2. EXPERIMENTAL SETUP

A well-designed pelton turbine with specifications as given in Table 1 is connected to the delivery pipe of the centrifugal pump whose specifications are also given in Table 1 with the required measuring instruments as shown in Figure 1. The schematic diagram exhibits how the three-phase alternator is coupled with the pelton turbine. At different discharges and different loads, the performance of the system [7] is studied. The gate valve is kept at 75% opened position and the alternator is loaded gradually from minimum to maximum. Correspondingly, the gate valve is opened to make up and maintain the speed at 1000 rpm. The discharge of water is calculated by collecting the water in the collecting tank per unit time and the motor input is also calculated. The difference in discharge due to the turbine load is noted at a constant speed of 1000 rpm. and is shown in Figure 2. This experiment is repeated with various discharges and at various turbine loads without changing the speed.

Finally, the turbine is removed and the gate valve is adjusted to match the already noted discharge and head values. In this condition, the motor input is measured and noted down. In the same way, the motor input is measured

at various heads and discharge values which are same as the previous values noted, when turbine develops some power. In this analysis, there is no considerable reduction in discharge due to the turbine load. So the performance of the centrifugal pump [8] is not affected by the turbine operation in the circuit.

The power developed by the three-phase alternator is utilized to run the secondary motor of 3 HP which is directly coupled with the primary motor of 7.5 HP. The turbine is adjusted to match the frequency of alternator with the frequency of available power supply. Thus the electrical power requirement to run the pump is reduced, i.e, a considerable amount of energy is conserved and utilized.

3. RESULTS AND DISCUSSION

In the present experimental set up, 7.46 kw (10 HP) three-phase induction motor is considered with star-delta starter to operate the centrifugal pump. Instead of using a single 10 HP motor, a one 7.5 HP motor, and one 3 HP motor (2.5 HP motor is not available in the market) available in the market are used to operate the same pump. Initially, the delivery valve is closed to 50% in order to reduce the motor load and the new primary motor 7.5 HP is started. After few seconds, the secondary motor of 3 HP is energized by the coupled pelton turbine-alternator set. Then the delivery valve is fully opened and the total load of the pump is shared by both the motors. In this situation, only 7.5 HP of input power is consumed, but 10.5 HP power is developed and supplied to the pump.

3.1 Preliminary Stage

The delivery valve remains in fully opened position and the Alternator load (Turbine load) is gradually increased from 0 to 100 % at suitable increments. For each and every load on the turbine at constant speed of 1000 rpm, the discharge of pump is calculated by using the calibrated measuring tank of size 0.5m x 0.5m x 0.5m. In addition to the above, the input power of main motor is also recorded corresponding to various turbine loads [9] and depicted in Figures 3-6.

When the load on the alternator increases above 2.2 kW, the pump does not discharge the required volume of water are the turbine speed decreases to some extent which is not advisable. Hence, the maximum power obtained from alternator is 2.2 kW. This case is studied for identifying the effects of inclusion of turbine in the water discharge side of the centrifugal pump.

3.2 Analysis Stage

In the second case of experiment, the turbine-alternator set is removed from the setup and water from the delivery pipe is directly discharged out without any power conservation. At the same discharge and head values as in the previous case, the input power values of the motor (10HP) are measured and shown in Figure 5.

There is no considerable difference in performance of the pump at various values of discharge and head with and without energy conservation system. From this, it is observed that only the exhausting energy is conserved from the discharge side of the pump.

3.3 Implementation Stage

The discharge of water is kept constant at a level and the turbine load is gradually increased with out maintaining the speed constant. The maximum power developed by the alternator and the motor input power (10HP) are measured and these results are shown in Figure 3. In this particular case, the maximum power of 2.3 kW is obtained. When the alternator load is increased above 2.3 kW, there is a huge drop in speed of the turbine.

When the ground water level is lower during summer season, the discharge of pump is lower, power requirement of pump is lower, and the power conserved from the delivery side is also lower, which is enough to run the secondary motor at reduced loaded condition.

Similarly, when the ground water level is higher during winter season, the discharge of pump, power requirement of pump and power conserved at delivery side are higher. In this stage also, the secondary motor (3HP) is effectively operated with the conserved energy.

4. CONCLUSIONS

Upon analysis of results and the data calculated, it is concluded that the extraction or the conservation of

energy from the delivery side of the pump does not significantly affect the performance of the pump.

In addition, the input energy consumption of the motor 10-HP is also not significantly increased due to the inclusion of the energy conservation system in the output side of the centrifugal pump.

The optimum power developed by the alternator (without affecting the normal performance of the primary motor and pump) is utilized to operate the secondary motor which is coupled with the primary motor. In this way, the total input external energy consumption is reduced which in turn increases the overall efficiency of the pump set. Approximately 25% of input energy is saved or conserved with this development. If a particular pump-set with 10 HP motor is considered, the amount of energy conserved over a considerable period of time is calculated as:

Energy saved / conserved per day (20 hrs) = 44 kW

Energy saved / conserved per hour = 2.2 kW

Energy saved / conserved per year (365 days) = 16060 kW

Approximate total cost saved per year @ Rs. 3.00/ kWh = 16060 x 3 = Rs. 48, 180.00

The approximate pay-back period is around 3 years.

REFERENCES

[1] "Testing Setup for Agricultural Pumps", Bureau of Indian Standards, IS 4029, 1967.

[2] G.C. Bakos, "Feasibility Study of a Hybrid Wind / Hydro Power-System for a Low-Cost Electricity Production", Applied Energy, Vol.72, 2002, pp.599-605.

[3] C.C. Warnick, "Hydropower Engineering", Prentice Hall of India, 1984.

[4] D.Manolakos, G.Papadakis, D.Papantonis and S.Kyritsis, "A Stand-alone Photovoltaic Power System for Remote Villages Using Pumped Water Energy Storage", International Journal of Energy, Vol.29, 2004, pp.57-63.

[5] R.R.Manakbadi, "Exploiting Irrigation Systems with Hydropower", Journal of Water Power and Dam Constructions, Vol.22, 1984, pp.37-44.

[6] S. Jungtiynont, "A Study on Turbine-Pump System of Utilization of Low Head Hydro Power", Journal of Institution of Engineers (I), Vol.82, 2000, pp.52-59.

[7] J.Lal, "Hydraulic Machines", Metropolitan Book Company Ltd., Delhi, 1975.

[8] S. Jungtiynont, "Performance Characteristics of Turbine for Low Head Hydro Power", Dissertation Project of UNU Training Programme, Indian Institute of Technology, NewDelhi, 1991.

[9] Y.I. Topcu and F.Ulengin, "Energy for the Future", An Integrated Decision Aid for the Case of Turkey International Journal of Energy, Vol.1,No.29, 2004, pp.137-144.

Table 1 Results of Preliminerary Stage

S.No.	Alternator Load (kW)	Water Collected in Tank			Discharge of Water (m^3/sec)	Motor Input Power (kW)	Head (m)	Turbine Speed (rpm)
		Height of Water Rise ('m')	Area of Cross Section of Tank (m^2)	Time taken for 0.5m of Water Level rise (sec)				
1	0.500	0.5	0.25	18.49	6.76×10^{-4}	4.37	7.00	1000
2	0.700	0.5	0.25	18.01	6.94×10^{-4}	4.42	6.95	1000
3	1.000	0.5	0.25	17.60	7.1×10^{-4}	4.48	6.90	1000
4	1.200	0.5	0.25	17.28	7.23×10^{-4}	4.54	6.80	1000
5	1.400	0.5	0.25	17.12	7.30×10^{-4}	4.65	6.75	1000
6	1.600	0.5	0.25	16.86	7.41×10^{-4}	4.72	6.70	1000
7	1.800	0.5	0.25	16.68	7.70×10^{-4}	4.90	6.65	1000
8	2.000	0.5	0.25	15.39	8.12×10^{-4}	5.17	6.55	1000
9	2.100	0.5	0.25	15.01	8.31×10^{-4}	5.29	6.50	1000
10	2.200	0.5	0.25	14.72	8.48×10^{-4}	5.40	6.45	1000

Table 2 Results of Analysis Stage

S.No.	Water Collected in Tank			Discharge of Water (m^3/sec)	Motor Input Power (kW)	Head (m)
	Height of Water Rise (m)	Area of Collecting Tank (m^2)	Time taken for 0.5 m of Water Rise (sec)			
1	0.5	0.25	18.50	6.76×10^{-4}	4.37	7.00
2	0.5	0.25	18.00	6.94×10^{-4}	4.42	6.95
3	0.5	0.25	17.60	7.10×10^{-4}	4.48	6.90
4	0.5	0.25	17.30	7.23×10^{-4}	4.54	6.80
5	0.5	0.25	17.20	7.27×10^{-4}	4.65	6.75
6	0.5	0.25	17.00	7.35×10^{-4}	4.72	6.70
7	0.5	0.25	16.60	7.53×10^{-4}	4.77	6.65
8	0.5	0.25	15.42	8.11×10^{-4}	5.17	6.55
9	0.5	0.25	15.10	8.28×10^{-4}	5.29	6.50
10	0.5	0.25	14.80	8.45×10^{-4}	5.40	6.45

Table 3 Results of Implementation Stage

S.No.	Water Collected in Tank			Discharge of Water (m^3/sec)	Motor Input Power (kW)	Alternator Load (kW)	Speed of Alternator (rpm)
	Height of Water Rise (m)	Area of Collecting Tank (m^2)	Time taken for 0.5 m of Water Rise (sec)				
1	0.5	0.25	14.74	8.48×10^{-4}	5.40	0.500	1000
2	0.5	0.25	14.74	8.48×10^{-4}	5.40	0.700	965
3	0.5	0.25	14.74	8.48×10^{-4}	5.40	1.000	905
4	0.5	0.25	14.74	8.48×10^{-4}	5.40	1.200	870
5	0.5	0.25	14.74	8.48×10^{-4}	5.40	1.400	840
6	0.5	0.25	14.74	8.48×10^{-4}	5.40	1.600	800
7	0.5	0.25	14.74	8.48×10^{-4}	5.40	1.800	765
8	0.5	0.25	14.74	8.48×10^{-4}	5.40	2.000	750
9	0.5	0.25	14.74	8.48×10^{-4}	5.40	2.200	690
10	0.5	0.25	14.74	8.48×10^{-4}	5.40	2.300	600

Table 4 Pump and Turbine Specifications

Pump		Turbine	
Head	53 m	Head	45m
Discharge	10.5 lit/sec	Discharge	10.5 lit/sec
Speed	2880 rpm	Speed	1000rpm
Input power	11.2kW	Output power	3.75 kW
Size	65mm x 65mm	Jet diameter	22mm
Impeller diameter	210mm	Jet ratio	12
		Pitch circle diameter	260mm
		Drum (Brake) diameter	300mm
		Rope diameter	12mm

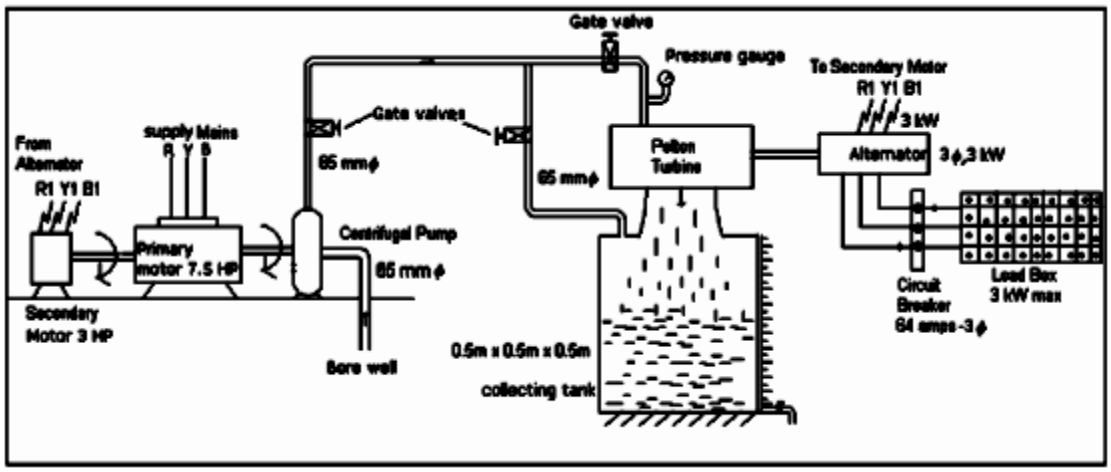

Fig. 1 Schematic diagram of the experimental setup

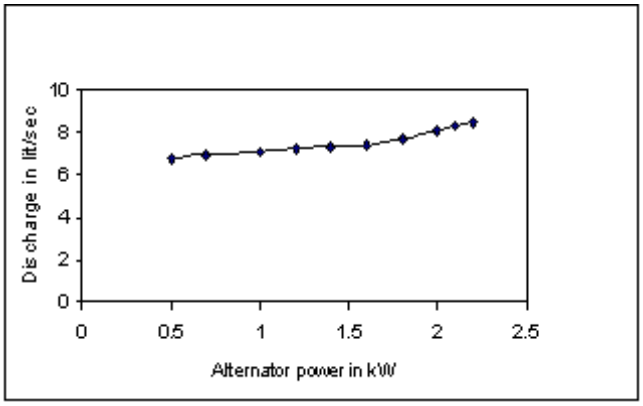

Fig. 2 Discharge Vs alternator power at constant speed 1000rpm (stage 1)

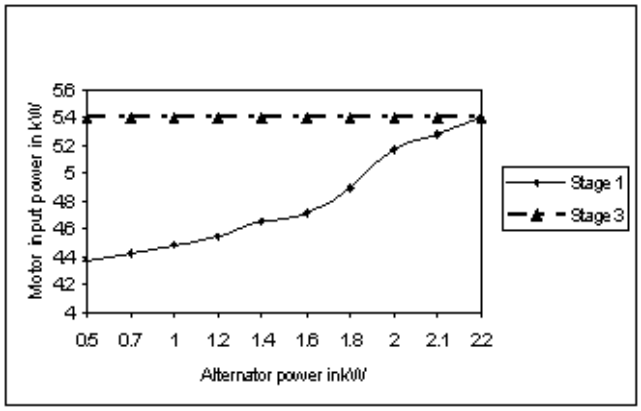

Fig. 3 Motor input power Vs alternator power at constant speed and maximum discharge

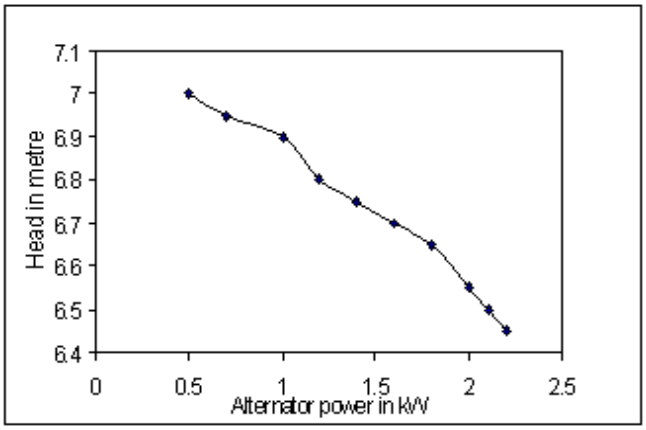

Fig. 4 Head Vs alternator power at constant speed of 1000rpm (stage 1)

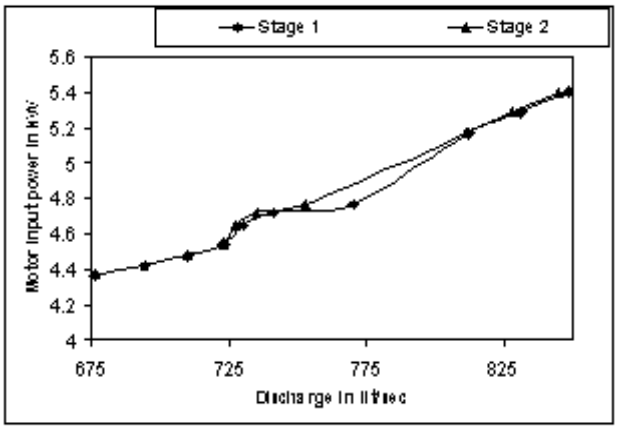

Fig. 5 Motor input power Vs discharge at constant speed of 1000 rpm

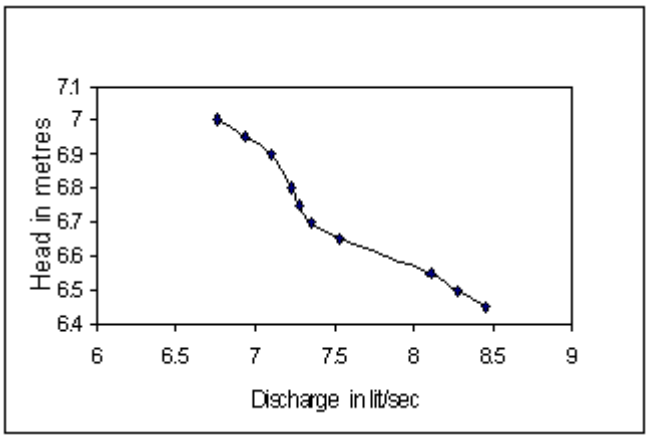

Fig. 6 Head Vs discharge at constant speed of 1000rpm (case 1)

EFFECTIVE USE OF SOLAR LIGHTING SYSTEM - A MELGHAT CASE STUDY

S.B. Thakre, N.W. Kale and S. J. Deshmukh
Department of Mechanical Engineering, Prof. Ram Meghe Institute of Technology & Research, Badnera Amravati, Maharashtra

(Received on 22 May 2007 and accepted on 18 October 2007)

Abstract

Chikhaldara and Dharni Tahesils of Amravati district of Maharashtra are together known as Melghat. This hilly area, covered by dense forests is a home for many tribals. Maharashtra Energy Development Agency (MEDA) have recently installed solar photovoltaic street lighting system in few of the villages in Melghat. Unfortunately very few of them are working today. This paper is aimed at identification of various problems of the solar lighting system in this remote area and search for probable remedies to these problems. Five pilot plants were setup at these locations, suggesting that by spending just 3.6% of the total installation cost, the system works satisfactorily for years together.

Keywords*: Melghat Region, Solar Photovoltaic Lighting System*

1. INTRODUCTION

Melghat is the place where the 'Ghats' meet. This southern tip of the central Indian highlands is the area encompassed by the Gawilgad ranges of the satpura hills. While northern boundary of the Melghat is unmarked by the river Tapi, river Sipna flows through the heart of the Melghat. Khandu, Khapra Gadga and Dolar are major tributaries of the Sipna. The flora and Fauna of this dry deciduous forest enjoys protection under Melghat tiger reserve, Gugamal National Park and Melghat Wild Life Sanctuary. The 'Adiwasis', i.e., the tribals of Melghat mainly include Korkus, Gonds and Nihals. The tract is so rugged, hilly and densely covered by forests that it is impossible to carryout major developmental activities in this region. Moreover carrying out such activities in protected areas is banned under wild life protection act and Indian forest act. As conventional source of energy, the electricity is not available, the energy requirement of the tribals are mainly met by fuel wood and animal dung.

2. USE OF RENEWABLE ENERGY IN MELGHAT

Maharashtra Energy Development Agency (MEDA), a Govt. Organisation aimed to popularization of various non-conventional energy sources, along with the Amravati (ZP) and Maharashtra State Electricity Board (MSEB) installed solar photovoltaic lighting system in fifty villages of Melghat region in 1989 and 1990. This consists of a set of photovoltaic panels, a compact fluorescent lamp, lead acid storage battery and inverter. The device is capable of working for 6 to 12 hours depending on the availability of sunlight with the help of light sensor. It gets switched on automatically in the evening and stops in the morning. Figure.l shows the schematic of this device. It was a very novel experiment of taking appropriate technology to the grass root level. But any efforts of changing the lifestyle of the people who are governed by some entirely different value system need much more homework. It demands in-depth study of situation from all the angles and Government agencies failed to do so. Unfortunately very soon, most of the installed systems ceased to work. The authors, therefore critically analyzed the problems with the existing system and proposed solutions were proposed for the same.

2.1 Problems with Existing System

A study group was then formed consisting of expert teachers and students for conducting detailed survey of various installations. The study group visited different villages, talked with people, carefully studied the design of existing system and gathered information regarding

problems with various installations. The study group also had detailed discussion with the authorities of ZP, MSEB, Forest Department, and Tribal Development Department etc.

Table 1 and figure 1 provide brief results of inspection of 50 installations. It is clear from the Table that only one solar lighting system was working out of 50 installations.

Table1Troubles and Total Number of Installations Total Number of Installations out of order is 49 out of 50

S.No	Causes/Trouble	No. of Systems Affected
1	Battery discharged / Out of order	32
2	Battery stolen	17
3	Broken solar photovoltaic panel	19
4	Solar panel not working / Generating poor voltage	02
5	Loose connection / Disconnected cables	42
6	Inverter / Regulator out of order	13
7	Fuse blown off	08
8	Fluorescent Tube Fused	06

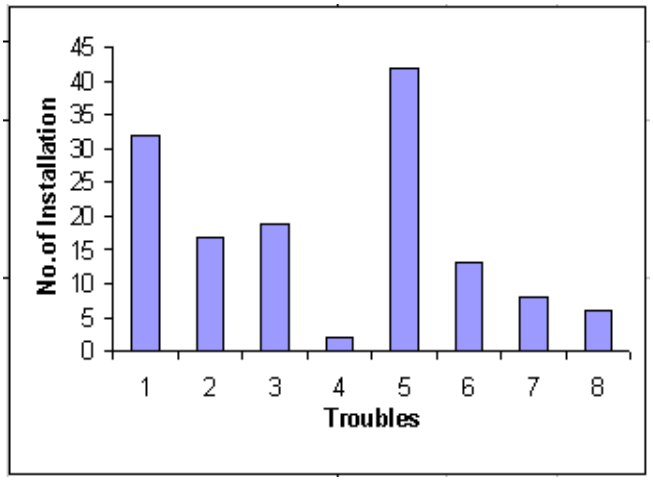

Fig.1 Troubles various number of installations

Table 1 reveals that out of 50 installations, hardly 15 installations are in operation due to critical reasons. Rest are simply laying idle due to negligence, lack of infrastructure available for carrying out repairs, etc. The main problems identified are as follows:

(i) Lack of public participation in this process. Probably this is most important reason behind the failure of this scheme. This has resulted into ignorance of tribals towards this device. As the tribals are not involved in the process of site selection, erection etc., for them this device is an alien.

(ii) Damage to the equipment from mischievous elements and children in the villages.

(iii) Thefts of battery, battery lugs, cables other components like fluorescent lamp, wires, etc.

(iv) Faulty design of the equipment in following respects:

- Solar panels are not properly shielded by using grill or wire mesh. This often results into broken solar panel due to stone pelting by mischievous children.
- Battery and other circuitry is mounted on the pole itself thus leaving sophisticated electronic component susceptible to weathering and corrosion.
- Height of the pole is short.
- Cabling work is not properly done.

(v) There is absolutely no provision for maintenance and repairs of this equipment, which is clear from Table 1. That many installations are inoperative simply due to some minor reasons, which can be corrected at local level itself. Neither MSEB nor ZP have planned programmed maintenance of these equipments.

(vi) Responsibility of safe guarding the equipment is not fixed.

2.2 Recommendations for Effective Use of Solar Lighting System

A report based on above studies was submitted to MSEB and ZP Some of the important recommendations for better utilization of solar energy are as follows:

(i) Seeking involvement of the local inhabitants. No non-conventional energy system can work without public participation. The process must begin with organizing a village meeting, wherein they should be convinced to adopt this concept. The emphasis should be on creating awareness regarding conservation of natural resources.

(ii) Formation of caretaker group. The responsibility of protection, routine maintenance should be given to a group of 4-5 enthusiastic youth from the village,

preferably 2 of them should be ladies. If possible they should be paid some honorarium.

(iii) Training for the care-taker group The care-taker group thus formulated should be trained to understand the working of this instrument, so that they will be able to carry out minor repairs of the device much as common battery care, replacement of fuses, fluorescent lamps, etc. at their place only. The group should be equipped with tool kit, common spares, fuses, fluorescent lamps, wires, lock for circuit box, etc.

(iv) The lighting unit should be redesigned in order to take care of various problems identified. The major changes suggested in design are as follows:

- The solar panels should be properly shielded by using wire mesh grill.
- The battery box and the circuit box should be kept properly in the nearby hut instead of mounting it on the pole.
- Height of the pole above the ground level should be at least six meters.
- Good quality cable should be used instead of using loose wires.

(v) If possible future installations should be supplied with dry/maintenance free batteries instead of lead acid batteries.

(vi) MSEB and ZP must take urgent steps to develop necessary infrastructure for carrying out repairs and maintenance of solar lighting systems.

(vii) If one really want to use appropriate technology for improving standard of living of the tribal, earning their faith is most important. These efforts will not be successful without their active participation. In order to achieve this, Government agencies should take help of local NGOs, conservation organization etc.

1. Pole
2. Solar Panel
3. Battery and Circuit Box
4. Fluorescent Lamp
5. Wire

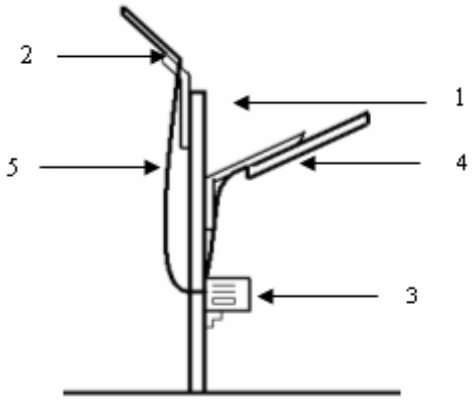

Fig.1 Existing solar lighting system

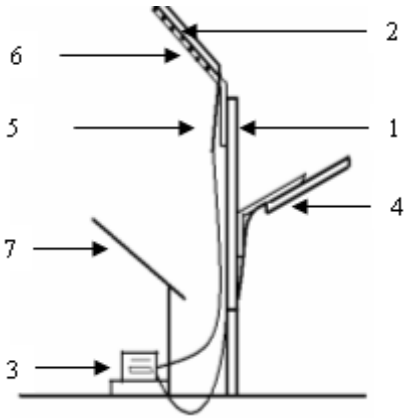

Fig. 2 Modified solar lighting system

1. Pole
2. Solar Panel
3. Battery and Circuit Box
4. Fluorescent Lamp
5. Wire
6. Wire Mesh Shield
7 Hut

3. THE PILOT PROJECT

As a pilot study, the author and study group decided to implement these suggestions to five of the fifty villages. Village meetings were called in which benefits of this device were told to people. As the outcome of this meeting, a caretaker group was formed. A brief two-day training was imparted to the caretaker group. They were taught about common battery care, replacement of fluorescent lamp, cleaning of solar panel, etc. The lighting units were redesigned as per the recommendations, the

battery and other electronic circuit was properly placed in the box which instead of mounting on the pole was kept in the hut adjacent to the site of installation, cabling was properly done. Figure 2 shows the schematic diagram of the redesigned unit. The installation was carried out with the help of the members of the caretaker group. Now after a period of one year all these five installations are working satisfactorily and it has been reported that in few other villages, inhabitants are insisting the "Gramsevak" to get the device repaired. Now for the people of these five villages, 'solar lighting system' is not a useless thing, which remains out of operation for years together. Even if any minor problem arises, they themselves can over come it. As per the record, cost of these 50 installations is Rs. 12,50,000/- (i.e. Rs. 25,000/- per installation). It is estimated that the extra expenditure on the design modification, cost of spares, expenditure over training, etc. is around Rs.45000/- (i.e. Rs. 900/- per installation) for these 50 installations, which is 3.6% of the total cost.

4. CONCLUSION

Throughout our country, in many remote areas like Melghat, thousands of such systems are laying idle due to more or less similar reasons. Just by spending little amount of extra money (Rs 900/-per system) the systems can be effectively used for years together. It can be further concluded that only Government agencies will not be able to handle this task. Government must take necessary steps to involve local NGOs, conservation organizations in this process.

REFERENCES

[1] Mehta Prachi "The Satpura Hills", Palvi, Nature Conservation Society, Amravati, Vol.5, 1995.

[2] MEDA, "Instruction Manual for Solar Photovoltaic Devices", Pune, 1992.

[3] Ministry of Non-conventional Energy Sources, "Annual Report", 1991-92.

[4] G.D. Rai, "Textbook of Non Conventional Energy Sources", 1992.

[5] Thakre S.B. *et al.*, "Solar Lighting Systems in Melghat-Project Report", College of Engg. Badnera,1996.

KINETIC STUDIES ON SORPTION OF BASIC ORANGE 14 AND BRILL RED 5B USING EICHHORNIA CRASSIPES PARTS OF RHIZOME AND ROOT

S. Renganathan[1], M. Dharmendira Kumar[2], R. Ravikumar[3] and M. Velan[4]

[1,2&4]Department of Chemical Engineering , Alagappa College of Technology, Anna University, Chennai- 600025, Tamil Nadu

[3]Department of Biotechnology, Bannari Amman Institute of Technology, Sathyamangalam - 638 401, Erode District, Tamil Nadu

E- mail: rengsah@rediffmail.com, ravi_cbe1@rediffmail.com

(Received on 03 October 2007 and accepted on 02 December 2007)

Abstract

Sorption capacity of different parts of Eichhornia crassipes like Rhizome and Root on Basic Orange 14 and Brill Red 5B was studied in a batch system. The percentage color removal of Basic Orange 14 dye using Root was found to be more when compared to other part Rhizome studied in the present investigation. The percentage color removal of Orange 14 and Brill Red 5B was observed as 92% (using Root) and 15% (using Root), respectively. The polynomial equations had been developed for two different parts of E. crassipes like Rhizome and Root on Orange 14 and Brill Red 5B using Basic programming language. It is a ready reckoner equation used to find out the percentage color removal of dyes at any time interval.

Keywords: *Basic Orange 14, Biosorption, Brill Red 5B, Eichhornia crassipes*

1. INTRODUCTION

Dyes are synthetic aromatic water soluble dispersible organic colorants, having potential application in various industries such as textiles, leather, paper, plastics, etc., to color their final products [1]. The extensive use of dyes often poses pollution problems in the form of colored wastewater discharge into environmental water bodies. Effluent containing dye is responsible for the water borne diseases such as dermatitis, ulceration of the skin and mucous membranes, kidney damage and a loss of bone marrow leading to anemia [2]. Removal of dyes using physical or chemical treatment processes include flocculation, floatation, membrane filtration, electro chemical destruction, ion exchange and ozonation are not economically feasible [3]. The above methods are involved with high initial investment and operation costs.

Adsorption employing activated carbon and various other adsorbents has been widely studied and applied, but the cost of carbon is limited to its application [4]. So a cheap and low cost adsorbents such as bagasse, peat, rice husk, fly ash, waste residues, wheat straw, corn cobs barley husks, agricultural residues, apple pomace and quaternised wood have been used for the color removal process through adsorption [5]. These low cost adsorbents are characterized by low adsorption capacity. In recent years, a number of studies have been focused on microorganisms such as fungal, bacterial and algae biomass as a potential biosorbent and the disposal of these adsorbent can be solved by recycling after regenerating the biosorbent using sodium hydroxide and organic solvents [6]. In the present investigation, biosorption experiment was focused on Orange 14 and Brill Red 5B using the E. crassipes parts of Rhizome and Root.

2. MATERIALS AND METHODS

2.1 Preparation of Sample

E. crassipes plants were collected from Nainar pond, Thirunelveli, India. They were washed with deionised water to remove dirt particles. Then it was separated into two parts (Rhizome and Root) and sun dried for 2 days and also they were crushed. The biosorbent used in the present investigation was utilized with the mesh size of 60.

2.2 Batch Experimental Process

The weighed amount of dried biomass (Rhizome and Root) was suspended in double distilled water and homogenized for 20 min. Orange 14 of 85 ml was prepared with 30 mg/L initial dye concentration and it was added with 15 ml of biomass suspension solution (to get the concentration of biomass in dye solution as 0.2 gm/L). Experiment was conducted in a temperature controlled shaker at 30oC and at 180 rpm. Samples were withdrawn for every 15 min interval, centrifuged at 12000 rpm for 10 min and the absorbance of the supernatant was analysed using Elico SL-177 mini spectrophotometer. The same experiment was repeated for Brill Red 5B.

2.3 Kinetic Studies

The biosorption mechanism and potential rate controlling steps have been investigated by using the Pseudo-first and Pseudo-second order kinetic models. The Pseudo-first order rate expression of Lagergren is

$$\frac{dq}{dt} = k_{1,ad}\,(q_{eq} - q) \qquad (1)$$

Where q is the amount of dye adsorbed on the biosorbent at time t and k1,ad (min 1) is the rate constant for first order biosorption. The integral form of Eq. (1) is

$$\log(q_{eq} - q) = \log q_{eq} - \frac{k_{1,ad}}{2.303} t \qquad (2)$$

A linear fit of log (qeq - q) versus t shows the applicability of this kinetic model.Expression for the Pseudo-second order kinetic model is

$$\frac{dq}{dt} = k_{2,ad}\,(q_{eq} - q)^2 \qquad (3)$$

(3)

Where k2,ad (g mg-1 min-1) is the rate constant of the Pseudo-second order biosorption. The integrated linear form of Eq. (3) is

$$\frac{t}{q} = \frac{1}{k_{2,ad}\,q_{eq}^{\,2}} + \frac{1}{q_{eq}}\,t \qquad (4)$$

If the experimental data fits (linear relationship) the plot of t/q versus t, the Pseudo-second order kinetic model is valid [7].

3. RESULT AND DISCUSSION

3.1 Comparison Studies

The E. crassipes Root particles showed maximum percentage of color removal on Orange 14 (92%) and Brill Red 5B (15%) when compared to the Rhizome part of the E. crassipes (Fig.1), because of high electrostatic attraction between negatively charged Root surfaces to positively charged dye cation. The effect of E. crassipes Root on the adsorption of dyes is well documented and similar results were observed in the literature [8].

3.2 Sem Imaging

Scanning Electron Microscopy (SEM) is a novel technique that has been increasingly used to examine biological specimens. The surface morphology of the different parts of the E. crassipes sorbent was exemplified by the Scanning Electron Micrograph (Fig.2). As shown in the SEM Micrograph, the rough and porous surface was found to be more in the Root part of E. crassipes when compared to Rhizome part studied in the present investigation. This surface property should be considered as a factor for providing an increase in the total surface area thereby increasing the percentage of color removal of Orange 14.

3.3 Kinetic Modeling

The Pseudo-first order and Pseudo-second order kinetic models are applied to the experimental data. From the slopes and intercepts of plots of log (qeq - q) versus t, the Pseudo-first order rate constant (k1,ad) and qeq values were determined. The linearized form of the Pseudo-first order model at 30 mg/L initial dye concentration for the period of 420 minutes was analysed. The correlation coefficients of the Pseudo-first order kinetic model obtained are very low (Table 1). Also the theoretical qeq values found from the Pseudo-first order kinetic model did not give acceptable values. Therefore, this biosorption system is not a Pseudo-first order reaction. The Pseudo-second order rate constant (k2,ad) and qeq values were also determined from the slope and intercept of the plots t/q versus t. The values of the parameters (k2,ad) calculated and experimental qeq values, together with correlation coefficients are presented in Table 1. The results indicate that the Pseudo-second order rate constants values for Root was found to be more when compared to Rhizome for all dyes studied in the present investigation.

The correlation coefficients for the Pseudo-second order kinetic model were almost equal to 1.00 for the dye concentration studied using E. crassipes parts of Root and Rhizome on Orange 14 and Brill Red 5B. The theoretical qeq values also agreed very well with the experimental qeq values in the case of Pseudo-second order kinetics. These results suggest that the sorption system is not a Pseudo-first order reaction and that the Pseudo-second order model, based on the assumption that the rate limiting step may be chemical biosorption involving valency forces through sharing or exchange of electrons [9].

Table 1 The Pseudo-first And Second Order Rate Constants, Calculated and Experimental Qeq Values for the Biosorption of Basicorange 14 and Brill Red 5b Using Rhizome and Root

		Pseudo first order			Pseudo second order		
	$q_{eq,exp}$	$k_{1,ad}$	$q_{eq,cal}$		$k_{2,ad}$	$q_{eq,cal}$	
Parts	(mg/g)	(L/min)	(mg/g)	R^2	(g/mg min)	(mg/g)	R^2
Basic Orange 14							
Rhizome	12.9	0.83	3.11	0.554	1.8	12.99	0.999
Root	13.65	2.14	9.86	0.911	2.3	13.76	0.999
Brill Red 5B							
Rhizome	0.075	0.33	15.44	0.836	7.29	0.09	0.867
Root	2.25	1.1	3.17	0.902	0.26	2.81	0.858

3.4 Polynomial Equations

In the present investigation, the polynomial equations had been developed for E. crassipes parts of Rhizome and Root on Orange 14 and Brill Red 5B (Table 2) using Basic Programming language. With the use of MS-Excel, the polynomial equations can be developed up to X6 terms only.

But using this Basic Program we can develop polynomial equations above X6 terms to Xn terms. This is the main advantage of this Basic program when compared to polynomial equations developed with the use of MS-Excel. It is a ready reckoner equation used to find out the percentage color removal of dyes at any time interval.

Table 2 Developed Polynomial Equations for the Biosorption of Basic Orange 14 and Brill Red 5b Using Rhizome and Root.

Parts of *E. crassipes*	Polynomial equation
Basic Orange 14	
Rhizome	$Y=27.00+221.97X-333.83X^2+230.00X^3-72.67X^4+8.53X^5$
Root	$Y=134.00-239.27X+358.67X^2-233.00X^3+69.33X^4-7.73X^5$
Brill Red 5B	
Rhizome	$Y=-0.90+4.81X-7.40X^2+5.10X^3-1.6X^4+0.19X^5$
Root	$Y=-0.60+21.84X-45.06X^2+42.13X^3-15.73X^4+2.02X^5$

3.5 Sorption Mechanisms

The most commonly used technique for identifying the mechanism involved in the sorption process is by fitting the experimental data in an intra particle diffusion plot. According to Weber and Morris, an intra particle diffusion coefficient Ki is defined by the equation

$$Ki = q/t0.5 \quad (5)$$

Thus the Ki (mg/ghr-1) value can be obtained from the slope of the plot of q (mg/g) versus t0.5 (hr) for two different parts of E. crassipes like Rhizome and Root on Orange 14 and Brill Red 5B. The Ki values obtained for Orange 14 and Brill Red 5B using Root was found to be

morewhen compared to the other part of Rhizome. The double nature of intra particle diffusion plot confirms the presence of both film and pore diffusion. In order to predict the actual slow step involved, the kinetic data were further analyzed using the Boyd kinetic expression.

Table 3 Intra Particle Diffusion Parameter (Ki) and Diffusion Coefficient (Di) for the Sorption of Basic Orange 14 and Brill Red 5b Using Root and Rhizome.

Parts of *E. crassipes*	Basic Orange 14		Brill Red 5B	
	Ki (mg/ghr^{-1})	Di (cm^2/s)	Ki (mg/ghr^{-1})	Di (cm^2/s)
Rhizome	0.5390	0.007741	0.0297	0.001752
Root	1.5324	0.009188	1.0087	0.004477

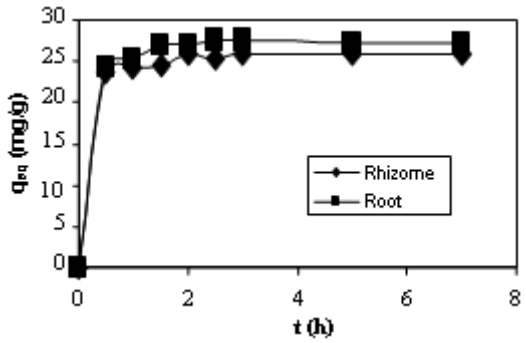

Fig.1 (a) Effect of E. crassipes sorbents on the color removal of orange 14

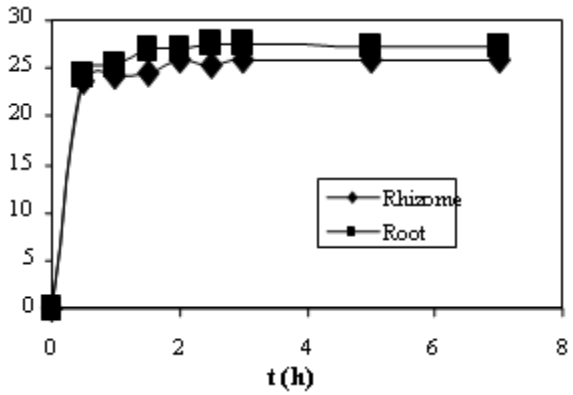

Fig.1 (b) Effect of E. crassipes sorbents on the color removal of brill red 5b

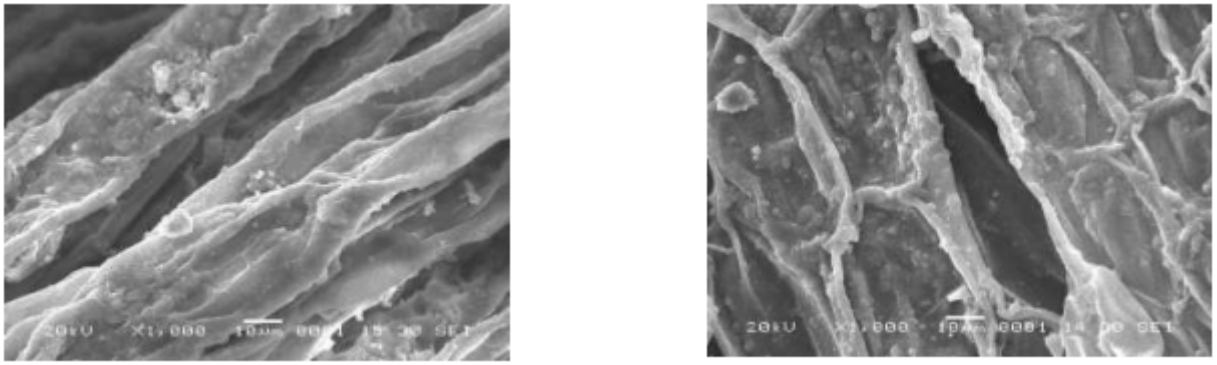

Fig. 2. SEM images of E. crassipes (a) Root (b) Rhizome

This kinetic expression predicts the actual slowest step involved in the sorption process for different sorbent systems. The Boyd kinetic expression is given by (9)

F = 1" (6/ð 2) exp (“Bt) (6) and
F = q/qo, (7)

Where, qo is the amount of dye adsorbed at infinite time (mg/g) and q represents the amount of dye adsorbed at any time t (min), F represents the fraction of solute adsorbed at any time t, and Bt is a mathematical function of F. Substituting Eq. (7) in (6), Eq. (6) simplifies to

1 “F = (6/ð 2) exp (“Bt) (8) Or
Bt = “0.4977”ln (1 “F) (9)

The Bt values at different contact times can be calculated using Eq. (9). The calculated Bt values were plotted against time t and is used to identify whether external transport or intra particle transport control the rate of sorption [10]. It was observed that the plots were linear but do not pass through the origin confirming that, for the studied initial dye concentration, external mass transport mainly governs the sorption process. The calculated Bt values were used to calculate the effective diffusion coefficient, Di (cm2/s) using the relation [11].

Bt = ð 2Di/r2 (10)

Where r represents the radius of the particle calculated by sieve analysis and by assuming spherical particles. The Di values obtained for different dyes Orange 14 and Brill Red 5B using Root was found to be more when compared to the Rhizome part of E. crassipes studied in the present investigation (Table 3). The similar sorption mechanism also explained by özer et al., using Enteromorpha proloera in a batch system [12].

4. CONCLUSIONS

The color removal for Orange 14 and Brill Red 5B using two different parts of E. crassipes like Rhizome and Root was investigated. The color removal for Orange 14 and Brill Red 5B using Root was found to be more when compared to the other part of Rhizome studied in the present investigation. Sorption results for the Orange 14 and Brill Red 5B using Root was found to be fitted very well to the Pseudo-second order kinetic model when compared to Pseudo-first order kinetic model.

The polynomial equations had been developed for two different parts of E. crassipes like Rhizome and Root on Orange 14 and Brill Red 5B using Basic Programming language had been studied in the present investigation.

The intra particle diffusion coefficient Ki obtained for Orange 14 and Brill Red 5B using Root was found to be more when compared to the other part of Rhizome. The effective diffusion coefficient (Di) values obtained for the sorption of Orange 14 and Brill Red 5B using Root was found to be more when compared to Rhizome studied in the present investigation.

REFERENCES

[1] K.C.Chen, J.Y.Wu, C.C.Huang, Y.M.Liang and S.C.J.Hwang, “Decolorization of Azo Dye Using Pva-immobilized Microorganisms”, Journal of Biotechnolgy, Vol.241, No.52, 2003, pp.101-108.

[2] A.El-Thalouth, K.Haggag and M.El-Zawahry, “Utilizing Sugar-cane Bagasse Pulp and Carbamoyl Ethyl Derivatives as Direct Dye Absorbent”, American Dyestuff Reporter, Vol.82, 1993, pp.36-41.

[3] I.M.Banat, P.Nigam, D.Singh and R.Marchant, “Microbial Decolorization of Textile Dye Containing Effluents: A Review”, Bioresource Technology, Vol.58, 1996, pp.217-227.

[4] G.S.Gupta., S.P. Shukla, G. Prasad and V.N. Singh, “China Clay as an Adsorbent for Dye House Waste Water”, Environmental Technology, Vol.13, 1992, pp. 925-936.

[5] B.S.Girgis, S.S.Yunis and M.Soliman, “Characteristics of Activated Carbon from Peanut Hulls in Relation to Conditions of Preparation”, Materials Letters, Vol.57, 2002, pp.164-172.

[6] B.S.Inbaraj, K.Selvarani and N.Sulochana, “Evaluation of a Carbonaceous Sorbent Prepared from Pearl Millet Husk for its Removal of Basic Dyes”, Journal of Scientific and Industrial Research, Vol.61, 2002, pp.971-978.

[7] Y.S.Ho and G..McKay, “A Kinetic Study of Dye Sorption by Biosorbent Waste Product Pith”, Resources, Conservation and Recycling, Vol.25, 1999, pp.171-179.

[9] Zumriye Aksu and Gonul Donmez, "A Comparitive Study on the Biosorption Characteristics of Some Yeast for Remazol Blue Reactive Dye", Chemosphere, Vol. 50, 2003, pp.1075-1083.

[10] V.K.Gupta, I.Ali and M.D.Suhas, "Equilibrium Uptake and Sorption Dynamics for the Removal of a Basic Dye (Basic Red) Using Low Cost Adsorbent", Journal of Colloid and Interface Science, Vol. 265, 2003, pp.257-264.

[11] V.K.Gupta and I.Ali, "Removal of DDD and DDE from Waste Water Using Bagasse Fly Ash, Sugar Industry Waste", Water Research, Vol.35, 2001, pp.33-39.

[12] A.Ozer, G.. Akkaya and M.Turabik, "Biosorption of Acid Red 274 (Ar 274) on Enteromorpha Proliera in a Batch System", Journal of Hazardous Materials, Vol.126,2005, pp.119-127.

PHASE CHANGE MATERIAL AS A THERMAL STORAGE MATERIAL FOR PEAK LOAD SHIFTING

M.Ravikumar[1] and P.S.S. Srinivasan[2]

[1]Department of Mechanical Engineering, Bannariamman Institute of Technology, Sathyamangalam - 638 401, Erode District, Tamil Nadu

[2]Department of Mechanical Engineering, K S Rangasamy College of Technology, Tiruchengode - 637 209, Namakkal District, Tamil Nadu

Email: kumarmravi74@yahoo.co.in, Email: drpss@yahoo.com

(Received on 22 May 2007 and accepted on 12 December 2007)

Abstract

As the demand for refrigeration and air-conditioning has been increased during the last decade, the cool storage systems can be used for economic advantage over conventional cooling plants. The cool storage system using phase change materials (PCMs) can be used for peak load shifting if they are installed in the building. In case of a sensible heat storage system, energy is stored or extracted by heating or cooling a liquid or a solid, which does not change its phase during the process. A variety of substances much as water, heat transfer oils and certain inorganic molten salts, and solids like rocks, pebbles, and refractory are used. The choice of substances used largely depends upon the temperature level of the application. PCMs are latent heat materials having low temperature range and high energy density of melting – solidification compared to the sensible heat storage. The thermal storage test was conducted in a room with PCM impregnated building materials and results showed that PCM impregnated material can be used as an alternative to the conventional cooling system.

Keywords: *Energy Storage, Natural Cooling, Phase Change Material (PCM), Salt Hydrate, Solar Chimney*

1. INTRODUCTION

Some devices store heat during peak power operation and release the same during reduced power operation. Phase change material are type of the thermal storage devices.

Heat is a constant demand for the household sector. An analysis of household energy consumption pattern reveals that the major use is for heating and cooling. The huge amount of time, money, physical energy expended and the immense health hazards in the conventional methods of cooling are enormous. This fact underlines the importance of utilizing the abundant solar energy as a supplier of heat. In a country like India, the sun shines gloriously for more than 300 days in a year. Thus, solar heating is an appropriate technology to solve the energy crisis. To solve the problem faced in conventional cooling and to fight against deforestation and air pollution, solar energy storage becomes an important aspect. Though there are many applications possible, an important factor is that solar energy is time dependent in nature. The energy needs for a wide variety of applications are also time dependent, but different in pattern and phase from that of solar energy supply. Hence, thermal energy storage systems are essential.

Renewable and natural energy sources that form the main components of sustainable energy systems, can only be made continuously available to users through thermal energy storage (TES). In addition to heating, TES provides several flexible alternatives for cooling systems. Recent discussions on topics like global warming and heat waves have brought attention once again to energy efficient cooling systems utilizing renewable energy sources. Cooling demand has already been increasing due to the evolving comfort expectations and technological development around the world. Climate change has brought additional challenges for cooling systems designers. Hence new cooling systems must use less and less electricity generated by fossil fuel based systems and still be able to meet the ever increasing and varying demand.

2. AN OVERVIEW OF PCMs

2.1 Classification and Properties of PCMs

In 1983, Abhat [1] gave the general classification of energy storage material fig.1 and the same was also proposed Lane [2,3], Dinser and Rosen [4]. These papers gave full details, like classification, characteristics, etc., Zalba [5] listed the properties of different PCM's (Organic, Inorganic, Fatty acids) much as density, specific heat, thermal conductivity and melting temperature. Hydrated salts are attractive materials for use in thermal energy storage due to high volumetric storage density, relatively high thermal conductivity and moderate costs compared to paraffin waxes. Glauber salt (Na2SO4. H2O), which contains 44% Na2SO4 and 56%H2O has been studied[6], and it is found to have a melting temperature of 32.4ºC, latent heat of 254 kJ/kg.

2.2 Selection of Phase Change Materials

The selection of PCMs for a specific application should be based on thermodynamic properties, kinetic properties and chemical properties. For low temperature applications ranging from 0 to 99°C, Salt Hydrates would be the best option owing to their availability in a less temperature range with a reasonable specific heat capacity of 133.4 (cal/deg.mol), thermal conductivity of 0.987 W/m-K, density of 1552 kg/m3 in solid phases respectively and phase transfer temperature ranging from 35 to 39°C.

The selection of PCMs is based upon the criteria discussed below:

2.2.1 Thermodynamic Criteria

The phase change materials should exhibit the following thermodynamics features:

- A melting point in the desired operating temperature range.
- High latent heat of fusion per unit mass, so that a lesser amount of material stores a given amount of energy.
- High density, so that a smaller container volume holds the material
- High thermal conductivity so that the temperature gradient required for charging the storage material is small.
- High specific heat that provides additional sensible heat storage effect and also avoid sub cooling.

2.2.2 Kinetic Criteria

The phase change materisls should exhibit little or no super cooling during freezing. The melt should crystallize at its freezing point. This is achieved through a high rate of nucleation and growth rate of the crystals.

2.2.3 Chemical Criteria

The phase change materials should exhibit the following chemical features:

- Chemical stability
- No chemical decomposition, so that the (LHTS) system life is assured.
- No corrosiveness to construction material
- The phase change material should be non-poisonous, non-flammable and non-explosive.

3 EXPERIMENTAL INVESTIGATIONS

3.1 Case Study

Bouchair *et al.* [7] reported that investigations on a full scale experimental solar chimney with both front and back walls maintained at the same uniform temperature by heating elements. It was shown that properly designed solar chimneys can be used for day time ventilation as well as night cooling in hot climates by driving cooler outdoor air into the building using the thermal energy stored during the day time. By introducing air movement across the room or by evaporative cooling of the incoming air, thermal comfort in buildings may be achieved using solar chimneys in buildings. Different designs of roof solar collector used to introduce natural ventilation into house were studied by Khedari *et al [*8]. Kumar *et al* [9] studied that indoor air quality in a prototype house with a solar chimney system and found that air ventilation is effective in reducing indoor air contaminants. By comparing the performance of a conventional brick solar chimney and a solar chimney with the sun facing wall replaced by glazing, Afonso and Oliverira [10] showed that the glazed solar chimney drew 10-20% more air through chimney.

3.2 Analysis

Assuming uniform air temperature at the same height inside the chimney, energy balance yields
qkw = QpCp(T_{avg} - T_{amb}, where 'h' is the height along the chimney, 'w' is the chimney width, 'q' is the heat flux, 'Q' is the air flow rate in the chimney, 'ñ' and 'Cp' are air density and specific heat capacity at ambient temperature respectively, 'T_{avg}' is the average temperature inside the chimney at a height of h and 'T_{amb}' is the ambient temperature. Stack pressure, ÄPs can be obtained by as follows:

$$\Delta P_S = \int_0^H \frac{(T_{avg} - T_{amb})\, pg \cos\alpha}{T_{amb}}\, dh = \frac{pBH \cos\alpha}{2Q} \quad (1)$$

where 'á' is the chimney inclination angle from vertical, 'H' is the chimney height and 'B' is the buoyancy flux

$$B = \frac{gqwH}{\rho Cp Tamb} \quad (2)$$

The pressure loss along the air path, ÄPL, may be expressed as given below:

$$\Delta P_L = C_{in}\frac{\rho(Q/A_{in})^2}{2} + C_{out}\frac{\rho(Q/A_{out})^2}{2} + f\left(\frac{H\rho(Q/A)^2}{2D_h}\right) \quad (3)$$

where 'A' is the channel cross sectional area, 'A_{in}' and 'A_{out}' are the inlet and outlet areas, 'f' is the friction factor of the wall, C_{in} and C_{out} are the inlet and outlet pressure loss coefficients, 'D_h' is the hydraulic diameter of chimney channel.

Balancing equations 2 & 3 the ventilation flow rate Q, for a chimney with uniform heat flux can be obtained as below:

$$Q = A\left(\frac{B\cos\alpha}{2\psi}\right)^{1/3}$$

Where

$$\psi = \frac{A}{H}\left(f\frac{H}{2D_L} + \frac{1}{2}\left(C_{in}\left(\frac{A}{A_{in}}\right)^2 + C_{out}\left(\frac{A}{A_{out}}\right)^2\right)\right)$$

From the above analysis it is seen that the air flow rate is affected by stack pressure and pressure losses at the inlet and outlet of the chimney.

4. EXPERIMENT

The experimental setup used in the present study is shown in figure1 below:

The solar chimney has internal dimensions of 1m height and 0.2 m width. This experiment was carried out in a 0.63 m x 0.63 m long x 0.465 m high prototype building. There was an opening arranged in the north side of 0.225m x 0.136 m and in the south side of 0.136m x 0.136 m. The inlet of the chimney was 0.465m above the floor. The sides of the wall and roof are coated with 2mm thick phase change material . Thermocouples are used to measure the temperature of roof and room air.

Fig.1 Schematic view of the experimental system

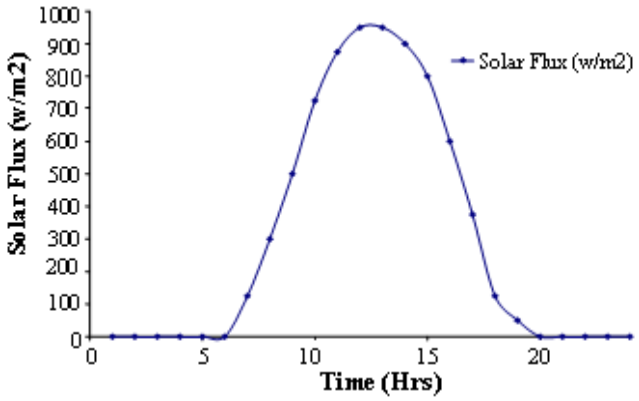

Fig. 2 Solar radiation data for coimbatore during June 2006

4.1 Material Property

The temperature distribution inside the room through the walls is analyzed using the software ANSYS "V-8.0". The parameters obtained for analyses are given in Table 1.

Table 1 Parameters of Analysis

Material	Density (Kg/m^3)	Thermal Conductivity (W/mK)	Specific Heat (J/Kg K)
Brick	1500	0.291	900
Plaster	1680	0.7792	1150
Phase Change Material	1522	0.8	
Concrete	2300	1.279	1130
Air	1.165	0.02675	1005

The physical model was designed as shown in Fig.1 to make more circulation of air with the attachment of solar chimney in the roof of the room.

4.2 Boundary Conditions

For right and left $\frac{\partial T}{\partial X} = 0$

Bottom surface, Convection, h_i =10w/m2k, T =25ºC
Top surface, Convection, h_o = 10w/m2k, T =hourly values
Solar radiation flux, q = hourly values

5. RESULTS AND DISCUSSION

5.1 Temperature Distribution along the Chimney Height

The solar radiation data for Coimbatore during June 2006 was recorded as shown in Fig 2.The temperature distribution along the axis of the chimney is recorded as shown in Fig.3. It shows that the temperature increases from the chimney base as the height increases resulting in creation of natural draught inside the room that makes the natural circulation of air inside the room. No appreciable difference in temperature is observed along the width of the chimney

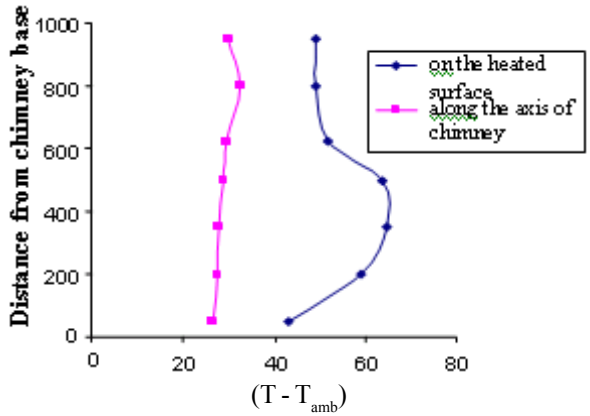

Fig 3 Temperature distribution along the chimney

5.2 Temperature Distribution Inside the Room

The PCM installed at the roof and walls of the building causes reduction of heat flow into the room and reduces the temperature inside the room. With the installation of PCM in the building structure, the inside room temperature are recorded and it is compared with the ambient temperature as shown in Fig 4. It shows a nearly 3^0C temperature drop for the PCM installed structure.

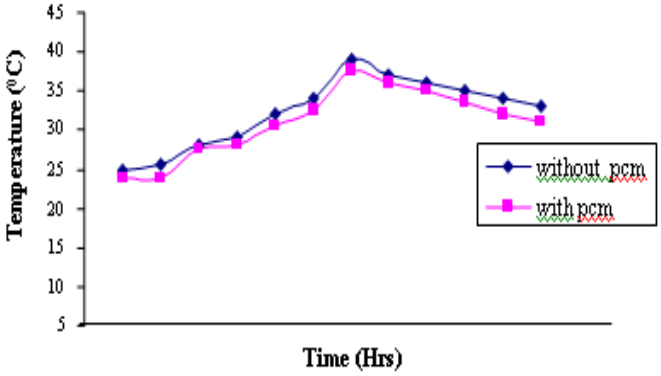

Fig. 4 Temperature distribution inside the room

5.3 Temperature Distribution in the Roof Structure

The temperature variation in the roof of the structure is compared for normal roof and PCM installed roof structure as shown in Fig.5 When PCM is installed along with withering course in the roof, it absorbs the heat entering in to roof. The maximum quantity of heat is absorbed when PCM changes its phase.

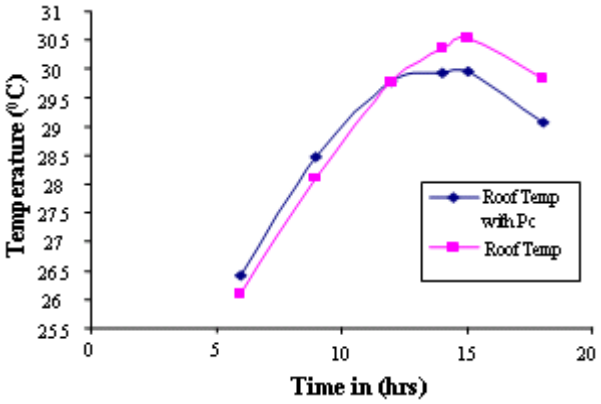

Fig. 5 Temperature distribution in the roof of the structure

For building cooling with PCM, only limited experimental studies have been conducted. Due to of high thermal mass of PCM walls, they are capable and very effective in minimizing the effect of large temperature fluctuations inside the building. The test was conducted by installing PCM in the walls of the test structure and temperature inside the room was reduced by 4°C and shifting the heating and cooling load to off-peak periods

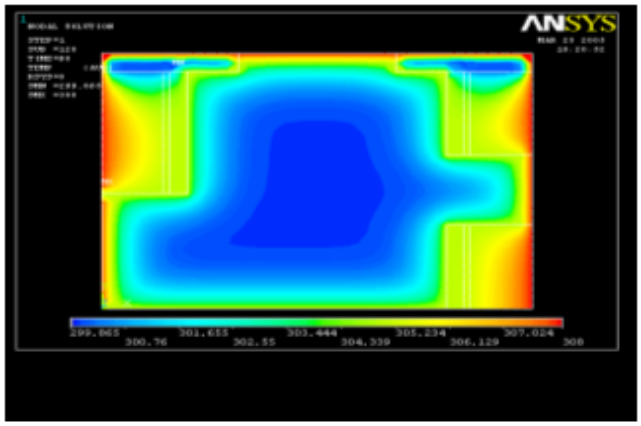

6. CONCLUSION

Natural cooling of buildings with phase change material was studied. The solar chimney effect was given additionally to improve the air movement inside the building structure. The solar chimney with uniform heat flux in the wall was investigated experimentally along the axis of the chimney. The maximum and minimum temperatures inside and outside the building are measured and analyzed by using ANSYS V-8.0. In the analysis carried out by varying the size of the element by smart size 10 and then smart size 5, the solutions was found to be convergent. With various combinations of PCM, the test can be repeated to find the best and effective material for cooling application.

REFERENCES

[1] A. Abhat, "Low Temperature Latent Heat Thermal Energy Storage, Heat Storage Materials, Solar Energy", Vol.30, 1983, pp.313-32.

[2] G.A.Lane, "Solar Heat Storage, Latent Heat Material", Technology, CRS Press, Boca Raton, FL, Vol 2, 1986.

[3] G.A.Lane, "Solar Heat Storage, Latent Heat Material", Background and Scientific Principles, CRC press, Florida, Vol 1, 1983.

[4] I.Dincer and M.A.Rosen, "Thermal Energy Storage, Systems and Applications", John wiley and Sons, Chickaester, (England), 2002.

[5] Belen Zalba, Jose M.Marin, Lusia Feabeza and Harald Mehling, "Review on Thermal Energy Storage with Phase Change Materials, Heat Transfer Analysis and Application", Applied Thermal Engg., Vol..23, 2003, pp.251-283.

[6] DR. Biswas, "Thermal Energy Storage Using Sodium Sulphate Decahydrate and Water, Solar Energy", Vol.19, 1977, pp.99-100.

[7] A. Bouchair, "Solar Chimney for Promoting Cooling Ventilation in Buildings in Southern Algeria, Building Service Engineering", Research and Technology, Vol.15. No.2, 1994, pp.81-93.

[8] J. Khedari, J.Hirunlabh and T.Bunnag, "Experimental Study of a Roof Solar Collector Towards the Natural Ventilation of New Houses", Energy and Buildings, Vol. 26, 1997, pp. 159-164.

[9] S.Kumar, S.Sinha and N.Kumar "Experimental Investigation of Solar Chimney Assisted Bioclimatic Architecture", Energy Conversion and Management, Vol.39, No.5-6, 1998, pp.441-444.

[10] C. Afonso and A. Oliveira, "Solar Chimneys: Simulation and Experiment, Energy and Buildings", Vol.32, 2000, pp.71-79.

KOH-CATALYST PRODUCTION OF MAXIMUM YIELD BIO-DIESEL FUEL FROM PUNGAMIA OIL

A.Murugesan[1], P.S.S.Srinivasan[2], R.Subramanian[3] and N.Neduzchezhain[4]

[1&2]Department of Mechanical Engineering, K.S.Rangasamy College of Technology, Tiruchengode - 637 215, Namakkal District, Tamil Nadu

[3&4]Department of Automobile Engineering, Institute of Road and Transport Technology, Erode - 638 316, Tamil Nadu

(Received on 19 December 2007 and accepted on 05 January 2008)

Abstract

Bio-diesel is gaining more importance as an alternative fuel due to the depletion of fossil fuel resources. Bio-diesel is a mono alkyl ester of long chain fatty acids derived from renewable feed stock like vegetable oils and animal fats. It is produced by transesterification process in which oil or fat is reacted with mono-hydric alcohol in the presence of catalyst. This process has been widely utilized for bio-diesel fuel production in many number of countries. In India, non-edible oils like pungamia oil, jatropha oil etc., are available in abundance, which can be converted into bio-diesel. In this study bio-diesel has been produced from pungamia (karanji) oil using KOH as catalyst. The experimental work revealed the maximum reaction condition for methanolsis of pungamia oil using KOH as catalyst and methanol as a solvent at a reaction temperature of about 65°C for a period of 70minutes. The yield of methyl ester was 93%. The unit consists of variable speed DC motor used to vary the speed of the stirrer (150 rpm to 800 rpm) and its speed is measured by speed sensor. Thermocouple is used to monitor the temperature of the unit and electric heater is used to heat the oil ranging from 40°C to 250°C. A simple transesterification method is explained and the fuel properties of methyl ester (bio-diesel) are compared with the conventional diesel fuel.

Keywords: *Bio-diesel, Pungamia Oil (Karanji), Transesterification*

1. INTRODUCTION

Self-reliance in energy is vital for overall economic development of our country. The need to search for alternative fuel which is renewable, safe and non-polluting assumes top priority in view of uncertain supplies and frequent price hikes of fossil fuels in the international market. Among the many species, this can yield oil as a source of energy in the form of bio-diesel. Pungamia has been found to be one of the most suitable species due to its various favourable attributes like its hard nature, high oil recovery and quality of oil, etc. It can be planted on degraded lands through joint forest management (JFM), formers field boundaries, and waste lands. Indigenous production of pungamia oil will save foreign exchange of worth several million dollars and also generate employment opportunities in rural areas [1]. Pungamia is one such forest-based tree-borne, non-edible oil with production potential of 135,000 million tones per year [2].

On the other hand, with the increasing demand of the use of fossil fuels, stronger threat to clean environment is being posed as burning of fossil fuels is associated with emission of like CO2, CO, SOX, NOX and particulate matter and are currently the dominant global source of emission [3]. The gases emitted by diesel driven vehicles have an adverse effect on the environment and human health. There is a universal acceptance of the need for reducing such emission [4]. The use of "clean" and renewable fuel such as bio diesel reduces net emissions of CO2 by 78.45% compared to petroleum diesel. In addition, bio-diesel provides modest reduction in total methane emissions compared to petroleum diesel; methane is another, even more potent, green house gas .

Apart from this, the world energy forum has focused on what is going to be the status of fossil fuel based materials like oil, gas and coal in the next 50 to 100 years. It is estimated by international forecasting that the available resources of fossil materials will get exhausted

with in the next 50 to 100 years, since those resources are non-renewable [3]. An attempt has been made in this work for conversion of pungamia oil to fatty acids of methyl ester. The latest studies by Rahemana and Phadatare [2] revealed a maximum yield of methyl ester of 750 ml of pungamia (karanja) methyl ester (bio-diesel) was obtained from one litre of pungamia oil [2]. Hence a study was under taken at our institution to produce a maximum yield of bio-diesel from pungamia oil by transesterification process using KOH as a catalyst.

2. MATERIAL AND METHODS

2.1 Extraction of Oil

The pungamia seeds are available at Tamil Nadu forest department in India and the oil is extracted from the kernel by mechanical expeller, the oil after mechanical extraction is filtered by using muslin cloth with 10 to 15 μm pore size.

2.2 Purification of Oil

The oil extracted from the crusher can be purified by the following methods.

2.2.1 Sedimentation

This is the easiest way to get clear oil, but it takes about a week until the sediment is reduced to 20-25% of the raw oil volume.

2.2.2 Boiling with Water

The purification process can be accelerated by boiling the oil with about 20% of water. The boiling should continue until the water has completely evaporated and bubbles of water vapour disappear. After a few hours, the oil then becomes clear.

3. PROPERTIES OF PUNGAMIA OIL

The fuel properties of pungamia oil (before transterification) compared with diesel are given in Table 1. It is observed from the Table that the viscosity of pungamia oil is around 74.14 centralstroke at 380C. The high viscosity of pungamia oil is due to its large molecular weight in the range of 600 to 900 which is about 20 times higher than that of diesel fuel. The flash point of pungamia oil is very high (i.e, 2000C). The volumetric heating value (calorific value) is 38.94 MJ/kg when compared to diesel fuel (43 MJ/kg). The presence of chemically bound oxygen in pungamia oil lowers its heating value by about 10% [6].

Table 1 Properties of Pungamia Oil and Diesel

PROPERTIES	DIESEL	PUNGAMIA OIL
Cetane No.	42	45
Specific gravity	0.84	0.925
Viscosity (cSt)	4.59	74.14
Calorific value (MJ/kg)	43	38.94
Flash point ^{0}C	50	200
Carbon residue %	86	74.45

Pungamia oil has the following properties that make it a suitable replacement for diesel fuel:

- Cetane number is comparable with diesel fuel.
- Calorific value (heating value) of pungamia oil is about 90% of that of diesel fuel.
- Long chain saturated and unbranched hydrocarbons are especially substitute for conventional diesel fuel. The long unbranched hydrocarbon chains in the fatty acids meet this requirement [6].

4. TRANSESTERIFICATION

Heating and blending of vegetable oil reduces the viscosity but its molecular structure remains unchanged; hence poly unsaturated character and low volatility problem exists. It has been reported that transesterification is an effective process to overcome all problems associated with vegetable oil [7]. Transesterification is the process of bringing the properties of the pungamia oil close to diesel fuel. It refers to conversion of an organic ester into another ester of the same acid by reacting it with methyl or ethyl alcohol to produce methyl or ethyl ester [8]. Purified pungamia oil is of yellow-orange to brown in colour which depends on standing. It has a bitter taste and disagreeable odour and hence not considered as edible. Vegetable oils and animal fats are chemically triglyceride molecules, in which three fatty acid groups are ester bonded to one glycerol molecule. The triglyceride molecules differ by the nature of the alkyl chain bound to glycerol.

Transesterification is the process of reaching a triglyceride such as mixing one of the vegetable oils with alcohol in the presence of a catalyst to produce fatty acid esters and glycerol. In this process, there is a displacement of alcohol part by a monohydric alcohol that yields three alkyl ester from one triglyceride molecule. The molecular weight of typical ester molecules is roughly one-third to that of straight vegetable oil molecules and has a viscosity approximately twice then that of diesel fuel. There is a decrease in viscosity and improvement in fuel properties of product fatty acid, alkyl esters in the process of transesterification

4.1 Transesterification Process

The pungamia oil is blended with alcohol and catalyst mixture. The purified pungamia oil is mixed with methanol and catalyst mixture in the transesterification unit. This solution is continuously stirred for 70 minutes. During the above process, glycerol present in the solution is separated out. After removing glycerol, the liquid bio-diesel is transferred to washing tank where the fuel is washed and purified bio-diesel is obtained.

4.2 Experimental Setup

The transesterification unit used for bio-diesel production is designed and fabricated in the laboratory. It consists of a stainless steel container, which has a capacity of 6 liters. The top of the container is fixed with the variable speed D.C motor attached with mechanical stirrer for the speed range of 150 rpm to 800 rpm. The speed of the stirrer can be easily varied with the help of a speed regulator and is monitored using photo-sensor along with digital speed indicator. The stirrer consists of 8 stainless steel blades each indicated at an angle of 45°.

The bottom of the container is fixed with 1.5 K.W heater for heating the oil. The temperature of oil is controlled in the range of 40° to 250°C using a microprocessor kit. The temperature of the oil was measured using a chromel Alumel (k-type) thermocouple with digital temperature indicator. Total control of the motor speed and temperature of the heater can be controlled by microprocessor based kit as per the requirement. The cooling fan is provided inside the microprocessor kit to recover heat from the transformer and integrated circuits. At the top of the container there is an inlet valve and at the bottom of the container a drain valve is provided.

Methanol (99.8%) and Potassium hydroxide pellets GR grade were procured from MERCK for experimentation.

4.4 Chemistry of Transesterification

Equation.1 gives the overall transesterifaction reaction. However three consecutive and reversible reactions are believed to occur. The chemistry of reactions is represented in Equation.2.

The first step in the conversion is from triglycerides to diglycerides followed by the conversion of diglycerides to monoglycerides and subsequently monoglycerides to glycerol yielding one methyl ester molecule from each glycerides at each step

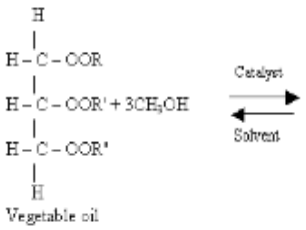

(1)

Triglycerides + ROH Di-glycerides +R1COOR

Di glycerides+ ROH Monoglycerides+R2COOR

Monoglycerides+ ROH Glycerol +R3COOR

4.5 Production of Maximum Yield of Bio-Diesel

Experimental work in the laboratory revealed that the maximum reaction condition for methanolysis of pungamia oil was 17 gms of Potassium Hydrochloride as catalyst, 2400 ml of pungamia oil and 400ml of methanol as a solvent with a reaction temperature of 650C for a period of 70 min and the maximum yield of 2230 ml of methyl ester was obtained as shown in Figure 1.

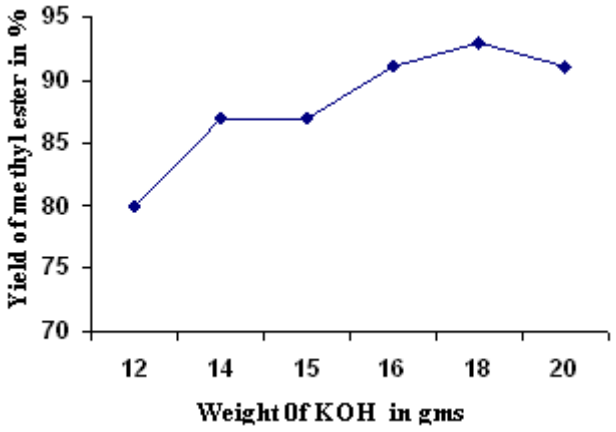

Fig. 1 Maximum yield of bio-diesel production

4.6. Separation of Bio-Diesel

After completion of the reaction, the product is kept for approx. 12 hours for separation of bio-diesel and glycerol layer as shown in figure2.

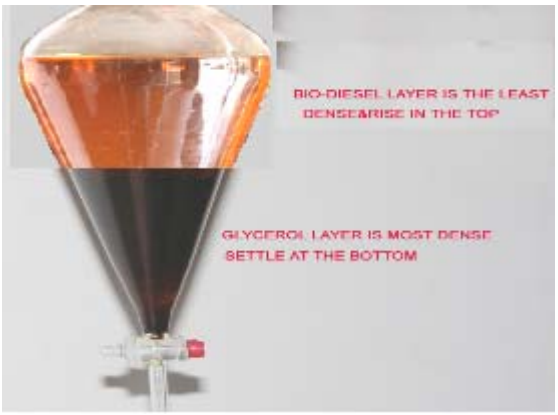

Fig. 2 Separation of glycerol from bio-diesel

Fig. 3 Pure bio-diesel

The mixture of KOH and methanol settles at the bottom of the funnel because of higher density as compare to bio-diesel. Whereas small amount of catalyst, methanol and glycerol are in the upper bio-diesel layer. The upper layer is collected for further purification by washing.

4.7 Properties of Bio-Diesel

If the fuel still appears somewhat cloudy after drying. The drying cycle should be repeated but the likely culprit is probably the presence of non-water soluble contaminants in the fuel (such as mono- and di-glycerine) [9]. The pure bio-diesel is collected and stored in the separating funnel as shown in Figure 3.

Bio-diesel is the generic name for the family of diesel fuel alternatives produced by transesterification of oils from agricultural feed-stock. Vegetable oils themselves form triglycerides, which are esters derived from long chain fatty acids and polyalcohol glycerol. The normal chain length is about 12-22 carbon atom with 0-3 double bond that are responsible for the physico-chemical properties of the oil [8]. The fuel properties of bio-diesel compared with the diesel is shown in the Table 2.

Some of the fatty acids have unsaturated chains also. Fatty acid methyl ester is also called as bio-diesel. Bio-diesel is a all fatty ester and has combustion properties similar to petroleum diesel; however, it is a mixture of complex hydrocarbons with carbon number largely between 12-18 and is obtained by distillation of crude mineral oil.

Table 2 Fuel Properties of Bio-Diesel and Diesel

Properties	Diesel	Bio-diesel (methyl ester)
Cetane No.	42	48
Specific gravity	0.84	0.934
Viscosity cSt	4.59	6.3
Calorific value (MJ/kg)	43	40
Flash point °C	50	80
Carbon residue %	86	83

5. RESULTS AND DISCUSSION

The results of the study based on the maximum yield are shown in Figure 1. Methanolsis of pungamia oil is carried out the KOH as a catalyst at a concentration of 13-19gms. It shows that an increase in the concentration of catalyst from 13-17 gms increases the yield of methyl ester from 87-93%. Further, increasing the concentration of catalyst up to 18gms reduced the yield of methyl ester by 91%. for further increasing of catalyst up to 19gms, the yield of methyl ester is reduced still and soap formation takes place. It clearly shows that an increase in the concentration of catalyst decreases in the yield of methyl ester and leads to the formation of soap in the presence of high amount of catalyst. The quality of oil is expressed in terms of important physical properties such as cetane number, specific gravity, viscosity, calorific value and flash point of the fuel. (Table 2).

6. CONCLUSION

It can be concluded from the present study that the maximum reaction condition for methonolysis of pungamia oil is 17gms of KOH as a catalyst and 400ml of methanol as a solvent at the reaction temperature of 65°C and the rate of mixing is 550rpm for a period of 70 minutes. The yield of methyl ester was 93%.

REFERENCES

[1] www.megcoperation.goe.in

[2] H. Raheman and A.G. Phadatare, "Diesel Engine Emissions and Performance from Blends of Methyle Ester and Diesel", Biomass and Bio-energy, Vol.27, 2004, pp.393 - 397.

[3] W. Raheman *et al,* "Esterifies Oil An Alternate Renewable Fuel for Diesel Engines in Controlling Air Pollution", Bio-Energy News, MNES, India, Vol 7, No 3, March 2003.

[4] K.C. Pant, "Report of The Committee an Development of Bio – Fuels", Planning commission 16 April 2003.

[5] K.S.Nagaprasad *et al*, "Effect of Injection Timming and Injection Pressure on Performance of C.I. Engine using Honge Oil", National Conference on Advances in Mechanical Engineering Sciences, Sri Siddhartha Institute of Technology, Tumkur, Karanataka. Sep. 2004, pp.24-25.

[6] A.K. Babu and G. Devaradjane, "Vegetable Oils and their Derivatives as Fuels for C.I. Engine-An Overview", SAE, 2003.

[7] Deepak Agarwal *et al,* "Technical Note Experimental Investigation of Control of Nox Emission in Bio-diesel Fueled Compression Ignition Engine", Renewable Energy Sources, Vol.31, 2006, pp.2356-2369.

[8] B.S. Murthy, "Bio-diesel and Ethanol", SAE India, Chennai, 11 June 2004.

[9] Rick Pelletier "Research Notes for Bio-Diesel", Revision 3.3, last updated on 31August 2005.

BEHAVIOUR AND ULTIMATE STRENGTH OF REINFORCED CONCRETE BEAMS WITH A CENTRAL TRANSVERSE HOLE

S. Sankaran[1], N. Arunachalam[2] and R. Sundararajan[3]
[1&2]Department of Civil Engineering, Bannari Amman Institute of Technology,
Sathyamangalam - 648 301, Erode District, Tamil Nadu
[3]A.C.College of Engineering & Technology, Karaikudi - 623 004, Tamil Nadu
(Received on 19 January 2008 and accepted on 10 February 2008)

Abstract

Openings in reinforced concrete beams occur quite often in practice to provide a convenient passage for utility ducts. Their accommodation eliminates a significant amount of dead space and results in a more compact and often, more economical design.

In order to study the flexural behaviour and strength of reinforced concrete beams having a central transverse hole of diameter 40mm to 100mm, five beams of dimensions 150mm x 230mm x 3000mm have been cast and tested under gradually increased flexural loading until collapse occurred. The behaviour of the beams have been studied by measuring deflections and drawing the load-deflection curves. The influence of the diameter of the hole on the ultimate flexural strength has been found out and reported in this paper.

Keywords: *Load-Deflection Curves, Reinforced Concrete Beams, Transverse Holes, Ultimate Strength.*

1. INTRODUCTION

In the construction of modern buildings, many pipes and ducts are necessary to accommodate essential services like water supply, sewage, air-conditioning, electricity, telephone and computer network. Usually, these pipes and ducts are placed underneath the soffit of the beam and, for aesthetic reasons, are covered by a suspended ceiling, thus creating a "dead space." An economical solution would be to take up these pipes through holes made perpendicular to the length of these beams.

Inspite of much of research work having been done on reinforced concrete structural elements world wide, no reliable information is available on the strength of such beams.

Hence, an attempt has been made to investigate experimentally the behaviour and strength of reinforced concrete beams having holes perpendicular to their longitudinal axis and subjected to flexural loading.

The programme includes casting and testing of a total of five rectangular beams. Three beams had a single hole of diameter of either 40mm, 80mm or 100mm and two beams were without holes.

Experiments were conducted to determine the ultimate flexural strength and to study the deformation characteristics and flexural rigidity.

2. MATERIALS USED

For the purpose of experimentation, Pozzolona Portland Cement conforming to Indian Standard Specifications was used along with locally available fine aggregate and 20mm coarse aggregate.

3. DETAILS OF THE BEAMS

The cross section of all beams was of 150mm x 230mm (depth). The depth of the compression zone was calculated based on the Whitney's stress block. It was found to be 47.8mm from top. The beam was designed as an under reinforced section with two numbers of 12mm RTS bars as main steel, two numbers of 8mm diameter RTS bars as hanger bars and 6mm diameter M.S bars as two legged vertical stirrups at 200mm c/c spacing.

4. METHOD OF CASTING OF BEAMS

4.1 Preparation of Formwork

Wooden formwork of inner dimensions 150 x 230 x 3000 mm was used. It had a square opening of size 120mm at the middle on both sides of the formwork. The centre of the opening was at 108mm (48+120/2) from the top of the mould (48mm being depth of Whitneys stress block and 120mm being the maximum provision for Dia of Hole). Aluminium plates of size 150mm x 230mm x 1mm thickness with a circular hole of predetermined size and location was used to get the desired hole. All the openings in the plates were concentric so as to provide the same level of opening in the tension zone of the beams. Plates without holes were used for covering the openings in the formwork for getting solid beams.

4.2 Concreting

Nominal mix of 1:1½: 3 has been adopted for the test specimens. The mix ratio and water-cement ratio have been kept the same for all beams. Along with each of the main beams, three cubes of size 150mm, three cylinders of 150mm diameter and 300mm height and three prisms of 100mm square and 500mm length were cast.

The main beams and the auxiliary specimens were cured by providing wet gunny bags for 28 days and air dried for 1 day before testing.

Table1 Details of Beam Specimens

Designation of Beam	Size	Diameter of Hole (mm)	Distance of Centre of Hole from Top (mm)
Beam 1	150 x 230 x 3000 mm	-	-
Beam 2	150 x 230 x 3000 mm	40	108
Beam 3	150 x 230 x 3000 mm	80	108
Beam 4	150 x 230 x 3000 mm	100	108
Beam 5	150 x 230 x 3000 mm	-	-

5. LOADING

Each beam had a simply supported span of 2.70m.The beams were subjected to two point loads each at a distance of 0.975m from the nearest support. Loading was applied by means of 15 Tonnes capacity hydraulic jack. The load applied by the jack was measured using a proving ring of capacity 50 Tonnes. At each increment of about 3.33 kN loading, the following measurements were taken

(a) Deflections at L/4, L/3, L/2, 3L/4.
(b) Strains in the compression and tension fibers
(c) Deflection at 10cm from support

The strains were measured on one face of the beam over a gauge length of 10cm at the centre of the span with a digital demountable strain gauge. The behaviour of the beams was keenly observed from the beginning till collapse. The appearance of initial crack, development and propagation of further cracks due to the increase of load were also recorded. The loading was continued till the collapse of the beams.

Fig.1 Photograph Showing the Test Setup

5.1 Testing of Auxiliary Specimens

The cubes, cylinders and plain concrete prisms were tested according to Indian Standards in the 100T capacity computerized Universal Testing Machine and the test results are tabulated below. The stress – strain characteristics of concrete and steel were obtained from the thus measured readings. The material properties as per the tested steel specimens are as given below

Table 2 Concrete Properties

Material	Average Ultimate Comp.Stress (N/mm2)	Average Split Tensile Strength (N/Mm2)
Concrete	24.20	3.44

Table 3 Steel Properties

Diameter of Secimen (Mm)	Yield Stress (N/Mm^2)	Ultimate Stress (N/Mm^2)
12	375.78	497.59

Table 4 Test Results

Beam	First Crack Load in kN	Ultimate Load in kN
Beam1	34	54.711
Beam2	31	48.044
Beam3	29	41.377
Beam4	23	38.044
Beam5	35	54.711

5.2 Deflection Profile Along the Length of the Beam

Deflected shapes of the beams were obtained by measuring the deflections along the length of the beam at L/4, L/3, L/2 and 3L/4 points at every load increment. The maximum deflection occurred at the mid span of the beams for all load stages. The deflected shapes are plotted for various loads. For comparison of deflected profiles of the beams with various sizes of openings, the deflected profiles of all the beams have been suitably plotted. It is observed from the figures that the beams with larger size of hole were found to deflect more as compared to those having small hole at the same load level. This is due to the decrease in stiffness of beams as the size of hole is increased.

The load-deflection relationships and the deflected shapes of the beams under loads are shown in Figs.2 to 4. These diagrams give a better picture of the behaviour of beams. The deflection of all the beams increased linearly with the applied load P up to the yield point. Beyond that for a very small increment of load, the beam showed large deformation. The load deflection response curves show that a fairly ductile response was obtained with large deflections being achieved in the inelastic region. The experimental values of deflections got for a load of 40.02 kN are given in Table - 5

Table 5 Deflection Profile along the Length of the Beam

Deflections Under a Load of 40.02kN								
Length in mm from left support	0	10	687.5	916.66	1375	2062.5	2740	2750
	Deflections in mm							
Beam1	0	1.95	6.26	7.12	8.12	5.78	1.83	0
Beam2	0	2.21	6.27	8	8.83	5.85	2.33	0
Beam3	0	2.34	7.58	8.71	10	6.75	1.74	0
Beam4	0	3.21	6.27	6.83	7.47	5.57	2.85	0

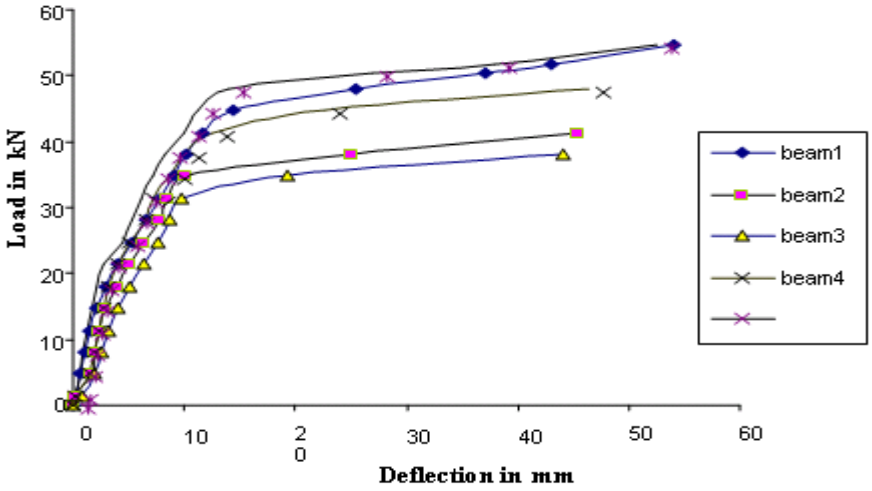

Fig. 2 Load Vs central deflection of all beams at midspan

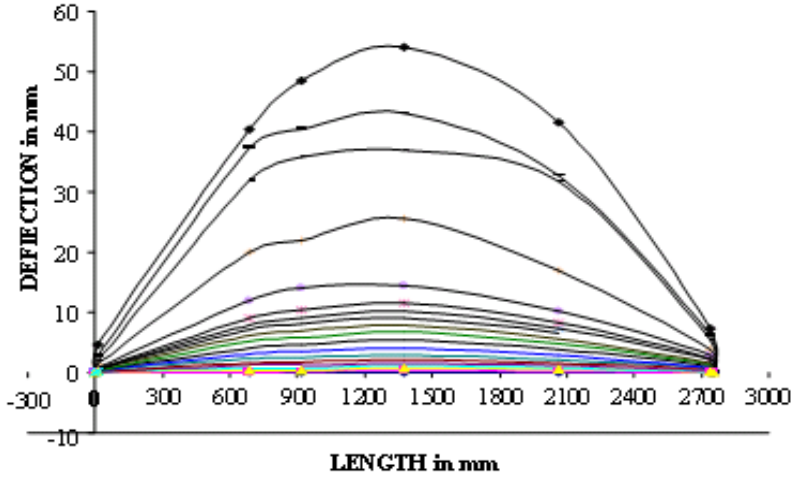

Fig. 3 Deflected shape of beam1 under various loads

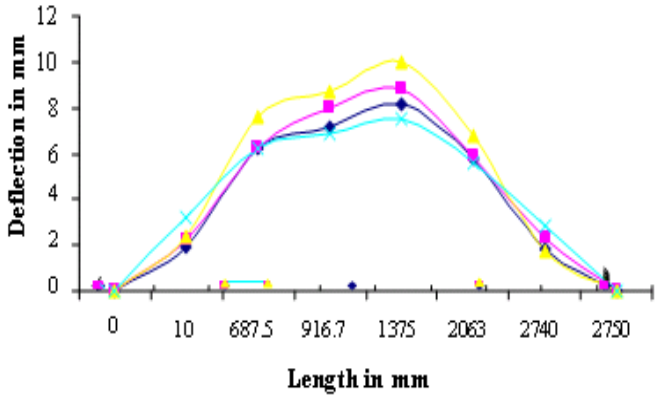

Fig.4 Deflected shape of beams under a load of 40.02kN

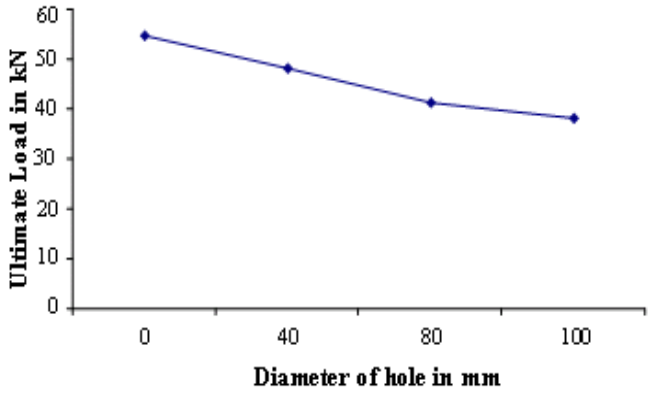

Fig.5 Variation of strength with dia. of hole

6. COMPARISONS AND CONCLUSIONS

The length of inelastic deformation is less for sections with openings.

The cracking load and the ultimate load carrying capacity of the beams with holes decreased as the size of the opening increased. As the diameter of the hole is increased, the Moment of Inertia of the mid-span section is reduced and hence the cracking load decreases. At ultimate load, depth of stress block may be more than the depth upto the top of hole, resulting in the lowering of the point of application of the resultant compressive force. This leads to the reduction in the length of lever arm and hence the ultimate flexural strength.

REFERENCES

[1] M.A.Mansur and Kiang-Hwee Tan, "Concrete Beams with Openings – Analysis and Design", CRC Press, 1999.

[2] I.Purna Chandra Rao, "Experimental Investigation of Flexural Behaviour of Reinforced Concrete Beams with Central Circular Web Openings", M.E. Thesis

[3] C.S.Whitney, "Plastic Theory of R.C. Design", Proceedings, ASCE, Vol.66, No.12, 1940, pp 1749-1780.

[4] Ashok K Jain "Reinforced Concrete Limit State Design", Nemchand & Brothers, 2002

[5] R.Park and T.Pauly, "Reinforced Concrete Structures", John Wiley & Sons, International Edition, 1979.

[6] M.A.Mansur, "Effects of Creating an Opening in Existing Beams"ACI Journal, Vol.96,No.6 November-December 1999.

SHEAR STRENGTH OF HIGH PERFORMANCE CONCRETE CONTAINING HIGH-REACTIVITY METAKAOLIN UNDER DIRECT SHEARING

R. Rathan Raj[1] and E.B.Perumal Pillai[2]

[1]Department of Civil Engineering, Bannari Amman Institute of Technology, Sathyamangalam - 638 401, Erode District , Tamil Nadu.

[2]Department of Civil Engineering, Coimbatore Institute of Technology, Coimbatore - 641 014, Tamil Nadu

Email: r.rathanraj@gmail.com

(Received on 20 November 2007 and accepted on 15 February 2008)

Abstract

High Performance Concrete (HPC) is becoming extremely popular now a days in applications, which require substantial improvements in structural capacity and resistance to aggressive environments. Several researchers have tried different mineral admixtures like Fly Ash (FA), Silica Fume (SF) and Ground Granulated Blast Furnance Slag (GGBS) in producing HPC. These admixtures are generally by-products of other industries and hence their properties are not identical and it is very difficult to assure the quality. This paper proposes a relatively new mineral admixture called High-Reactivity Metakaolin (HRM) with potential for utility in the production of High Performance Concrete.

In the present work, experimental investigation has been carried out to study the performance of High Performance Concrete with varying percentage of replacement of High-Reactivity Metakaolin. This experimental investigation formulates a simplified mix design procedure for HPC by combining Bureau of Indian Standards (BIS) and ACI code methods of mix design and available literatures on HPC. Based on the above mix design procedure M50 and M60 grade HPC mix was arrived and investigations were carried out to study the compressive strength of cube specimens and shear strength of push-off specimens with and without side face reinforcement.

Keywords: *High-Reactivity Metakaolin, High-Performance Concrete, Push-Off Specimen*

1. INTRODUCTION

There has been a phenomenal increase in the development and use of High Performance Concrete (HPC) in the last two decades. Any concrete which satisfies certain criteria proposed to overcome limitations of Conventional Cement Concrete (CCC) may be called High Performance Concrete. Admixtures play an important role in the production of HPC. Developments in mineral and chemical admixtures have made it possible to produce concretes with relatively much higher strengths than was thought possible. Presently concrete with strengths of 90 to 112 MPa are being commercially produced and used in the construction industry in many countries [1]. Several researchers have tried different mineral admixtures such as Fly ash (FA) Pulverized Fuel Ash (PFA), Silica fume (SF), and Ground Granulated Blast Furnance Slag (GGBS) in producing HPC [2-4]. The search is still going on for identifying different mineral admixtures for improving the cementitious properties so that high compressive and flexural strengths can be achieved.

High-Reactivity Metakaolin (HRM) has been recently identified as a new mineral admixture that confirm to ASTM C 618, Class N pozzolan specification. Bureau of Indian Standards have recommended the use of Metakaolin in mortar and concrete as mineral admixture in IS: 456-2000. HRM unique feature is that, it is not the by-product of an industrial process or an entirely natural material; it is derived from a naturally occurring mineral and manufactures specially for cementing applications. HRM is a thermally activated aluminosilicate material obtained by calcining Kaolin clay within the temperature range of 700-8500C [5-7]. It contains typically 50-55% SiO2, 40-45% Al2O3, and is highly reactive. In recent years, there has been an increasing interest in the utilisation of HRM in concrete as partial substitution or

addition of cement. Due to its high pozzolanic activity, the inclusion of HRM greatly improves the mechanical and durability properties of concrete [5-15]. It has been reported that the replacement of cement by 5-15% HRM results in significant increase in compressive strength for high performance concretes and mortars at age of up to 28 days, particularly at early ages [6,11,12]. The replacement also results in improved concrete durability properties, including the resistance to chloride penetration, freezing and thawing, and deicing, salting, scaling [11,14].

While a number of studies have been conducted on HPC incorporating HRM was focused only on determining early age properties, mechanical properties and durability properties. The present study is concerned with the High-Reactivity Metakaolin High Performance Concrete under direct shear. The shear strength of the HPC incorporating HRM is assessed from Push-off specimens with and without side face reinforcement of size 150 mm X 150 mm X 450mm were cast. The results are also compared with those obtained for push-off specimen with side face reinforcement and for push-off specimen without side face reinforcement. The stress distribution of those specimens was analyzed by developing models using Ansys software.

2. MATERIALS AND EXPERIMENTAL DETAILS

2.1 Materials

The materials used in this study were Ordinary Portland Cement (OPC), 53 Grade conforming to BIS: 12269 – 1987 and High-Reactivity Metakaolin (HRM) as mineral admixture in dry densified form conforming to ASTM C 618 class N Pozzolan. The physical and chemical properties of these materials are given in Table 1, where the data for OPC and HRM were provided by the suppliers. Superplasticizer (chemical admixture) based on Sulphonated Naphthalene Formaldehyde condensate – CONPLAST SP 430 conforming to BIS: 9103 – 1999 and ASTM C-494, which had a solids content of 40%, was used to produce an appropriate paste consistency. Locally available quarried and crushed granite stones confirming to graded aggregate of nominal size 12.5 mm (Table 2) as per BIS: 383 – 1970 with specific gravity of 2.82 and fineness modulus of 6.73 as Coarse aggregates (CA) and Karur river sand conforming to Grading zone II of BIS: 383-1970 with specific gravity of 2.60 and fineness modulus of 2.96 as fine aggregates (FA) was used (Table 4).

Table 1 Chemical and Physical Properties of OPC and HRM

Parameters	Cement	HRM
SiO_2 (%)	21.80	52.30
Al_2O_3 (%)	4.80	44.90
Fe_2O_3 (%)	3.80	0.40
CaO (%)	63.30	0.50
MgO (%)	0.90	0.20
NA_2O (%)	0.21	0.12
K_2O (%)	0.46	0.02
TiO_2 (%)	-	0.51
SO_3	2.20	-
Insoluble residue	0.40	-
Loss of ignition (%)	2.00	0.80
Specific gravity	3.15	2.54
Specific surface (m^2/gm)	0.32	17

2.2 Mix Proportions

Concrete mix design is a process by which the proportions of the various raw materials of concrete are determined with an aim to achieve a certain minimum strength and durability, as economically as possible. The main difference between mix design of HPC and CCC is that the emphasis is laid on performance aspect besides strength. At present, no standard mix design procedure is available for the mix proportioning of HPC. The present study is also concerned, to formulate a simplified mix design procedure for HPC using HRM and Superplasticizer as a mineral and chemical admixture. Based on the simplified mix design procedure, a HPC mixture proportions with a characteristic target mean compressive strength of 50 MPa and 60 MPa was designed without any mineral admixtures. However, the use of several trial mixtures is important in the design of HPC. Therefore, to get the optimum proportions, trial mixes were arrived by replacing 0, 2, 4, 6, 8, 10, 12 and 14 percent of the mass of cement by HRM respectively. A total of 8 trial mixes of combinations were arrived. In all the above 8 combinations, a superplasticizer by name CONPLAST SP430 was used at 3% by weight of the binder for obtaining workable concrete. The quantities of different material requirement per m3 of concrete for the 8 trial mixes are given in Table 2 and Table 3.

2.3 Sample Preparation

The concrete mixture prepared in this study included M50 and M60 grade HPC with HRM contents of 2% to 14% by replacement of cement and a control HPC without HRM content. The water/binder ratio for all M50 and M60 grade concrete was 0.360 and 0.328. The concrete were mixed in a mechanical mixer. Small amounts of Superplasticizer (3% by weight of binder) were added to achieve an adequate consistency. Cube specimens of 150mm x 150mm x 150mm in dimension were cast in cast-iron steel moulds. The inside of the moulds were applied with oil to facilitate the easy removal of specimens. Cube specimens were removed from the moulds after one day and were then cured in water at 27^0C. The shear strength of concrete is determined by fabricating a new type of specimen called push-off specimen of size 150 x 150 x 450 mm, which was suggested by American Concrete Institute material Journal [16]. The push-off specimens were cast in steel moulds with and without side face reinforcement. They were removed from the moulds after one day and were then cured in water at 270C. The geometry and dimensions of the push-off specimen units with and without side face reinforcement were given in figures 1 & 2.

Fig.1 Push-off speciman without side face reinforcement

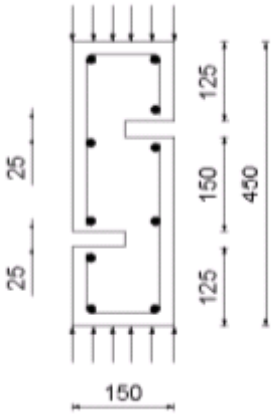

Fig.2 Push-off speciman without side face reinforcement

Table 2 Details of HPC Trial Mixes for M_{50} Grade

Mix	HRM (%)	W/B ratio	Cement (kg)	HRM (kg)	FA (kg)	CA (kg)	Super-plasticizer (lit)	Water (lit)
MK_0	0	0.36	402.78	0	923.82	995.15	8.26	143.80
MK_2	2	0.36	394.72	8.06	922.09	995.15	8.26	143.80
MK_4	4	0.36	386.87	16.11	920.19	995.15	8.26	143.80
MK_6	6	0.36	378.61	24.17	918.63	995.15	8.26	143.80
MK_8	8	0.36	370.56	32.22	916.90	995.15	8.26	143.80
MK_{10}	10	0.36	362.50	40.28	915.17	995.15	8.26	143.80
MK_{12}	12	0.36	354.45	48.33	913.44	995.15	8.26	143.80
MK_{14}	14	0.36	346.39	56.39	911.71	995.15	8.26	143.80

Table 3 Details of HPC Trial Mixes for M_{60} Grade

Mix	HRM (%)	W/B ratio	Cement (kg)	HRM (kg)	FA (kg)	CA (kg)	Super plasticizer (lit)	Water (lit)
MK_0	0	0.328	442.07	0	844.72	1044.91	9.06	143.22
MK_2	2	0.328	433.23	8.84	842.82	1044.91	9.06	143.22
MK_4	4	0.328	424.39	17.68	840.93	1044.91	9.06	143.22
MK_6	6	0.328	415.55	26.52	839.03	1044.91	9.06	143.22
MK_8	8	0.328	406.70	35.37	837.13	1044.91	9.06	143.22
MK_{10}	10	0.328	397.86	44.21	835.23	1044.91	9.06	143.22
MK_{12}	12	0.328	389.02	53.05	833.33	1044.91	9.06	143.22
MK_{14}	14	0.328	380.18	61.89	831.44	1044.91	9.06	143.22

2.4 Compression Test and Direct Shear Test

The compressive strength of M50 and M60 grade HPC cubes with 0-14% replacement of cement by HRM were determined at the age of 1, 7, 14, 28, and 56 days. All the cubes were tested in saturated condition, after wiping out the surface moisture. For each trial mix combination, three cubes were tested at different age of curing. The tests were carried out at a uniform stress after the specimen has been centered in the testing machine. The ultimate load divided by the cross sectional area of the specimen is equal to the ultimate cube compressive strength.

The shear strength of M50 and M60 grade HPC push-off specimens with and without side face reinforcement with 0-4% replacement of cement by HRM were determined at the age of 28 days curing using 100 ton capacity Universal Telling Machine. The tests were carried out for adopting same procedure of compression test.

The specimen was designed to fail in shear at a known plane. The shear strength is equal to the ultimate shear load divided by the area of shear plane.

3. RESULTS AND DISCUSSION

3.1 Compressive Strength

The results of the average cube compressive strength at the age of 1, 7, 14, 28, and 56 days tests are shown in Table 4, where each value is the average of three measurements. It can be seen that the HPC containing 2-14% HRM had higher compressive strengths than the control at all tested age hanging from 1 to 56 days, with the HPC containing 8% HRM performing the best. This is due to the fact that the higher compressive strength of concrete is due to the pozzolanic reaction and filler effects of HRM. This observation is similar to those observed by Curcio *et al.* [12] for mortars with a w/b ratio of 0.33, Zhang and Malhotra [14] for concrete with a w/b ratio of 0.4 and by Poon *et al*. [15] for cement pastes and mortars with a w/b ratio of 0.3.

Table 4 Cube Compressive Strength of HPC Trial Mixes for M_{50} & M_{60} Grade

Mix	HRM %	1 Day		7 Day		14 Day		28 Day		56 Day	
		M_{50}	M_{60}	M_{50}	M_{60}	M_{50}	M_{60}	M_{50}	M_{60}	M_{50}	M_{60}
MK_0	0	28.40	35.50	32.40	48.60	39.54	55.78	52.04	60.74	57.32	66.49
MK_2	2	31.28	37.00	39.29	50.56	44.20	57.24	54.59	61.47	59.98	68.20
MK_4	4	33.46	39.40	42.78	54.78	46.62	59.92	59.26	66.27	64.74	71.77
MK_6	6	36.78	44.75	47.36	56.14	49.48	62.35	63.04	72.64	67.37	79.44
MK_8	8	37.42	47.65	49.96	58.40	52.63	64.24	65.32	75.52	68.42	81.12
MK_4	10	36.78	46.80	48.40	57.88	51.20	63.72	64.48	74.99	67.30	80.59
MK_{12}	12	33.55	40.28	43.86	54.46	49.83	54.32	62.90	70.36	65.47	76.56
MK_{14}	14	31.20	38.56	38.58	52.27	47.44	62.46	57.85	66.80	62.28	72.20

3.2 Shear Strength

The results of shear strength of HPC push-off specimen with and with out side face reinforcement under direct shear at the age of 28 days are shown in table 5. From the test results, it can be observed that the maximum shear strength of HPC push-off specimen with and without side face reinforcement is obtained for mixes with 8% replacement of cement by HRM. The shear strength of concrete increases with increase in HRM content up to 8% and thereafter, it gradually decreases. It is seen that the strength of concrete in compression and strength of concrete in shear are closely related and the ratio of the two strengths depends on the general level of strength of concrete. In other words, for higher compressive strength shows higher shear strength, but the rate of increase of shear strength is less. It is also observed that shear strength of push-off specimens without side face reinforcement is higher than those specimens with side face reinforcement. This is due to the fact that the developments of horizontal shear in the specimens without side face reinforcement.

Table 5 Shear Strength of HPC Trial Mixes for M_{50} & M_{60} Grade

Mix	HRM %	Average Shear Strength in MPA (28 days)			
		Without side face reinforcement		With side face reinforcement	
		M_{50}	M_{60}	M_{50}	M_{60}
MK_0	0	2.86	3.54	2.38	3.02
MK_2	2	2.98	3.72	2.49	3.24
MK_4	4	3.07	4.02	2.62	3.45
MK_6	6	3.16	4.12	2.78	3.62
MK_8	8	3.26	4.25	2.92	3.88
MK_{10}	10	3.23	4.20	2.90	3.79
MK_{12}	12	3.17	3.93	2.76	3.54
MK_{14}	14	3.06	3.73	2.63	3.47

4. CONCLUSIONS

The aim of this paper is to assess the progress of the shear strength on high performance concrete with varying percentage of replacement of HRM. A series of tests on the compressive strength and shear strength of high performance concrete with varying percentage of replacement of HRM has been carried out. Comparisons have been made with the results obtained from HPC with varying replacement of HRM and controlled HPC (Nil replacement of HRM), and with those obtained by other researchers with different w/b ratios. Also, comparisons have been made for shear strength on HPC with side face reinforcement and without side face reinforcement for all replacement levels. Based on the results and discussions, the following conclusions are drawn.

- Due to its high pozzolanic reactivity, HRM resulted in a higher rate of compressive strength development for the high performance concrete when compared with controlled concrete (Nil replacement of HRM).
- Increasing level of HRM in HPC produce increased resistance to cracking.
- The failure in shear was observed at a known shear plane.
- The shear capacity of concrete depends on adhesive strength of hydration cement paste-aggregate transition zone, cement-aggregate interaction along the cracked surface.
- That the strength of concrete in compression and strength of concrete in shear are closely related and the ratio of the two strengths depends on the general level of strength of concrete. In other words, higher compressive strength shows higher shear strength, but the rate of increase of shear strength is less for HPC.

REFERENCES

[1] S.P. Shah and S.H.Ahmad, "High Performance Concrete and Applications", Edward Arnold, London, 1994.

[2] P. Zia, M.L. Leming, S.H. Ahmad, J.J. Schemmel, R.P. Elliot and A.E. Naaman, "Mechanical Behaviour of High Performance Concretes", Strategic Highway Research Program, National Research Council, Washington, D.C., Vol.1, 1993, pp.98.

[3] P. Zia, M.L. Leming, S.H. Ahmad, J.J. Schemmel, and R.P. Elliot, "Mechanical Behaviour of High Performance Concretes", Strategic Highway Research Program, National Research Council, Washington, D.C., Vol.2, 1993, pp.92.

[4] P. Zia, M.L. Leming, S.H. Ahmad, J.J. Schemmel, and R.P. Elliot, "Mechanical Behaviour of High Performance Concretes", Strategic Highway Research Program, National Research Council, Washington, D.C., Vol.3, 1993, pp.116.

[5] J.A.Kostuch, V.Walters and T.R.Jones, "High Performance Concretes Incorporating Metakaolin: A Review", R.K. Dhir, M.R. Jones (Eds.), Concrete 2000, E&FN Spon, London, UK, 1993, pp.1799-1811.

[6] B.B.Sabir, "High Strength Condensed Silica Fume Concrete", Magazine of Concrete Research, Vol.47, No. 172, Sep. 1995, pp.219-226.

[7] J. Ambroise, S.Maximillen and J.Pera "Properties of Metakaolin Blended Cements" Adv. Cem. Based Mater. Vol.1, No.4, 1994, pp.161-168.

[8] DD. Vu *et al,* "Strength and Durability Aspects of Calcined Kaolin-Blended Portland Cement Mortar and Concrete" Cement & Concrete Composites, Vol.23, 2001, pp. 471- 478.

[9] J. Bai, S.Wild and B.B.Sabir, "Workability of Concrete Incorporating Pulverized Fuel Ash and Metakaolin", Magazine of Concrete Research, Vol.51, No.3, 1999, pp.207-216.

[10] J.J.Brooks, M.A.M. Johari and M. Mazloom, "Effects of Admixtures on the Setting Time of High Strength Concrete", Cement and Concrete Composites, Vol. 22, No.1, 1994, pp. 293-301.

[11]M.A. Caldarone, K.A. Gruber and R.G. Burg, "High Reactivity Metakaolin (Hrm): A New Generation Admixture for High Performance Concrete", Concrete International, Vol.16, No.11, 1994, pp.37-40.

[12] F.Curcio, B.A.Deangelis and S. Pagliolico, "Metakaolin as Pozzolanic Micro Filler for High Performance Mortars", Cement and Concrete Research, Vol.28, No.6, 1998, pp.800-809.

[13]J.T. Ding and Z.J. Li, "Effects of Metakaolin and Silica Fume in Properties of Concrete", ACI Materials Journal Vol.99,No.4, 2002, pp.393-398.

[14]M.H.Zhang and V.M.Malhotra, "Characteristics of a Thermally Activated Aluminosilicate Pozzolanic Material and its use in Concrete", Cem. Concr. Res., Vol.25, No.8, 1995, pp.1713-1725.

[15]C.S.Poon, L. Lam, S.C.Kou, Y. L.Wong and Ron Wong "Rate of Pozzolanic Reaction of Metakaolin in High Performance Cement Pastes" Cem. and Con. Res., Vol.31, 2001, pp.1301-1306.

[16]American Concrete Instoitute Material Journal ACI, Vol.94 No.6, pp.592-601.

[17] R. Rathan Raj and E.B. Perumal Pillai, "A Partial Replacement of Cement with High-Reactivity Metakaolin in High Performance Concrete - An Experimental Investigation", Proceedings of the International Conference on Recent Developments in Structural Engineering – RDSE-2007, Manipal Institute of Technology, Manipal, India, August 30-31 & September 01, 2007, pp.834-845.

[18] R. Rathan Raj, "Experimental Investigation on Mechanical and Durability Characteristics of M110 Grade High Performance Concrete Using Silica Fume And Superplasticizer" Proceedings of the National Conference on Recent Advances in Structural Engineering, JNTU College of Engineering, Kakinada, 11-12 Feb, 2006, pp 224-229.

FINITE ELEMENT FORMULATION OF MULTILAYERED AXI-SYMMETRIC DEGENERATED SHELL ELEMENT

J. Raja Murugadoss[1], M. G. Rajendran[2] and S. Justin[3]
[1]Department of Civil Engineering, Bannari Amman Institute of Technology,
Sathyamangalam - 638 401, Erode District, Tamil Nadu
[2&3]Department Civil Engineering, Karunya Institute of Technology and Sciences (DU),
Coimbatore - 641 114, Tamil Nadu
Email: rajamurugadoss@gmail.com
(Received on 30 October 2006 and accepted on 22 February 2008)

Abstract

In the present work Finite Element (FE) formulation for the free vibration analysis of laminated composite shells using Multi-layered Axi-symmetric Degenerated Shell Element (M-ADSE) is derived by extending the concept of degeneration. The results in terms of fundamental frequency are compared with those literature and are found to be in good agreement, confirming the accuracy of the FE model.

Keywords: *Composites, Free Vibration Analysis, Multi-Layered Kegenerated Shell Element*

1. INTRODUCTION

For the past few decades, the introduction of lightweight composite materials has boosted the construction of weight sensitive structures in various industrial applications such as vehicles ranging from boats to aircraft. It is mainly due to the high strength/weight and stiffness/weight properties of composite materials. Light weight composite structures when subjected to loads or displacements, behave dynamically necessitating accurate design standards for dynamic analysis. Very often the dynamic response of these weight sensitive structures becomes critical and alters the stiffness and mass of the structural system due to the designers' choice in material properties, boundary conditions and other geometric parameters. Therefore, a thorough knowledge is much essential in tailoring the directional dependent properties of composites to achieve the expected strength and stiffness.

In the present work, laminated composite shells have been modeled by FE approach using multi-layered axi-symmetric degenerated shell element by extending the concept of degeneration of Ahmed *et al* [1]. Numerical integration is carried out in a different fashion using gauss quadrature to evaluate the element stiffness matrix in such a way that the integral limits vary from -1 to +1 for each layer of the laminate. The mass matrix is computed using lumped mass system. The accuracy of the FE approach is verified by comparing the fundamental frequency of isotropic and orthotropic cylindrical shells with those reportal else where [2.3].

2. CONCEPT OF DEGENERATION

The concept of degeneration can be explained by forming a beam element (line element) from a plane element (i.e. 2 Delement) as shown in Fig. 1.

$$\left.\begin{aligned} u_1^* &= u_1 + \frac{t.\theta_1}{2} \quad u_3^* = u_2 - \frac{t.\theta_2}{2} \\ u_2^* &= u_2 + \frac{t.\theta_2}{2} \quad u_4^* = u_1 - \frac{t.\theta_1}{2} \end{aligned}\right\} \quad (1)$$

where, u_1^*, u_2^*, u_3^* and u_4^* are the corner-node displacements of the real element; u1 and u2 are the horizontal nodal displacements of the degenerated beam element; similarly v_1^*, v_2^*, v_3^*, v_4^*, and v1, v2 are the corner-node and mid-node vertical displacements respectively. Here and = v1 and and= v2. θ1 and θ2 are the rotational component, 'L' is the length of the element and 't' is the thickness of the element.
Therefore each node has three degrees of freedom with two translations and one rotational component and therefore Equation. 1 can be rewritten as:

$$\begin{bmatrix} u_1^* \\ u_2^* \\ u_3^* \\ u_4^* \\ v_1^* \\ v_2^* \\ v_3^* \\ v_4^* \end{bmatrix} = \begin{bmatrix} 1 & 0 & \frac{t}{2} & 0 & 0 & 0 \\ 0 & 0 & 0 & 1 & 0 & \frac{t}{2} \\ 0 & 0 & 0 & 1 & 0 & -\frac{t}{2} \\ 1 & 0 & -\frac{t}{2} & 0 & 0 & 0 \\ 0 & 1 & 0 & 0 & 0 & 0 \\ 0 & 0 & 0 & 0 & 1 & 0 \\ 0 & 0 & 0 & 0 & 1 & 0 \\ 0 & 1 & 0 & 0 & 0 & 0 \end{bmatrix} \begin{bmatrix} u_1 \\ v_1 \\ \theta_1 \\ u_2 \\ v_2 \\ \theta_2 \end{bmatrix}$$

3. CO-ORDINATE SYSTEM FOR AN AXI-SYMMETRIC SHELL ELEMENT

A system of curvilinear co-ordinates 'ξ' and 'η' defined inside the axi-symmetric shell element with typical top and bottom nodes is shown in Fig. 2. The normal direction 'ξ', as defined by such points is only approximately normal to the mid-surface. However, it is in this direction 'ξ' that the linearity constraint is imposed. The co-ordinates 'r' and 'z' at any point within the element are linked to the nodal coordinates using the curvilinear coordinates by Equation. 3

$$\begin{Bmatrix} r \\ z \end{Bmatrix} = \sum N_i \frac{(1+\xi)}{2} \begin{bmatrix} r_i \\ z_i \end{bmatrix}_{top} + \sum Ni \frac{(1-\xi)}{2} \begin{bmatrix} r_i \\ z_i \end{bmatrix}_{bot}$$

where, 'Ni' is the shape function. The element extends from ξ = -1 to ξ = +1 and η = -1 to η = +1 in the usual manner; $\begin{bmatrix} r_i \\ z_i \end{bmatrix}_{top}$, $\begin{bmatrix} r_i \\ z_i \end{bmatrix}_{bot}$ are the co-ordinates in 'r' and 'z' direction of ith node at top and bottom of surface of the axi-symmetric shell element respectively. Equation.3 can be rewritten in terms of mid surface co-ordinates and angle of the normal 'ϕ_i' and the scalar length of the normal or the thickness of the element (t_i) at i^{th} node as given below:

$$\left.\begin{aligned} &-\sum N_i \left[\frac{1}{2}\begin{bmatrix} r_i \\ z_i \end{bmatrix} + \frac{\xi}{2}\begin{bmatrix} r_i \\ z_i \end{bmatrix}\right]_{top} + \sum N_i \left[\frac{1}{2}\begin{bmatrix} r_i \\ z_i \end{bmatrix} - \frac{\xi}{2}\begin{bmatrix} r_i \\ z_i \end{bmatrix}\right]_{bot} \\ &= \sum N_i \left[\frac{1}{2}\begin{bmatrix} r_i \\ z_i \end{bmatrix}_{top} + \frac{1}{2}\begin{bmatrix} r_i \\ z_i \end{bmatrix}\right]_{bot} + \sum N_i \left[\frac{\xi}{2}\begin{bmatrix} r_i \\ z_i \end{bmatrix}_{top} - \begin{bmatrix} r_i \\ z_i \end{bmatrix}_{bot}\right] \end{aligned}\right\} \quad (4a)$$

$$= \sum N_i \begin{bmatrix} r_i \\ z_i \end{bmatrix}_{mid} + \sum N_i \frac{\xi t_i}{2} \begin{bmatrix} \cos\varphi_i \\ \sin\varphi_i \end{bmatrix} \quad (4b)$$

$$\begin{Bmatrix} r \\ z \end{Bmatrix} = \begin{bmatrix} N_1 N_2 N_3 N_4 & 0 & 0 & 0 & 0 & N_5\cos\varphi_1 & N_6\cos\varphi_2 & N_7\cos\varphi_3 & N_8\cos\varphi_4 \\ 0 & 0 & 0 & 0 & N_1 N_2 N_3 N_4 & N_5\sin\varphi_1 & N_6\sin\varphi_2 & N_7\sin\varphi_3 & N_8\sin\varphi_4 \end{bmatrix} \begin{bmatrix} r_1 \\ r_2 \\ r_3 \\ r_4 \\ z_1 \\ z_2 \\ z_3 \\ z_4 \\ 1 \\ 1 \\ 1 \\ 1 \end{bmatrix}$$

where, $\begin{bmatrix} N_5 \\ N_6 \\ N_7 \\ N_8 \end{bmatrix} = \begin{bmatrix} N_1 \xi t_1/2 \\ N_2 \xi t_2/2 \\ N_3 \xi t_3/2 \\ N_4 \xi t_4/2 \end{bmatrix}$ and $\begin{bmatrix} r \\ z \end{bmatrix} = [N] \begin{bmatrix} \bar{r} \\ \bar{z} \\ 1 \end{bmatrix}$

4. DISPLACEMENT PATTERN UNDER AXI-SYMMETRIC LOADING

The general displacement 'u' and 'v' are defined by the displacement of mid surface nodes in the 'r' and 'z' directions respectively and the rotation of the normal at such nodes u_i, v_i, α_i as in Fig. 3. The general displacement is based on the assumption that the normal are straight and non-extensible.

$$\begin{bmatrix} u \\ v \end{bmatrix} = \sum N_i \begin{bmatrix} u_i \\ v_i \end{bmatrix} + \sum Ni \frac{\xi t_i}{2} \begin{bmatrix} -\sin\varphi_i \\ \cos\varphi_i \end{bmatrix} \alpha_i \qquad (7)$$

where, 'α_i' is the angle of rotation of the normal.

$$\begin{bmatrix} u \\ v \end{bmatrix} = \begin{bmatrix} N_1 N_2 N_3 N_4 & 0 & 0 & 0 & 0 & -N_5\sin\varphi_1 & -N_6\sin\varphi_2 & -N_7\sin\varphi_3 & -N_8\sin\varphi_4 \\ 0 & 0 & 0 & 0 & N_1 N_2 N_3 N_4 & N_5\cos\varphi_1 & N_6\cos\varphi_2 & N_7\cos\varphi_3 & N_8\cos\varphi_4 \end{bmatrix} \begin{bmatrix} u_1 \\ u_2 \\ u_3 \\ u_4 \\ v_1 \\ v_2 \\ v_3 \\ v_4 \\ \alpha_1 \\ \alpha_2 \\ \alpha_3 \\ \alpha_4 \end{bmatrix}$$

5.EVALUATION OF ELEMENT CHARACTERISTICS

The element characteristics such as stiffness matrix can be determined in the usual manner. The stiffness matrix is defined as given below:

$$[K]=\int[B]^T[C][B]d[vol] \quad (9)$$

where, [B] = strain displacement matrix; [C] = constitutive matrix; [K] = stiffness matrix. [B] relates the local strains [ε] to the nodal displacements and therefore

$$[\varepsilon] = [B][\delta]$$

Now, consider local orthogonal co-ordinates z1 parallel to a surface. The ξ = constant with in the shell and r^1 created truly normal to this, with the corresponding displacement components v^1 and u^1. Neglecting the strain normal to the mid surface in accordance with the shell assumptions and writing hoop strain directly in global coordinates, the strain in these local co-ordinates are given by

$$(\varepsilon)=\begin{bmatrix}\varepsilon_{z'}\\ \varepsilon_{\theta}'\\ \gamma_{r'z'}\end{bmatrix}=\begin{bmatrix}\dfrac{\partial v'}{\partial z'}\\ \dfrac{u}{r}\\ \dfrac{\partial u'}{\partial z'}+\dfrac{\partial v'}{\partial r'}\end{bmatrix} \quad (10)$$

It is necessary to write these strains in terms of nodal displacements and local co-ordinates 'ξ', 'η'. The second term of Equation. 10 can be obtained from Equations. 5 and 8. Transformations are required for obtaining other two terms, which are given below. Initially the r, z derivatives of u, v are derived from their 'ξ'and 'η' derivatives. This process is well known as

$$\begin{bmatrix}\dfrac{\partial v}{\partial z} & \dfrac{\partial u}{\partial z}\\ \dfrac{\partial v}{\partial r} & \dfrac{\partial u}{\partial r}\end{bmatrix} = [J]^{-1}\begin{bmatrix}\dfrac{\partial v}{\partial \xi} & \dfrac{\partial u}{\partial \xi}\\ \dfrac{\partial v}{\partial \eta} & \dfrac{\partial u}{\partial \eta}\end{bmatrix} \quad (11)$$

where, [J] is the Jacobian matrix which can be defined as

$$[J]=\begin{bmatrix}\dfrac{\partial z}{\partial \xi} & \dfrac{\partial r}{\partial \xi}\\ \dfrac{\partial z}{\partial \eta} & \dfrac{\partial r}{\partial \eta}\end{bmatrix} \quad (12)$$

Transforming to local orthogonal coordinates it can be rewritten as

$$\begin{bmatrix}\dfrac{\partial v^1}{\partial z^1} & \dfrac{\partial u^1}{\partial z^1}\\ \dfrac{\partial v^1}{\partial r^1} & \dfrac{\partial u^1}{\partial r^1}\end{bmatrix}=[\theta]^T\begin{bmatrix}\dfrac{\partial v}{\partial z} & \dfrac{\partial u}{\partial z}\\ \dfrac{\partial v}{\partial r} & \dfrac{\partial u}{\partial r}\end{bmatrix}[\theta] \quad (13)$$

where, [è] is the matrix of direction cosines of the 'z1' and 'r1' axes as shown in Fig. 4 and therefore 'θ' can be defined as

$$\theta=\frac{1}{\sqrt{\left(\dfrac{dr}{d\eta}\right)^2+\left(\dfrac{dz}{d\eta}\right)^2}}\begin{bmatrix}\dfrac{dz}{d\eta} & -\dfrac{dr}{d\eta}\\ \dfrac{dr}{d\eta} & \dfrac{dz}{d\eta}\end{bmatrix} \quad (14)$$

In the Equation.13, all the derivatives are obtained numerically from Equation.10. The [B1] matrix, which defines the local strains in terms of the nodal displacement, now be evaluated at any point with the element.

$$[\varepsilon'] = [B']\begin{bmatrix}u_1\\ v_1\\ \alpha_1\\ \vdots\\ u_i\\ v_i\\ \alpha_i\end{bmatrix} = [B']^e \quad (15)$$

The corresponding constitutive matrix [C] for an isotropic material is now easily written as

$$[C]=\frac{E}{(1-\upsilon^2)}\begin{pmatrix}1 & 0 & 0\\ 1 & 0 & 0\\ 0 & 0 & \dfrac{1-\upsilon}{2k}\end{pmatrix} \quad (16)$$

where, 'E' and 'ð' are the elastic modulus and Poisson's ratio respectively. The factor 'k' is included to account for more accurate shear strain energy. As the displacements vary linearly across the thickness of the shell, the shear stresses are sensibly constant. However they are known to be approximately parabolic, and the factor k = 1.2 is included to improve the representation. Finally the volume integration for an annular element is defined as,

$$d\,(volume) = 2\pi\, r\,(|J|\,.\,d\eta\,.\,d\xi) \quad (17)$$

The actual integration is numerically carried out within the limits of ±1 using several gauss points, two gauss points are required in the thickness direction (ξ- direction) and 3 to 4 in the η direction, depending upon whether the element is parabolic or cubic. The transformation of axi-symmetric pressure loading to consistent nodal loads may be carried out to arrive at the load vector [F].

6. EXTENSION TO LAYERED SHELL ELEMENT

6.1 Constitutive Matrix for Layered Shell Element

A laminate is an integral structural element that is bonded together with two or more fiber reinforced composite laminate such as Boron/Epoxy, Carbon/Epoxy, Glass/Epoxy, etc. The principal material directions of a lamina can be tailored to achieve the required stiffness and strength. With reference to the middle plane of the laminate, the stacking sequence of the laminae is classified as symmetric or anti-symmetric. During the analysis, the constitutive matrices of composite materials at element integration points must be calculated before the stiffness matrices are assembled from element level to global level. For fiber reinforced composite laminated materials, each lamina can be considered as an orthotropic layer as shown in Fig. 5. The stress strain relation for a lamina in the material co-ordinate (1, 2, 3) at an element integration point can be written as

$$\{\bar{\sigma}\} = [\bar{Q}]\{\bar{\varepsilon}\} \qquad (18)$$

$$\begin{Bmatrix} \sigma_1 \\ \sigma_2 \\ \tau_{12} \\ \tau_{13} \\ \tau_{23} \end{Bmatrix} = \begin{bmatrix} \frac{E_{11}}{1-\upsilon_{12}\upsilon_{21}} & \frac{\upsilon_{12}E_{22}}{1-\upsilon_{12}\upsilon_{21}} & 0 & 0 & 0 \\ \frac{\upsilon_{21}E_{11}}{1-\upsilon_{12}\upsilon_{21}} & \frac{E_{22}}{1-\upsilon_{12}\upsilon_{21}} & 0 & 0 & 0 \\ 0 & 0 & G_{12} & 0 & 0 \\ 0 & 0 & 0 & s_f G_{13} & 0 \\ 0 & 0 & 0 & 0 & s_f G_{23} \end{bmatrix} \begin{Bmatrix} \varepsilon_1 \\ \varepsilon_2 \\ \gamma_{12} \\ \gamma_{13} \\ \gamma_{23} \end{Bmatrix} \qquad (19)$$

where, 's_f' is the shear correction factor (5/6) to account for the shear being parabolic and $E_{11}, E_{22}, G_{12}, G_{13}, G_{23}, \upsilon_{12}, \upsilon_{21}$ are the elastic constants. The constitutive equation for the lamina in the element co-ordinate (z', θ', r') becomes

(20)

(21)

$$[T] = \begin{bmatrix} \cos^2\theta & \sin^2\theta & \sin\theta\cos\theta & 0 & 0 \\ \sin^2\theta & \cos^2\theta & -\sin\theta\cos\theta & 0 & 0 \\ -2\sin\theta\cos\theta & 2\sin\theta\cos\theta & \cos^2\theta - \sin^2\theta & 0 & 0 \\ 0 & 0 & 0 & \cos\theta & \sin\theta \\ 0 & 0 & 0 & -\sin\theta & \cos\theta \end{bmatrix} \qquad (22)$$

where, $\{\sigma'\} = \langle \sigma_{z'}, \sigma_{\theta'}, \tau_{z'\theta'}, \tau_{z'r'}, \tau_{\theta'r'} \rangle$ and

$\{\varepsilon'\} = \langle \varepsilon_{z'}, \varepsilon_{\theta'}, \gamma_{z'\theta'}, \gamma_{z'r'}, \gamma_{\theta'r'} \rangle$

and 'θ' is measured counterclockwise about the element r' axis from the element local axis to the material '1' axis. The element coordinate system is a system different from the structural global coordinate system. Equation 21 results in the transformation of out-of-plane shear stresses, independent of the transformation of the in-plane normal and shear stresses. Because of axi-symmetric property the in-plane shear stress ($\tau_{z'\theta'}$) and the out-of-plane shear stress ($\tau_{r'\theta'}$) associated with θ` direction are zero. If G13 and G23 are taken equal to G12, the shear stress ($\tau_{r'z'}$) can be directly written as $s_f G_{12}$. Therefore the resulting transformed constitutive relation in the element coordinate is

$$x \begin{Bmatrix} \sigma_{z'} \\ \sigma_{\theta'} \\ \tau_{r'z'} \end{Bmatrix} = \begin{bmatrix} Q_{11} & Q_{12} & 0 \\ Q_{12} & Q_{22} & 0 \\ 0 & 0 & s_f G_{12} \end{bmatrix} \begin{Bmatrix} \varepsilon_{z'} \\ \varepsilon_{\theta'} \\ \gamma_{r'z'} \end{Bmatrix} \qquad (23)$$

where, Q_{11}, Q_{12}, Q_{22} obtained from Equation. 4.40 are given as

$$\left.\begin{aligned} Q_{11} &= \bar{Q}_1\cos^4\theta + 2\bar{Q}_2\cos^2\theta\sin^2\theta + \bar{Q}_{22}\sin^4\theta + 4\bar{Q}_{33}\cos^2\theta\sin^2\theta \\ Q_{12} &= \bar{Q}_1\cos^2\theta\sin^2\theta + \bar{Q}_2\left(\cos^4\theta + \sin^4\theta\right) + \bar{Q}_{22}\cos^2\theta\sin^2\theta - 4\bar{Q}_{33}\cos^2\theta\sin^2\theta \\ Q_{22} &= \bar{Q}_1\sin^4\theta + 2\bar{Q}_2\cos^2\theta\sin^2\theta + \bar{Q}_{22}\cos^4\theta + 4\bar{Q}_{33}\cos^2\theta\sin^2\theta \end{aligned}\right\} \qquad (24)$$

6.2 Element Stiffness Matrix for Layered Shell

The integral equations can be evaluated using Gauss-Quadrature formulae. But in the case of layered shell, the constitutive matrix varies from layer to layer. In order to apply Gauss Quadrature integrals the limit should vary from -1 to 1. This is achieved by modifying the variable ξ to ξi in any ith layer such that ξi varies between -1 and 1 in that layer. Thus $[K_e]$ is defined as

$$\left.\begin{aligned} [K_e] &= 2\pi \sum_{i=1}^{n} \int_{-1}^{1}\int_{-1}^{1} [B]_i^T [Q]_i [B]_i \det[J]\, r\, d\xi_i\, d\eta_i \\ [K_e] &= 2\pi \sum_{i=1}^{n} \left[\sum_{\xi_i=1}^{ng}\sum_{\eta_i=1}^{ng} f(\xi_i, \eta_i)\; W\xi_i\, W\eta_i \det[J] \right] \end{aligned}\right\} \qquad (25)$$

where 'n' is the total number of layers and 'ng' is the number of gauss points. The 3-point Gauss Quadrature has been applied for numerical integration. Layers have to be numbered sequentially starting from inner surface of the shell and the fundamental frequency can be evaluated using the relation, $\omega = \sqrt{\frac{K}{M}}$, where 'M' is the mass matrix that is computed using lumped mass system.

7. VALIDATION OF FE MODEL

To confirm the validity of the FE model, initially a convergence study has been carried out with the help of an isotropic simply supported cylindrical shell for maximum fundamental frequency with linear, quadratic and cubic elements and with different number of elements. Accordingly the results are presented in Table 1. It is found that 8 number of cubic element converge to the fundamental frequency of 3760.56 rad/sec which is in close agreement with the closed form solution of [2].

Analysis is further extended for an orthotropic simply supported cylindrical shell made of Boron/Epoxy. The fundamental frequency obtained using M-ADSE is then compared with the one obtained using axi-symmetric solid elements of another [3] and the results (vide Table 2) are found in good agreement confirming the accuracy of the M-ADSE.

8. CONCLUSION

A finite element formulation is developed using multi-layered axi-symmetric degenerated shell element to perform free vibration analysis of laminated composite shells. Fundamental frequencies are found to converge rapidly with minimum number of elements and are found in good agreement with the published results.

REFERENCES

[1] S. Ahmed, B.M. Irons, and O. C. Zienkiewicz, "Curved Thick Shell and Membrane Elements with Particular Reference to Axi-Symmetric Problems", Proceedings of Second Conferences on Matrix Method in Structural Mechanics" Wright – Patterson, Air Force Base, Ohio, 1968.

[2] J.Ramachandran, "Thin Shells, Theory and Problems", Universities Press Ltd, India, 1993.

[3] A. Schokker, S. Sridharan, and A. Kasagi, "Dynamic Buckling of Composite Shells", Computers and Structures, Vol.59, No.1, 1996, pp. 43-53.

ASSESSMENT OF POLLUTION POTENTIAL OF THE GROUNDWATERS OF VRISHABHAVATHI VALLEY BASIN IN BANGALORE, KARNATAKA

B.S.Shankar[1] and N.Balasubramanya[2]

[1]Department of Civil Engineering, East Point College of Engineering, Bangalore- 560 049, Karnataka

[2]Department of Civil Engineering, M S Ramaiah Institute of Technology, Bangalore- 560 054, Karnataka

E-mail: shankar_bs1@yahoo.co.uk

(Received on 27 February 2008 and accepted on 15 March 2008)

Abstract

The present study aims to assess the water quality and pollution potential of groundwaters in and around the Vrishabhavathi Valley; an erstwhile fresh water stream, today carrying huge quantities of industrial, agricultural and domestic effluents from the western part of Bangalore metropolis. Groundwater samples have been drawn from both bore-wells and open-wells along the Vrishabhavathi watershed and subjected to a comprehensive physico-chemical and bacteriological analysis. The study revealed that 57% of samples were non-potable due to the presence in excess of several water quality parameters, as per the BIS, with Nitrate and total hardness accounting for 43.33% and 40% of the samples respectively. About 50% of the samples examined, indicated bacterial contamination of the groundwater. Further, the water quality indices of these samples were determined, considering ten critical parameters to assess their suitability for drinking purpose and the results indicate that 50% of samples fall in the category of poor, very poor, and unfit water. Appropriate measures for improving the water quality in the affected areas have also been suggested.

Keywords*: Contamination, Groundwater, Pollution, Quality*

1. INTRODUCTION

The urban environment is deteriorating day by day with the major cities reaching saturation levels and unable to cope up with the increasing pressure on their infrastructure [1]. Bangalore city has meager water resource in its neighbourhood, being a part of semi-arid peninsular India. The undulating topography of the city has been meticulously managed in the past, to build a chain of water storage lakes in the Valley areas. But, the city has been heading towards fresh water crisis, mainly due to improper management of water resources and environmental degradation, which has led to lack of access of safe water supply.

The Department of Mines and Geology carried out investigations to evaluate the groundwater quality in Bangalore Metropolis (1995) and based on the analysis, reported that 51 percent of samples were found to be non-potable due to the presence in excess of one or more water quality parameters [2]. But Nitrate was found to be the major cause, accounting for 45 percent of non-potability.

2. STATEMENT OF THE PROBLEM

The Vrishabhavathi River, once a major source of water, is now entirely contaminated from household, agricultural and industrial wastes [3]. While the original river has dried up, at present, it is carrying sewage and industrial effluents from more than 100 industries of various kinds. The waste water flowing into the Vrishabhavathi Valley is about 300 Million Litre Perday. It receives improperly treated and /or untreated effluents and domestic waste water from the Bangalore Water Supply and Sewerage Board (BWSSB) treatment plant, containing various organic materials, toxic elements and pathogens [4]. As surface water is accessible for irrigation in the study area, it is highly polluted with waste effluents and groundwater is the most utilized source in the area. A majority of the farmers own both dug wells and bore wells for irrigating various crops [4]. In the recent years, pollution of groundwater in the Vrishabhavathi locality has emerged as a severe environmental issue, constraining its use drastically. In this context, the present study assumes great importance.

The Vrishabhavathi is one of several tributaries of the river Cauvery. It drains a major part of Bangalore metropolis in the west and is the outlet channel for domestic and industrial effluents in the area. An erstwhile freshwater stream has now become the carrier of heavy pollutants. Vrishabhavathi, a tertiary tributary of the river Cauvery, drains an aerial extent of 545 sq km before it joins the Suvarnamukhi River at Bhadragundadoddi of Kanakapura Taluk, Bangalore District. It is encompassed by North Latitudes 12^0 45^1 to 13^0 03^1 and East Longitudes 77^0 23^1 to 77^0 35^1. The topographic coverage of the area is available on the topo sheets 57H/5 and 57H/9 published on scale 1: 50,000.

3. MATERIALS AND METHODS

Thirty water samples were collected from bore wells and open wells in the study area during April 2007 in two litre PVC containers and sealed. These samples were analyzed for the major physico-chemical parameters in the lab [5]. Ten samples were analyzed for bacterial contamination in the wake of reported bacterial infection of groundwater causing water borne diseases such as Cholera, Typhoid, etc.

The physical parameters such as p^H and electrical conductivity were determined in the field at the time of sample collection. The chemical analysis including metals and bacteriological analysis were carried out as per standard methods [5] for examination of water and wastewater (APHA, 1995). The results obtained were evaluated in accordance with the standards prescribed under 'Indian Standard Drinking Water Specification IS 10500: 1991 of Bureau of Indian Standards [6].

4. COMPUTATION OF WATER QUALITY INDICES

Water Quality Index (WQI) is one of the most effective ways to communicate information about the quality of water to all concerned citizens and policy makers. It thus becomes an important parameter for the assessment and management of groundwater. WQI may be defined as a rating reflecting the composite influence of a number of water quality parameters on the overall quality of water. The main objective of WQI is to turn complex water quality data into information that is understandable and useable by the public. WQI, based on some important parameters, can provide a simple indicator of water quality. It gives the public, a general idea of the possible problems with water in a particular region.

The WOI has been calculated using the formula [7] as given below:

$$WQI = \text{Antilog } [\text{“}W_{n=1}^{n} \log_{10} q_n] \quad (1)$$

where,

W = Weightage factor (Table 3) computed as

$$W_n = K / S_n \quad (2)$$

K = Proportionality constant derived from equation (3)

$$K = [1 / (\text{“}n_{n=1} \; 1 / S_n)] \quad (3)$$

S_n is the recommended drinking water standard as per B.I.S.

Quality rating q is calculated using the formula,

$$q_{ni} = [(V_{actual} - V_{ideal})/(V_{standard}-V_{ideal}) \text{ X } 100] \quad (4)$$

q_{ni} = quality rating of i^{th} parameter for a total of n parameters.

V_{actual} = Value of water quality parameter obtained from laboratory analysis

V_{ideal} for p^H = 7 and equivalent to zero for other parameters.

$V_{standard}$ = B.I.S. parameters.

Based on the above WQI values, the groundwater is rated as excellent, good, poor, very poor and unfit for consumption (Table 4)

5. RESULTS AND DISCUSSION

Thirty groundwater samples were drawn from open-wells and bore wells which included hand pumps, piped water supplies and mini-water supply schemes and were analyzed for twenty physico-chemical parameters including trace metals. Further, ten groundwater samples were drawn for the bacteriological analysis. The results of the physico-chemical analysis are presented in Table 1 and the diagrammatic interpretations of the results are presented in Figures 1&2. Out of the thirty samples analyzed for physico-chemical parameters, 17 samples (56.67%) were found to be non-potable as per B.I.S.

The main causative constituents for the non-potability of the samples are nitrates and total hardness, which accounted for 43.33% and 40% of unsafe samples respectively, followed by Calcium, as a result of which 23.33% of samples were found to be unsafe. Total dissolved solids, Fluorides and Iron, each accounted for 13.33% of samples being non-potable. Chlorides and Iron each rendered 10% of samples non- potable.

The study area has shown excessive concentrations of nitrates which have contributed to 43.33% of samples being rendered non-potable as reported earlier. The maximum, minimum and average concentrations of nitrates are found to be 157 mg/l, 05 mg/l and 47.60 mg/l (Table 2, which also gives the concentrations for other critical parameters and their BIS limits). Nitrates in several samples are alarmingly high, when compared to a BIS permissible limit of 45 mg/l. In the study area, organic origin is probably the cause for most of such occurrences, which can be assigned fairly to drainage of water through soil containing domestic and industrial wastes, vegetable and animal matter. Septic tanks and garbage dump disposal may also be responsible for the high nitrate content in the study area. Beyond 45 mg/l, this may cause Methaemoglobinemia or blue baby disease in infants. It may also be carcinogenic to adults.

Total hardness attributing to 40% of non potability of samples has shown maximum, minimum and average concentrations of 1960 mg/l, 70 mg/l, & 563.67 mg/l as CaCO3 respectively. The maximum permissible limit as per BIS is 600 mg/l. The high degree of hardness in the study area is definitely attributed to the disposal of untreated / improperly treated sewage and industrial wastes [8].

The fluoride value ranges from 2.5 mg/l to nil. The high levels of fluoride account for the non-potability of 13.33% of samples. Apart from natural processes which cannot be controlled, considerable amount of fluorides may have been contributed to man-made reasons, such as the use of fluoride salts in large number of industries in the study area such as steel, aluminum, brick and tile manufacturing units. Fluorides in excess of 1.5 mg/l may lead to a crippling and painful disease called fluorosis, which may be in the form of dental fluorosis, skeletal fluorosis and non-skeletal fluorosis.

The concentration of total dissolved solids varies from 200 mg/l to 2850 mg/l and account for 13.33% of the non-potability. Water with high total dissolved solids (>2000mg/l) is of inferior palatability and may induce an unfavourable physiological reaction in the transient consumer and gastro-intestinal irritation.

Iron concentration was high at 1.24 mg/l and four samples are found to have iron in excess of the maximum permissible limit of 1 mg/l. The higher value may be due to rusting of casing pipes, non-usage of bore-wells for long periods and disposal of scrap iron in open areas due to industrial activity.

Chlorides resulting in 10% of the non-potability have a peak value of 1338 mg/l, as against the BIS limit of 1000mg/l. The high value can definitely be attributed to the discharge of industrial effluents in the area.Only two samples were affected by excess Chromium and one sample by Copper.

Out of ten samples analyzed for bacteria, five samples (50%) were found to be contaminated, mainly in sewage contaminated and slum areas, with an alarmingly high peak MPN value of 350 in an open-well as against the maximum limit of 10/100ml. (Table 5). Excessive Coliforms may be responsible for the out-break of a number of water-borne diseases as mentioned earlier.

Water quality index has been calculated to determine the suitability for drinking purposes. WQI values revealed that 50% of the 30 groundwater samples are of excellent and good category and hence can be used for humanconsumption. about 5samples are of poor quality (WQI,be1. tween51-75)4samples of very poor quality (WQI between 76- 100) and 6 samples are totally unfit for consumption (WQI > 100).

Table 1 Physico-Chemical Analysis of Groundwater Samples

Sample no	pH	Turbidity NTU	Total Hardness mg/las $CaCO_3$	Ca mg/l	Mg mg/l	Na mg/l	K mg/l	Fe mg/l	HCO_3 mg/l	CO_3 mg/l	Cl mg/l	NO_3 mg/l	SO_4 mg/l	PO_4 mg/l	TDS mg/l	EC umhos/ cm	F, mg/l	Cu mg/l	Pb mg/l	Cr mg/l	WQ I	Rating
	1	2	3	4	5	6	7	8	9	10	11	12	13	14	15	16	17	18	19	20		
1	7.42	0.1	190	52	14	26	02	0.16	204	nil	100	18	10	0.3	328	520	1.3	nil	nil	nil	62.94	P
2	7.60	nil	210	56	18	30	1.4	0.04	275	nil	90	32	40	0.8	390	620	1.2	nil	nil	nil	22.73	E
3	7.5	5.1	210	50	16	32	0.6	1.24	200	nil	82	54	16	1.9	340	540	1	0.1	nil	nil	269.2	UFD
4	7.84	nil	688	130	69	55	1.1	0.2	544	08	210	52	42	0.1	840	976	1.3	nil	nil	nil	77.27	VP
5	7.15	0.4	492	128	41	76	03	0.2	309	nil	137	157	84	0.8	806	1210	.98	nil	nil	nil	69.5	P
6	7.26	nil	416	102	38	56	02	0.24	270	nil	120	109	56	2.8	646	1050	0.9	nil	nil	nil	78.89	VP
7	7.62	0.7	584	108	76	54	1.3	0.12	458	06	220	10	44	06	628	1010	1.3	nil	nil	nil	52.24	P
8	7.48	0.7	480	64	72	48	1.2	0.04	471	nil	205	34	45	0.5	744	1174	1	nil	nil	nil	21.88	E
9	7.42	0.1	430	108	40	54	1.0	0.2	427	nil	235	10	56	1.1	714	1100	0.9	nil	nil	nil	69.02	P
10	7.22	nil	380	88	39	44	1.4	0.1	280	nil	160	36	29	1.0	530	850	0.7	nil	nil	nil	38.82	G
11	7.60	0.2	360	56	54	48	2.2	0.02	442	nil	130	09	31	0.4	550	830	1.4	nil	nil	nil	14.12	E
12	7.6	0.5	392	94	38	35	2.6	0.22	300	10	130	12	25	0.8	490	780	1.9	nil	nil	nil	87.9	VP
13	8.21	nil	280	55	35	48	3.0	0.02	402	12	164	12	14	0.6	510	810	0.4	nil	nil	nil	10.72	E
14	7.80	nil	626	202	30	52	3.4	0.52	549	nil	265	70	30	1.0	930	1350	0	nil	nil	0.1	53.08	P
15	7.55	nil	560	118	65	46	3.2	1.08	442	nil	350	11	31	0.4	840	1330	0	nil	nil	nil	89.33	VP
16	6.92	nil	388	106	31	203	20	0.1	630	nil	212	20	56	2.0	990	1520	0.5	nil	nil	nil	35	G
17	6.55	0.4	432	110	40	200	14	0.04	580	nil	150	05	80	2.6	1000	1520	.06	nil	nil	nil	11.56	G
18	7.20	nil	612	150	58	40	1.0	0.08	225	nil	300	54	28	1.0	730	1120	1.4	nil	nil	nil	38.54	G
19	7.32	1.2	608	144	60	120	03	0.1	328	12	306	52	30	1.4	860	1340	0.5	nil	nil	nil	36.64	G
20	7.82	nil	672	202	40	40	1.4	0.12	321	nil	275	20	34	1.0	764	1240	0	nil	nil	nil	18.06	
21	8.42	0.5	618	204	26	72	2.0	0.03	336	nil	285	60	51	1.2	880	1450	0.1	nil	nil	nil	10.96	E
22	6.79	1.4	1960	386	249	202	10	0.8	286	nil	1338	84	216	6.2	2850	4270	0.8	nil	nil	nil	188.8	UFD
23	6.76	0.8	604	155	36	140	5.2	0.4	494	nil	232	153	51	4.0	1045	1712	0.6	nil	nil	Nil	104.7	UFD
24	7.70	nil	620	142	64	220	30	0.09	540	nil	400	10	150	06	1310	2010	0.6	nil	nil	nil	35.89	G
25	6.60	Nil	70	15	08	14	0.4	0.12	140	nil	60	38	18	nil	200	310	0	nil	nil	nil	17.38	E
26	6.80	0.8	570	108	73	36	1.1	0.02	407	nil	305	20	18	1.8	746	1220	0.6	nil	nil	nil	11.48	E
27	7.12	Nil	416	100	40	48	2.2	0.05	332	nil	320	24	40	1.2	742	1260	0.7	nil	nil	nil	22.9	E
28	7.40	12	960	300	50	86	3.1	1.04	608	nil	1012	80	120	2.6	2042	3370	1.8	nil	nil	nil	274.1	UFD
29	7.62	26	1062	330	58	78	3.6	1.02	570	nil	1044	84	90	2.0	2008	3270	2.3	nil	nil	nil	288.4	UFD
30	7.80	14	1095	270	101	106	4.0	0.28	700	80	780	98	90	4.3	2200	4010	2.5	nil	nil	0.2	114.8	UFD

Table 2 Concentrations of Critical Parameters and BIS Permissible Limits

Sl. No	Parameter	Maximum	Minimum	Average	BIS limits
1	pH	8.42	6.55	7.40	6.5 to 8.5
2	Chlorides	1338	60	320.63	1000
3	TDS	2850	200	921.77	2000
4	Total Hardness	1960	70	563.67	600
5	Calcium	386	15	137.83	200
6	Magnesium	249	08	52.63	100
7	Nitrate	157	05	47.6	45
8	Sulphate	216	10	54.17	400
9	Fluoride	2.5	nil	0.87	1.50
10	Iron	1.24	Nil	0.225	1.0

All parameters except pH in mg/L

Table 3 Water Quality Parameters, Standards and Unit Weights

Parameter	Standard (S_n)	Weightage (W_n)
pH	8.5	0.026
Total Hardness	300	0.00073
Calcium	75	0.00293
Magnesium	30	0.00733
Chloride	250	0.00088
Nitrate	45	0.00049
Sulphate	200	0.0011
TDS	500	0.00044
Fluoride	1	0.22
Iron	0.3	0.73

Table 4 Water Quality Index Categories

Water Quality Index	Category
0 -25	Excellent (E)
26- 50	Good (G)
51- 75	Poor (P)
76- 100	Very poor (VP)
> 100	Unfit for drinking(UFD)

Table 5 Results of Bacteriological Analysis (MPN)

Sample. No	Coliform organisms/ 100 ml of water
3	NIL
11	01
15	NIL
16	23
18	04
19	350
22	23
23	120
25	NIL
29	35

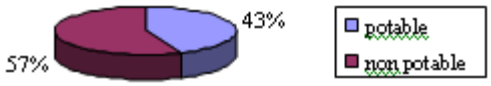

Fig. 2 Potability of Samples

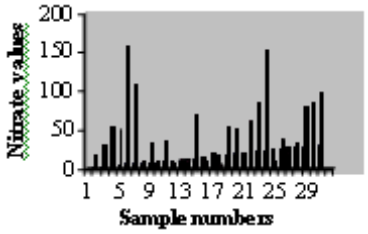

Fig. 3 Variation of nitrate in groundwater

6. CONCLUSION

The analysis of groundwater samples reveals that nearly 57% of the samples are non-potable. Strict legislation on industries being setting-up and operating their effluent treatment plants should be enforced mandatorily. Replacement of damaged pipelines and lining of sewer drains is a must. Augmenting the ground water resources by recharging the ground water aquifer through rain water harvesting and thus reducing the high concentration of chemical parameters is a very important measure. Use of bio fertilizers by farmers instead of chemical fertilizers in agricultural activities is another very important control measure. The public should be instructed to use boiled water for drinking, as the study areas have shown considerable hardness, mostly of temporary type. Public awareness programmes should be initiated to create a sense of know-how to safeguard against the perils of water-borne diseases.

REFERENCES

[1] S.S. Asadi, "Remote Sensing and GIS Techniques for Evaluation of Groundwater Quality in Municipal Corporation of Hyderabad (Zone-5), India", Int.Jour.Environ.Res.Public Health, Vol.4, No.1, 2007, pp.45-52.

[2] T.M.Shivashankar, "Evaluation of Groundwater Quality in Bangalore Metropolis", Technical Report, Department of Mines and Geology, Bangalore, 1995.

[3] R.L. Gaikwad, " Urbanization and its Effects on Environment-Groundwater Pollution by Sewage in the Vrishabhavathi Valley near Bangalore Metropolis - A Case Study", Department of Mines and Geology, No.260 , 1994.

[4] Praveen, "Drinking Water in Urban Areas: Why and How is it Getting Worse?", Proceedings of Drinking Water Supply of IWMI-TATA Partners Meet, Anand, Gujarat, 2005, pp.24- 26.

[5] AW. Apha , "Standard Methods for the Examination of Water and Wastewater", 16th edition, American Public and Health Association, Washington D.C., USA, 1995.

[6] BIS, "Indian Standard Drinking Water Specification", Bureau of Indian Standards, New Delhi, IS: 10500, 1991.

[7] T.N.Tiwari, "Assessment of Water Quality Index", Indian Journal of Environmental Protection, Vol.5, No.4, 1985, pp.276-279.

[8] C.S.Ramasesha, "Water Quality and Health", Proceedings of National Conference on Groundwater Pollution - Sources and Mitigation, Bangalore, India, 2005, pp.55-57.

ANALYSIS OF MANUAL VS AUTOMATED SOFTWARE COST ESTIMATING METHODS FOR LARGE SCALE PROJECTS

K. Thangadurai[1] and A. Shanmugam[2]
[1]Department of Computer Science, PSG College of Arts and Science, Coimbatore - 641 004, Tamil Nadu
[2]Bannari Amman Institute of Technology, Sathyamangalam - 638 401, Erode District, Tamil Nadu
Email: ktramprasad04@yahoo.com
(Received on 01 August 2007 and accepted on 22 March 2008)

Abstract

For large projects, automated estimates are more successful than manual estimates in terms of accuracy and usefulness. In addition, successful estimates for large projects must be adjusted to match specific development processes, to match the experience of the development team, and to match the results of the programming languages and tool sets that are to be utilized. Requirement issues abound in system development despite many models and methods intended to verify that requirements are complete. This paper highlights the untility of function point analysis (FPA), and the software sizing technique incorrect estimation. It also delivers value as a structured requirements review and the parametric models have been shown to give accurate estimates of cost and duration for given accurate inputs of the project. This paper also focuses on scope estimates for new development, and is applicable for the new development portion of maintenance builds especially in large scale projects.

Keywords*: Constructive Cost Model, Cost Estimation, Effort Estimation, Function Points*

1.INTRODUCTION

Software has achieved a bad reputation as a troubling technology. Large software projects ten to have a very high frequency of schedule and cost overruns, quality problems, and outright cancellations. While this bad reputation is often deserved, it is important to note that some large software projects are finished on time, stay within their budgets, and operate successfully when deployed.

The life cycle of software cost estimation[1] is made of many parts, beginning with input parameters at the concept stage and continuing through the function and implementation stages. Many consider estimating project scope to be the most difficult part of software estimation. After all, how one can input scope early in the life cycle when the requirements are still vaguely understood? Consider also that scope must be estimated, quantified, and documented in a manner that is understandable to management, end users, and estimating tools. This paper focuses on scope estimates for new development, including maintenance builds.

This paper also addresses projects where user requirements are articulated (or should be) and outlines how function point analysis (FPA) can be an additional tool to identify missing requirements, gauge requirements completeness, and uncover potential defects.

2. MAJOR FEATURES OF SOFTWARE COST ESTIMATION TOOLS

The major features of commercial software-estimation tools circa 2005 include these attributes:

- Sizing logic for specifications, source code, and testcases.
- Phase-level, activity-level, and task-level estimation.
- Adjustments for specific work periods, holidays, vacations, and overtime.
- Adjustments for local salaries and burden rates.
- Adjustments for various software projects such as military, systems, commercial etc.
- Support for function point metrics, lines of code (LOC) metrics, or both.
- Support for backfiring or conversion between LOC and function points.
- Support for both new projects and maintenance[2]and enhancement projects.

- Some estimating tools also include more advanced functions such as the following:

Quality and reliability estimation
Risk and value analysis
Return on investment
Sharing of data with project management tools
Measurement models for collecting historical data
Cost and time-to-complete estimates mixing historical data with projected data
Support for software process assessments
Statistical analysis of multiple projects and portfolio analysis.

- Currency conversion for dealing with overseas projects.
- Estimates for large software projects.

2.1 Adjustment Factors for Software Estimates

When being used for real software projects, the basic default assumptions of estimating tools must be adjusted to match the reality of the project being estimated. These adjustment factors are a critical portion of using software estimating tools. Some of the available adjustment factors[3] include the following:

- Staff experience with similar projects
- Client experience with similar projects
- Type of software to be produced
- Size of software project
- Size of deliverable items (documents, test cases, etc.)
- Requirements methods used
- Review and inspection methods used
- Design methods used
- Programming languages used
- Reusable materials available
- Testing methods used
- Paid overtime
- Unpaid overtime

2.2 The Estimating Life Cycle

First, it is important to recognize the limitations of software cost estimating at the macro level. As shown in Figure 1, the typical accuracy of cost estimates varies based on the current software development stage. Early uncertainty in the estimate is largely based on variances in the estimate's input parameters. Later uncertainty in the estimate is based on the variances of the estimating models.

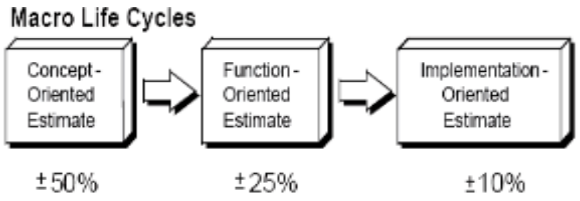

Fig.1 Typical cost estmating accuracies

The percentages shown in Figure 1 match the author's personal experience and are roughly comparable with figures found in the Project Management Institute's "A Guide to the Project Management Body of Knowledge". However, actual numbers will vary widely based on the type of applications involved, the estimators' experience and policies, and other factors. Initially, at the concept stage a vague project definition can be presented. Though the requirements may not yet be fully understood, the general purpose of the new software can be recognized.

At this point, estimates with an accuracy of ± 50 percent are typical for an experienced estimator using informal techniques (i.e., historical comparisons, group consensus, and so on). After the requirements are reasonably well understood, a function-oriented estimate may be prepared. At this point, estimates with an accuracy of ± 25 percent are typical for an experienced estimator using the techniques described above. Finally, after the detailed design is complete, an implementation-oriented estimate may be prepared. This estimate is typically accurate within ± 10 percent.

2.3 Estimating Program Scope

The first step in preparing an estimate is to determine an estimate of the project scope, or volume. Scope is typically estimated using a variety of metrics, as different portions of the application may be compatible with different scope metrics. One measure of program scope is the number of source lines of code (SLOC). A source line of code is a human-written line of code that is not a blank line or comment. Do not count the same line more than one time even if the code is included multiple times in an application. Typically one works with a related number - thousands of SLOC (KSLOC) - when estimating.

Table 1 Estimation

Project Type	Linear Productivity Factor (Person Months/KSLOC)
COCOMO II Default	3.13
Embedded Development	3.60
E-Commerece Development	3.08
Web Development	2.51

The Constructive Cost Model (COCOMO) popularized SLOC as an estimating metric. The basic COCOMO model and the new COCOMO II model remain the most well-known estimating approaches because of their prevalence in both academic research settings and as models embedded into estimating tools. Let us jump ahead and look at how we can convert from the number of KSLOC to an estimate for the project. We will then discuss approaches to estimating KSLOC in more detail. Begin with the simplest estimate as shown in Table 1. If one is aware of the number of KSLOC the developers must write, and you knows the effort required per KSLOC, then multiply these two numbers together to arrive at the person-months of effort required for the project. This concept is the heart of the estimating models.

Table 1 shows some common values that cost expert researchers have found for this linear productivity factor. Now, let us apply this approach to build an e-commerce system consisting of 15,000 LOC. How many person-months of effort would this take using just this equation. The answer is computed as follows:

Effort = Productivity x KSLOC = 3.08 x 15 = 46 Person Months

Table 2 Typical Size Penalty Factors

Project Type	Linear Productivity Factor (Person Months/KSLOC)
COCOMO II Default	1.072
Embedded Development	1.111
E-Commerce Development	1.030
Web Development	1.030

Table 2 shows some typical size penalty factors for various project types. Again, the COCOMO II value comes from work by Boehm, and values for embedded, e-commerce, and Web development come from work by cost expert group [2] and its customers. These values have been validated by hundreds of cost expert group customers/projects, and are updated over time as warranted by the research. Note that because the size factor is an exponential factor rather than linear, it does not change with project size, but changes impact on the end result with project size.

After a size penalty adjustment, is done the number of person-months of effort required by 15,000 lines of code e-commerce system is computed as follows:

Effort = Productivity x KSLOCPenalty =
3.08 x 151.030 = 3.08 x 16.27 =
50 Person Months

All of this is pretty straightforward. The next logical question is, "How do one knows that the project will end up as 15,000 SLOC?" There are two approaches to answering this question naturally direct estimation and function points (FPs) with backfiring. Using either approach, the fundamental input variables are determined through expert opinion, often with the developers as the experts.

The Delphi technique, involving multiple experts iterating towards a consensus decision, is a good way to cross-check the input variables. Normally, the first step in estimating the number of LOC is to break down the project into modules or some other logical grouping. For example, a very high-level breakdown might be front-end processes, middle-tier processes, and database code. The developers then use their experience building similar systems to estimate the number of LOC required. It is strongly recommended to obtain three estimates for each input variable: a best-case estimate, a worst-case estimate, and an expected-case estimate. With these three inputs, the mean and standard deviation can be calculated as follows:

$$\text{Mean} = \frac{(\text{best} + \text{worst} + (4 \times \text{expected}))}{6}$$

$$\text{Standard Deviation} = \frac{(\text{worst} - \text{best})}{6}$$

The standard deviation is a measure of how much deviation can be expected in the final number. For example, if the statistical description of the project is correct and risk factors not included in the statistical

spread are ignored the mean plus three times the standard deviation will ensure that there is a 99 percent probability that the project will be completed with in the estimate.

2.4 An Alternative Approach to Sizing/Estimating

Parametric or model-based estimating takes the following alternate approach(Fig.2):

- It determines the size of the software elements breaking them down into common low-level software implementation units (IUs).
- It creates a model-based first cut estimate using a productivity assumption (preferably historically based), the project size, and the critical constraints.
- It performs what-if modeling until an agreed-upon estimate has been created.
- It creates the detailed plans for the project.

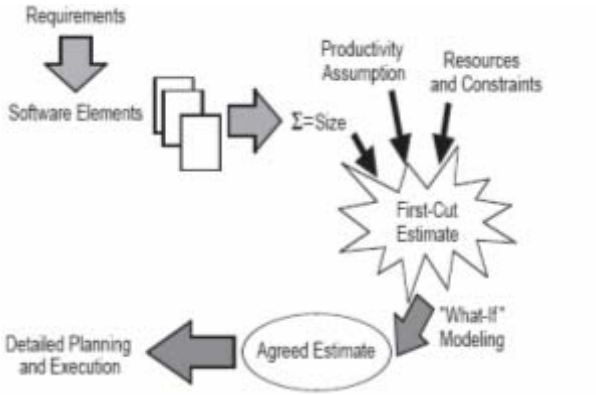

Fig. 2 Alternative Sizing and Estimating Approach

Figure 2 the key to the success of this methodology is an accurate size and a productivity assumption that is consistent with the organization's capabilities.

3. COCOMO SUITE METHODOLOGY AND EVOLUTION

Over the years, software managers and software engineers have used various cost models such as the Constructive Cost Model (COCOMO) to support their software cost and estimation processes[4]. These models have also helped them to reason about the cost and schedule implications of their development decisions, investment decisions, client negotiations and requested changes, risk management decisions, and process improvement decisions. Since that time, COCOMO has cultivated a user community that has contributed to its development and calibration. COCOMO has also evolved to meet user needs as the scope and complexity of software system development has grown. This eventually led to the current version of the model: COCOMO II.2000.3.

The growing need for the model to estimate different aspects of software development served as a catalyst for the creation of derivative models and extensions that could better address commercial off-the-shelf software integration, system engineering, and system-of-systems architecting and engineering. The COCOMO [5] suite that includes extensions and independent models. The underlying methodologies and the logic behind the models and how they can be used together to support larger software system estimation needs are describes below:

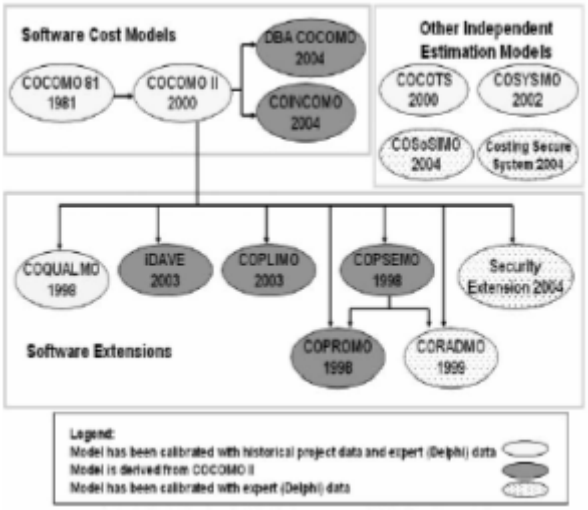

Fig.3 Historical overview of cocomo suite of models

Figure 3 shows the evolution of the COCOMO suite categorized by software models, software extensions, and independent models. The more mature models have been calibrated with historical project data as well as expert data via Delphi surveys. The newer models have only been calibrated by expert data.

Table 3 includes the status of the 12 models in the COCOMO suite. All of these models have been developed using the following seven-step methodology: (1) analyze existing literature, (2) perform behaviour analysis, (3) determine form of model and identify relative significance of parameters, (4) perform expert-judgment/Delphi assessment, (5) gather project data, (6) determine Bayesian A Posteriori update, and (7) gather more data, refine model. The checkmarks in Table 1 indicate the completion of that step for each model.

Table 3 Status of the Models

Model `	Description	Literature	Behavior	Significant Parameters	Delphi	Data
COCOSMO II	Construction Cost Model	✓	✓	✓	✓	>200
COINCOMO	Constructive Incremental COCOMO					
DBA COCOMO	Data Base(Access) Doing Business As COCOMO II					
COQUALMO	Constructive Quality Model	✓	✓	✓	✓	6
iDAVE	Information Dependability Attribute Value Estimation	✓	✓	✓	✓	-
COPLIMO	Constructive Line Investment Model	✓	✓	✓	✓	-
COPSEMO	Constructive Phased Schedule and Effort Model	✓	✓	✓	✓	-
CORADMO	Constructive Rapid Application Development Model	✓	✓	✓	✓	16
COPROMO	Constructive Productivity – Improvement Model	✓	✓	✓	✓	-
COCOTS	Constructive Commercial Off-the-Shelf Cost Model	✓	✓	✓	✓	29
COSYSMO	Constructive Systems Engineering Cost Model	✓	✓	✓	✓	14
COSOS/MO	Constructive System-of-Systems Integration Cost Model	✓	✓	✓	✓	-

Table 4 Model Factor Types

Model Name	Scope of Estimate	Number of Additive Factors	Number of Exponential Factors	Number of Multiplicative Factors
COCOMO	Software development effort and schedule	1	1	15
COCOMO II	Software development effort and schedule	1	5	17
COSYSMO	Systems engineering effort	4	1	14
COCOTS	COTS assessment tailoring and integration effort	3	1	13
COSOSMO	SoS architecture and integration effort	4	6	-

The number of factors in each of the models is shown in Table 4. The general rationale for whether a factor is additive, exponential, or multiplicative comes from the following criteria:

- A factor that has effect on only one part of the system - such as software size – has a local effect on the system. For example, adding another source instruction, function point entity, module, interface, operational scenario, or algorithm to a system has mostly local additive effects on project effort.

- A factor is multiplicative or exponential if it has a global effect across the overall system. For example, adding another level of service requirement, development site, or incompatible customer has mostly global multiplicative or exponential effects. If the size of

4. TYPES OF EFFORT CURRENTLY ESTIMATED

The next step was to identify a comprehensive set of high level, software-intensive system life-cycle activities, the typical development organizations responsible for the performance of these activities, and the scope of the activity typically performed by each development organization. Then each activity covered by each of the primary cost models was identified. For example, the system engineering organization typically responsible for the system/subsystem requirements and design, and the software development organization participates in a support or review role. Other activities, such as management, are often performed at various levels with each development organization having primary responsibility at their respective levels. The results of this effort are shown in Table 5.

Table 5 Life Cycle Activities

Activity	Responsibilities			
	Software Development (COCOMO II and COCOTS)	**Hardware Development**	**System Engineering (COSYSMO)**	**LSI (COSOSIMO)**
Management	Primary for Software Level	Primary for Hardware Level	Primary for System Level	Primary for SoS Level
Support Activities(e.g., Configuration Management and Quality Assurance)	Software Level	Hardware Level	System Level	SoS Component Level
SoS Definition			SoS Component	SoS Level
Source Selection and SoS Component Procurement				Lead
Subsystem Requirements	Review	Review	Elaboration* Lead	Inception Lead
System Subsystem Design	Support	Support	Lead	Review
Hardware/Firmware Development		Lead		
Software Requirements Analysis	Elaboration* Lead		Inception Lead	
Software Product Design	Lead		Review	
Software Implementation/ Programming	Lead		Support	
Software Test Planning	Lead		Review /Support	
Software Verification and Validation	Lead		Review /Support	
System Integration/Test	Support	Support	Lead	Review
System Acceptance / Test	Support	Support	Lead	Review
SoS Integration / Test	Support	Support	Review /Support	Lead
SoS Acceptance / Test	Support	Support	Review /Support	Lead
Manuals(User, Operator, Maintenance)	Software Lead	Hardware Lead	System Lead	SoS Level Lead
Transition(Deploy and Maintain	Support	Support	System Lead	SoS Level Lead

The shaded activities under Software Development [6]are currently covered in COCOMO II and COCOTS. The shaded activities under System Engineering are currently estimated by COSYSMO. The shaded activities under LSI are currently estimated by COSOSIMO. The activities that are not shaded are currently not covered by any of the models in the COCOMO suite. And, since the focus of the COCOMO suite is on software-intensive systems, none of the items under the hardware development column are currently covered.

5. FUTURE TRENDS, IMPLICATIONS IN COST ESTIMATION MODELS

5.1 Trends in Software Productivity, Estimating Accuracy

In principle, an organization should be able to continuously measure, recalibrate, and refine models such as COCOMO II to converge uniformly towards perfection in understanding the software applications and in accurately estimating the costs and schedules. In practice, convergence towards perfection in estimation is not likely to be uniform.

Two major phenomena are likely to interrupt your progress in estimation accuracy:

- As the understanding increases about the nature of applications domain, it is possible to improve the software productivity and quality by using larger solution components and more powerful applications definition languages. Changing to these construction methods will require to revise the estimation techniques, and will cause estimation error to increase.

- The overall pace of change via new technologies and paradigm shifts in the nature of software products, processes, organizations, and people will cause the inputs and outputs of software estimation models to change. Again, these changes are likely to improve software productivity and quality, but cause the estimation error to increase.

6. ESTIMATION ACCURACY

6.1 The Bottom Line

If only our software engineering domain understanding, product and process technology, and organization and people factors stayed constant, we could get uniformly better and better at estimating. But they do not stay constant, and their changes are generally good for people and organizations. The need to continually rethink and re-engineer our software estimation models is a necessary price to pay for the ability to incorporate software engineering improvements. Coping with Change: COCOMO II

We are trying to ensure that COCOMO II will be adaptive to change by trying to anticipate trends in software engineering practice, as discussed in the Introduction. The resulting three-stage set of COCOMO II models (application composition, early design, post-architecture) anticipates some dimensions of future change. Other dimensions are addressed by the new or extended cost drivers such as process maturity, architecture and risk resolution, team cohesion, multi site development, use of tools, and the various reuse parameters.

6.2 Coping with Change: COCOMO II and Many Organization

COCOMO II can be a useful tool for many organization to use in adapting to future change, both at the project level and at the organizational level.

6.2.1 Coping with Change during Project Definition

Figure 4 shows how COCOMO II can be used to help address issues of change at the project definition level. You can enter your organization's customary values via the COCOMO II parameters, and indicate which ones will undergo change. COCOMO II will estimate how these changes will affect the project's expected cost and schedule, and will provide you and your stakeholders with a framework for re scoping the project if estimated cost and schedule are unsatisfactory.

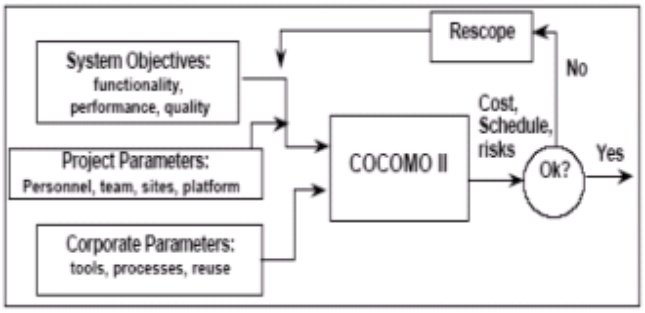

Fig. 4 Using COCOMO II to cope with change

6.2.2 Coping with Change during Project Execution

Frequently, changes in project objectives, priorities, available componentary , or personnel occur during project execution. If these are anticipated, COCOMO II can support a variant of the project definition process above to converge on a stakeholder- satisfactory re scoping of the project. A more serious case occurs when the changes are unanticipated and largely unnoticed: via personnel changes; COTS product, reusable component, or tool shortfalls; requirements creep; or platform discontinuities.

In such cases, COCOMO II phase and activity distributions can be used to develop a quantitative milestone plan or an earned-value system for the project, which enable plan deviations to be detected, and appropriate corrective actions to be taken involving COCOMO II in project re scoping.

6.2.3 Coping with Required COCOMO II Model Changes

At times, unanticipated project changes are indications that your COCOMO II model needs to be recalibrated or extended. The more management data you collect on actual project costs and schedules, the better you will be able to do this (see Figure 5).

Recalibration might be appropriate, for example, if your organization is acquired by or merged into an organization with different definitions of project endpoints, or with different definitions of which types of employees are directly charged to the project vs. being changed to overhead. As described in Chapter 4 of Software Cost Estimation with COCOMO II, techniques are available to recalibrate COCOMO II 's base coefficients and exponents for cost and schedule estimation. Some COCOMO II tools such as USC COCOMO II and COSTAR, a commercial product from Soft Star Systems, provide such calibration features.

Extending the model will be appropriate if some factor assumed to be constant or insignificant turns out to be a significant cost driver. For example, the COCOMO 81 TOOL Factor[8] was not in the original 1978 TRW version of COCOMO, as previous TRW projects had operated with a relatively uniform set of mainframe tools. The TOOL Factor was added after TRW had completed some microprocessor software projects with unexpectedly high costs.

After investigation, the scanty microprocessor tool support was the primary factor that accounted for the extra project effort and cost. Subsequent data from other organizations confirmed the validity of the TOOL variable as a significant COCOMO 81 cost driver. Similarly, several variables were added to COCOMO 81 to produce COCOMO II, in response to affiliate indications of need and our confirmation via behavioral analysis.

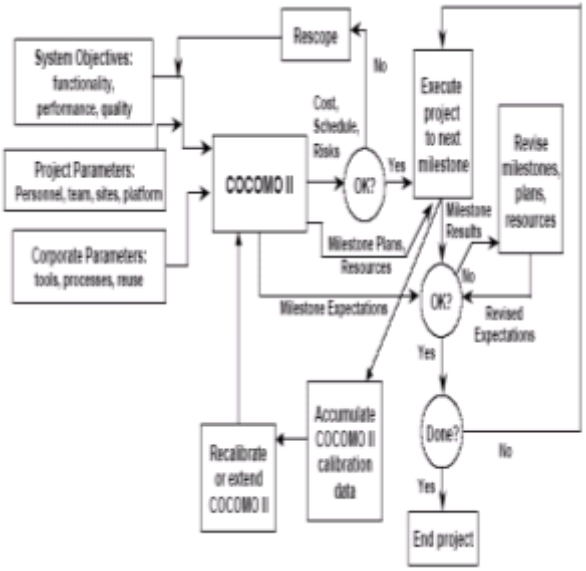

Fig. 5 Using COCOMO II to cope with change III

7. FUNCTION POINT MEASURES

Function points (FPs) measure the size of a software project's logical user functionality as opposed to the physical implementation of those functions as measured by lines of code (LOC). FPA examines the functional

user requirements to be supported or delivered by the software. It then assigns a weighted number of FPs to each logical user function as outlined in Function Point Counting Practices Manual and calculates the software's FP size.

In simplest terms, FPs measure what the software must do from an external, user perspective irrespective of how the software is constructed. While analogies from other industries such as building construction and manufacturing attempt to describe how function point analysis works with software, none provides a perfect fit. In basic terms, FPs reflect the functional size of software, independent of the development language and physical implementation. FPs can be likened to the functional area of a building by summing up its floor plan size. FPs quantify the functional user requirements (the floor plan) by summing up the size of its functional components. As with building construction, project management is not possible if only square foot size is known. System development cannot be managed purely on the basis of FP size.

7.1 Estimating Function Points

An alternative to direct SLOC estimating is to start with FPs, then use a process called backfiring to convert from FPs to SLOC. Backfiring is described on page 6, consists of converting from FPs to SLOC using a language-driven table lookup function. FPs were first utilized by IBM as a measure of program volume.

Table 5 Function Point Conversion

Raw Type	Function Point Conversion Factor
External Inputs	4
External Interface files	7
External Outputs	5
External Queries	4
Logical Internal Tables	10

7.1.1 Factor

To convert from these raw values into an actual count of FPs, you multiply the raw numbers by a conversion factor from Table 5 on page 6 (again, this approach is a simplification). So, if we had a system consisting of 25 data-entry screens, five interface files, 15 reports, 10 external queries, and 20 logical internal tables, how many FPs would we have? The answer is computed as follows:

(25 x 4) + (5 x 7) + (15 x 5) + (10 x 4) +
(20 x 10) = 450 FPs

7.1.2 Backfiring

The only remaining step is to use backfiring to convert from FPs to an equivalent number of SLOC. This is done using a table of language equivalencies. Some common values are shown in Table 6 (C++, COBOL, and SQL from work by Capers Jones and other values from research by Cost Xpert Group): So, to implement the above project (450 FPs) using Java 2 would require approximately the following number of SLOC:

450 x 46 = 20,700 SLOC

and would require the following effort to implement, assuming that this was an ecommerce system:

Effort = Productivity x KSLOCPenalty = 3.08 x 20.71.030 = 3.08 x 22.67 =69.8 Person Months

There are also other approaches to calculating equivalent SLOC from a higher level input value. These other approaches include Internet points, Domino points, and class-method points to name just a few. All of them work in a fashion analogous to FPs as just described.

Table 6 Language Equivalencies

Language	SLOC per Function Point
C++ Default	53
COBOL Default	107
Delphi 5	18
HTML 4	14
Java 2 Default	46
Visual Basic 6	24
SQL Default	13

8. EVOLVING FUNCTION POINTS

Function points have been shown to be a definite indicator of development effort, and are still fundamentally sound.

8.1 Semantically Difficult

Function point standards were codified in the early 1980s by a standards body hailing from a traditional

management information system world. Since then the standards document has not been drastically overhauled. Its language reflects this with seemingly arcane terms such as "record element types, external inputs, etc." While such careful language insulates a relatively complex metric from everyday misunderstanding, it also impedes learning and acceptance by a wider audience.

8.2 Too Many Steps

The function point counting methodology is complex. It takes several days to learn function points, which is more time than most harried software engineers are willing to spend. Furthermore, some of that methodology is mathematically suspect while potentially adding no benefit.

8.3 Incomplete

Function points were defined from the user interface's vantage. Although a clever angle, this caused major criticism that all the functionality built into a software system might not be captured. Many argued that substantially internal functionality, without much manifestation at the user interface, might be missed.

8.4 Arbitrary Weightings

Once identified, raw function points go through two numeric transformations. The first is meant to weight them for relative size—low, average, high. The second is intended to make different types of points comparable such as equating an external input to an external output. The problem is that the scalar values behind these transformations were developed more than 20 years ago under very particular circumstances. At worst, these values may now be arbitrary.

8.5 No Automatic Count

No generally automated method is available for counting function points, even in completed systems. In contrast, lines of code counts can be obtained using simple line counting utilities. This paper does not address the automatic counting issue; innovations eventually may emerge from computer aided software engineering vendors.

9. SIMPLE SEMANTIC CHANGES

The following changes are intended to make function points[7] easier to learn and eliminate inconsistencies.

9.1 Simpler Names

Function points' key innovation is that they approach software size from an intuitive perspective—user interface artifacts such as inputs, outputs, and files a software developer understands. Why call these external inputs, external outputs and internal logical files when more straightforward terms work equally well? Figure 6 offers a simplified nomenclature.

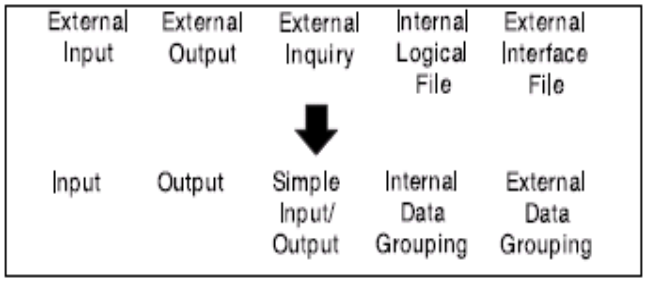

Fig.6 Simplified naming scheme

9.2 Simplified Weighting Terms

The function point methodology describes a function in terms of size. Actually, the standard refers to "complexity" but complexity is an algorithmic factor that should be orthogonal to a size metric, so we are unilaterally changing the label. Consistent with this change, low, average, and high complexity become small, medium, and large. Size is determined by counting a function's attributes.

The standard refers to these as data element types, record element types, and file types referenced—simpler terms are field for the first item and data groupings accessed for the latter two. Figure 7 illustrates how size is determined then labeled using the alternative nomenclature outlined here.

		Total Number of Fields		
		1 to 5	6 to 19	20 or more
Data Groupings Accessed	1	Small	Small	Medium
	2 to 3	Small	Medium	Large
	4 or more	Medium	Large	Large

Fig. 7 Size determination matrix

10. ACCOUNTING FOR HIDDEN FUNCTIONALITY

Function points are determined at an application's external interface, the layer where interaction with the outside world occurs. However, attributes at the external interface sometimes provide little indication of how substantial underlying code is. Examples include algorithmically intense software (encryption, image processing) or systems with underlying "layers" that are out of the user's view. Judged from the external interface, the size of these systems will be understated. Two very different methods for capturing hidden size have been suggested but never before specified for use in a single framework.

10.1 An Internal Function Point

Numerous researchers have suggested a new function point to capture functionality missed by the other categories. It even has been implemented in competing functional metrics schemes. Figure 8 illustrates the idea behind the "internal function." As depicted an internal function is a truly extraordinary input or output. It easily bests other functions that form an external perspective resembling it in size but have nowhere near the underlying amount of code.

These functions should occur rarely, no more than a few times in the average system. When an internal function is found, it probably should be sized by analogy against standard function points. Compare an internal function against other known inputs or outputs in the system—it could equal several. Remember that an internal function is an input or output with a misleadingly simple external interface; sizing by analogy corrects this misjudgment.

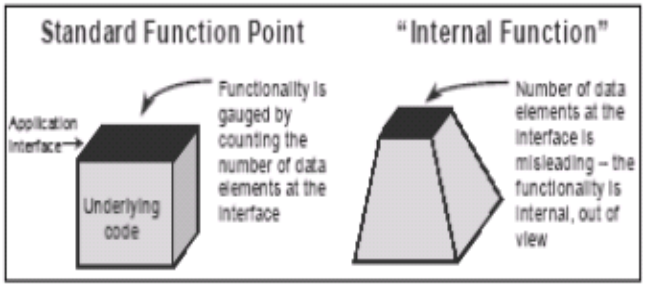

Fig. 8 The internal function "Iceberg"

10.2 Layers

Other hidden functionality can be captured by a change of perspective. A cornerstone of the function point framework is that software functionality, except key data structures, is not functional unless it interacts with the outside world. This external interface provides a consistent vantage while accounting for the entire system. However, this level can also conceal the inner workings of a complex system (see Figure 9).

Component-to-component interaction can be revealed with internal layers, an innovation first proposed for full function points. Beneath the external interface, layers are intended as equally valid perspectives from which to count function points. To prevent misinterpretation and over counting, a layer must be strictly defined. All software has many functions interacting with one another; these do not justify layers. Internal layers are characterized by a well defined internal interface that every function in a system lies either above or below. They are tantamount to secondary application boundaries. Layers certainly exist when there are wholly constituted systems within systems, such as with middle-ware and operating system utilities. Inputs or outputs counted at each layer still must satisfy the counting rule that an internal file (data grouping) is modified.

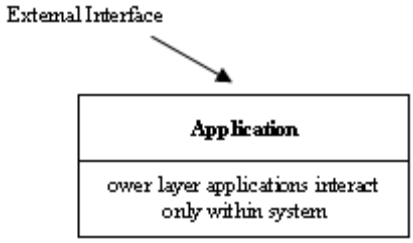

Fig. 9 Layers

11. SUMMARY AND CONCLUSION

Software estimating is simple in concept, but difficult and complex in reality. The larger the project, the more factors there are that must be evaluated. The difficulty and complexity required for successful estimates of large software projects exceeds the capabilities of most software project managers to produce effective manual estimates. In particular, successful estimation of large projects needs to encompass non-coding work.

The various simplifications proposed do not change counting results; meanwhile, extensions to account for hidden functionality would only rarely apply. Other suggestions are intended to increase the acceptance of function points and involve no changes to the underlying standard. Functional size metrics are here to stay. As software technology continues to evolve, they eventually may be preferred to lines of code. The question is whether lingering concerns about function points will remain unanswered or whether many of the changes advocated here will be adopted.

REFERENCES

[1] B. Boehm, M. Kellner and D. Perry,(eds.), "Proceedings, ISPW 10: Process Support of Software Product Lines", IEEE Computer Society, 1998.

[2] D. Reifer, "Practical Software Reuse", John Wiley and Sons, 1997.

[3] "The Function Point Counting Practices Manual (CPM)", The International Function Point Users Group (IFPUG), 1999.

[4] B.Boehm, *et al.,* "Software Cost Estimation with COCOMO II", Prentice Hall, 2000.

[5] B. Boehm, A. Abts, W. Brown, S. Chulani, B. Clark, E. Horowitz, R. Madachy, D. Reifer and B. Steece, "Software Cost Estimation with COCOMO II", Prentice Hall, June 2000.

[6] University of Southern California Center for Software Engineering. "Unification Workshop Minutes", 19th Forum on COCOMO and Software Cost Modeling, 26 October 2004.

[7] M. Maier, "Architecting Principles for Systems-of-Systems", Systems Engineering, 1998.

[8] B. Boehm and D. Port, "Escaping the Software Tar Pit: Model Clashes and How to Avoid Them", ACM Software Engineering Notes, January 1999.

[9] Annual Research Review, "Corporate Affiliate Survey", University of Southern California Center for Software Engineering, 16 March 2004.

REALTIME 3D ULTRASONOGRAPHY – TECHNICAL ADVANCEMENTS AND CHALLENGES

M.Ezhilarasi[1], M.Rajaram[2] and S.N.Sivanandham[3]

[1]Department of BMIE, Avinashilingam University for Women, Coimbatore - 641 108, Tamil Nadu

[2] Department of Electrical and Electrionics Engineering, Thanthai Periyar Institute of Technology, Vellore - 632 002 , Tamil Nadu

[3]Department of Computer Science and Engineering, PSG College of Technology, Coimbatore - 641 004, Tamil Nadu

E-mail: ezhilrasi@yahoo.co.in

(Received on 10 September 2007 and accepted on 25 March 2008)

Abstract

The evolution of Ultrasonography is very rapid in recent years with advances in piezoelectric materials, transducer array geometries, beamforming methods, signal processing, image formation & processing methods and volume surface rendering. For many who design medical ultrasound imaging systems, the ultimate goal is to obtain images that closely resemble the idealized pictures of medical school anatomy texts. An on-line, real time three-dimensional (3D) image that is analogous to that of the human eye and which can be manipulated to obtain any desired view or cross-section remains the ideal for medical imaging. High frequency ultrasound, harmonic imaging and ultrasound contrast agents are some of the advanced techniques adopted to improve the quality of imaging. Improvement in accuracy of image data, contrast and resolution with simultaneous reduction of noise and slice thickness has taken ultrasonography to a new milestone. It is hoped that this paper will provide new comers to the field a glimpse of the present state-of-the-art in ultrasonography development.

Keywords: *Beamforming, Harmonic Imaging, Transducer Array, Ultrasonography, Ultrasound Imaging, Volume Surface Rendering*

1. INTRODUCTION

Ultrasound, as currently practiced in medicine, is a real-time tomographic imaging modality. Not only does it produce real-time tomograms of scattering, but it can also be used to produce real-time images of tissue and blood motion, elasticity, and flow in the tissue (perfusion). The most common form of imager is the B-scanner (the B stands for brightness). The cross-sectional image format of ultrasound B-scans originated by Wild and Reid [l] in 1952 has been adopted for computed tomography and magnetic resonance imaging. Since the most widely used ultrasound is currently only a two-dimensional imaging modality, many investigators are researching multi-dimensional modalities such as three-dimensional imaging or are combining flow with scattering images in several dimensions. There has been significant previous work in 3-D ultrasound imaging. In 1953, Howry et al. [2] and in 1967, Brown [3] described pulse-echo 3-D ultrasound scanners: but these were too slow for practical clinical use. In 1966, Thurstone [4] described 3-D ultrasound holography for biomedical applications.

The combination of ultrasound imaging with therapeutics such as hyperthermia or drug injections, or with ultrasound ablation, is developing quickly. Intravascular and intracavitary imaging methods for both imaging and therapeutics are being investigated at fast pace in both commercial development and basic research laboratories. Even ultrasonic microscopy is developing to surpass a resolution of 1 micron[5]. Technical advances in ultrasound supported by mathematics include computed tomography (inverse scattering)[6], scatterer number density calculations (statistics), wave elastic tissue interaction (viscoelasticity)[7], ferroelectric transducer development (ceramic physics)[8], and wave equation modeling of ultrasound in viscoelastic materials such as tissue.

2. BACKGROUND INFORMATION

An ultrasonic pressure pulse about a microsecond long is launched into the tissue by a transducer consisting of an array of individually pulsed piezoelectric elements. This pulse is reflected from the various scatterers and reflectors within the tissue under investigation. The scattered pressure wave is detected by the transducer array and the data is processed and cted as an image[9].

The multi-element transducer at the end of a relatively long (about 2-m) cable, contains 48 to 256 micro-coaxial cables (very expensive!)(Figure 1). In most systems, several different transducer probe heads are available. The probes are selected via high voltage (HV) relays. The phased-array digital beamformer systems are also expensive due to the need for full electronic control of all channels. The Tx beamformer determines the delay pattern and pulse train that set the desired transmit focal point and outputs of the beamformer are then amplified delivered to the transducer elements. On the receiver (Rx) side, there is a T/R switch, generally followed by a low-noise amplifier (LNA) and one or more variable-gain amplifiers (VGAs which provides increased gain for signals from deeper in the body) and then the beamformer. Finally, the Rx beams are processed to show either a gray-scale image, Color flow overlay on the 2-D image, and/or a Doppler output.

3. OBJECTIVES OF THE STUDY

The objectives of this study are: to find out the technological challenges yet to be solved in the field of ultrasound imaging in general, to specifically identify the problems in the field of ultrasound physics, signal acquisition, instrumentation, signal processing and in post processing of images and to briefly highlight few software modules which are useful in solving these problems.

4. STATEMENT OF PROBLEM

Mathematics and physics have greatly influenced the development of ultrasonic imaging, and many challenging problems from physics and the mathematical sciences remain to be solved. Beam forming in nonhomogeneous and usually nonisotropic materials such as biologic tissue is not at all well developed theoretically[10]. Adaptive beam forming, which corrects for variations in refractive index within the imaged field, is a problem that is not solved. Inverse scattering is not a solved problem for geometries in which the sound is either traversing (forward scattering) or reflecting (backscattering) from the object. Acoustic models for the behavior of transducers with the complicated geometries of today's scanners are not well developed.

5. ANALYSIS AND DISCUSSION OF ADVANCEMENTS AND THE CHALLENGES

5.1 Acoustic Transducer

Ultrasonic transducer is an integral part of any ultrasonic device which may be used in a variety of applications ranging from medical imaging to bubble detection. The transducers cover a wide spectrum of frequencies from a few kilohertz to a few gigahertz. Although they carry such an importance in the performance of an ultrasonic device, there are many aspects of ultrasonic transducer engineering still poorly understood. In fact in current ultrasonic imagers, the transducer performance is a major limiting factor in preventing these systems from reaching the theoretical resolution.

One of the challenges is the large acoustic impedance mismatch between the transducer elements and the body. Novel piezoelectric material developments[7], modeling of transducers and arrays, multidimensional array design and fabrication, interconnection strategies, and recent progress in therapeutical devices are also the main topics in recent research.

5.2 Transducer Array Geometry

They are mainly classified into: Linear, Phased, 2D and Annular. Out of all these the 2D array is the most versatile transducer since one doesn't have to move the transducer to scan a volume if a phased array approach is used. The biggest drawback of the 2-D array is that the complexity increases by N2[11]. People have tried using sparse arrays, to alleviate the complexity increase, but so far nobody has made a commercially successful electronically steerable 3-D system.

Another major problem is also the need for much larger cables to access the additional elements. The cable is one of the most expensive items in an ultrasound system, plus they become very stiff and unwieldy for 256 and

more micro-coax cables. Because of this, high voltage multiplexers need to be used in the transducer handle to reduce the number of cables.

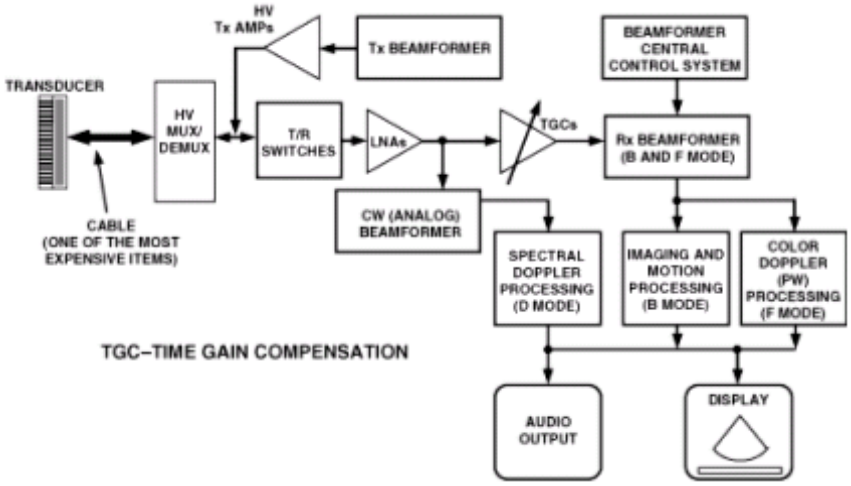

Fig. 1 Block diagram of ultrasonography

5.3 Beamforming and Signal Processing

The design of transmit and receive aperture weightings is a critical step in the development of ultrasound imaging systems. Current design methods are generally iterative, and consequently time consuming and inexact.

Operating frequencies for medical ultrasound are in the 1-40 MHz range and as the frequency increases the resolution increases but the penetration depth decreases. Because transmit power is cannot be increased beyond needed to render ultrasound data in three dimensions. But, still the 3D ultrasound datasets are typically fuzzy, contain a substantial amount of noise and speckle, and suffer from several other problems that make extraction of continuous and smooth surfaces extremely difficult.

6. CONCLUSION

The real-time 3D medical imaging has the ability to view elements of the anatomy in its "natural" three-dimensional state in real-time whether through direct acquisition of 3D images, or their later reconstruction from a series of axial 2D images, is still considered a young technology. The above mentioned challenges illuminate the growth of the real-time 3D ultrasonography yet to be achieved.

REFERENCES

[l] J. J. Wild and J. M. Reid, "Application of Echo-ranging Techniques to the Determination of Structure of Biological Tissues", Science, Vol. 115, 1952, pp. 226-230.

[2] D. H. Howry, G. J. Posakony, C. R. Cushman and J. H. Holmes, "Three-Dimensional and Stereoscopic Observation of Body Structures by Ultrasound", J. Appl. Physics, Vol.9, 1956, pp.304- 306.

[3] T. G. Brown, "Visualization of Soft Tissues in Two and Three Dimensions - Limitations and Development", Ultrasonics, Vol. 5, pp.ll8-124.

[4] F. L. Thurstone, "Ultrasound Holography and Visual Reconstruction", Proc. Symp. Eiomed. Eng., Marquette Univ., Milwaukee, WI: Vol. 1, 1966, pp. 12-15, reprinted in Acoustical Holography, Metherell, El-Sum, and Larmore. Eds. NewYork: Plenum Press, Vol. 1, 1969, pp. 120-125.

[5] R. Demirli and J.Saniie, "Ultrasonic Microscopy Using Low Frequency Transducers", IEEE Ultrasonics Symposium, Vol.1, 1999, pp.589-592.

[6] M. Cheney, G. Beylkin, E. Somersalo and R. Burridge, "Three-Dimensional Inverse Scattering for the Wave Equation with Variable Speed: Near-field Formulae Using Point Sources", IOP Journal, Vol.1, 1989, pp. 1-6.

[7] G. C. Cruywagen, I.P.K.Mainie and J. D. Murray, "Travelling Waves in a Tissue Interaction Model for Skin Pattern Formation", J.Math.Biol., Vol.33, 1994, pp.193-210.

[8] J. G. Gualtieri, J. A. Kosinski and A. Ballato, "Piezoelectric Materials for Surface Acoustic Wave Applications", in Proc. IEEE Ultrasonics Symp., Oct. 1992, pp.403-412.

[9] TL. Szabo, "Diagnostic Ultrasound Imaging: Inside Out. Burlington", MA: Elsevier; 2004.

[10] C. Fritsch, M.Parrilla, A.Ibanez, R.C.Giacchetta and O. Martinez, "The Progressive Focusing Correction Technique for Ultrasound Beamforming", IEEE Transactions on Ultrasonics, Ferroelectrics and Frequency Control, Vol. 53, No.10, 2006, pp.1820 – 1831.

[11] Andreas Austeng and Sverre Holm, "Sparse 2D Arrays for 3D Phased Array Imaging", IEEE Transactions on Ultrasonics, Ferroelectrics and Frequency Control, Vol.49, No.8, August 2002, pp.1073-1086.

ROLE OF SEWING NEEDLE IN SEWING PERFORMANCE - A CRITICAL REVIEW

M.Bharani, S.Mohanraj and R.V.Mahendra Gowda
Department of Fashion Technology, Bannari Amman Institute of Technology, Sathyamangalam - 638 401, Erode District, Tamil Nadu
E-mail: rvm_gowda@rediffmail.com
(Received on 20 March 2008 and accepted on 13 May 2008)

Abstract

New fibers, new threads, new ideas contribute to the garment manufacturer's need for a larger assortment of sewing machine needles so the perfect stitch can be achieved. The sewing needle plays an important role in making finished garments durable, pleasing and attractive and hence selection of the right needle is very crucial in garment manufacture. Selection of improper needle tarnishes the seam appearance, seam durability and mars the productivity of the sewing process. In addition, it also damages the fabric and the thread. Poor quality, improper size, and styles of sewing needle are some of the major causes for skipped stitches and severe thread breakage during sewing. Therefore, it is necessary to understand various aspects of sewing needles, which are critically analysed and described in this paper.

Keywords: *Performance of Needles, Sewing Needles*

1. INTRODUCTION

The Egyptians, five thousand years ago, used wooden needles. Steel needles were first made in England in 1545, which were, cut and pointed by machinery. Needles are used in the process for creating garments from fabric, embellishing constructed garments, and repairing worn and damaged clothing [1]. The choice of discriminating sewers world-wide is that the needles provide an uncompromising, consistent quality of producing the perfect stitch every time. The sewing machine needle is the most crucial element in stitch-forming process. In this context, the selection of suitable sewing needle is one of the most important parameters for ensuring an effective and fault-free sewing process. Needle is a pointed piece of metal that carries the sewing thread through the fabric. This task requires good knowledge of basic characteristics of a sewing needle, i.e., needle type, shape of point and needle fineness. Also, a good knowledge of sewing materials is desirable, for instance, fine fabrics should be sewn with fine sewing needles and heavier fabrics with heavier sewing machine needles. The garment manufacturer has to ensure that these issues are resolved by selecting the right needle. The selection of a suitable sewing needle has to be carried out based on the analysis of influential sewing parameters with an application of machine learning process.

2. NEEDLE MANUFACTURING

The process and the number of steps required to make a needle is amazing. The sewing machine needles have been manufactured to exact standards since 1851. Needles are required in a range of sizes since garments are customarily constructed using a thread of a similar weight to the fabric being sewn. Larger needles are made of bone, metal or wood; small needles similar to those used today are made from metal, usually copper alloy or iron. Needle production, a process consisting of more than 100 steps is a combination of precision engineering, chemical technology and metallurgy [2]. Needle manufacturing can be divided into two stages name Needle Production and Needle Quality Control.

2.1 Needle Production

The needle production includes the following major steps in sequence:

- Selection of wire
- Swaging
- Shank making
- Die pressing and punching
- Milling
- Barb grinding and soft pointing

- Hardening
- Chemical de-burring
- Plating
- Final pointing and polishing

2.1.1 Wire Selection

It is key to high quality needle production. Sewing needle is made by high carbon steel wire. A numbers of physical, chemical and metallurgical tests are conducted on wire, before selection.

2.1.2 Swaging

Swaging is the process, where wire is cold forged to final thickness of the needle blade as shown in Figure 1.

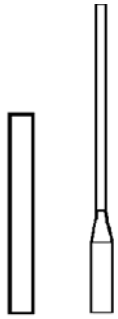

Fig. 1 Swaging needle blade

2.1.3 Shank Making

In this stage the company name/trade mark as well as the needle marking is done as shown in Figure 2.

Fig. 2 Shank making

2.1.4 Die Pressing and Punching

It is the most important step where master tool is made which intern used to press the eye section of the needle. Each needle has to be accurately die pressed to give the same depth of scarf, perfect eye rounding and other dimensions that are critical for stability (Figure 3).

Fig. 3 Die pressing stage of needle

2.1.5 Milling

It is a process where the long groove of the needle is milled in a special purpose machine. Long groove is the path through which sewing thread travels (Figure 4).

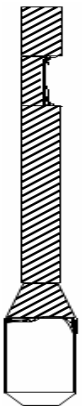

Fig.4 Milling stage of needle

2.1.6 Barb Grinding and Soft Pointing

The barb which results during die press operation is ground on automatic machine. Subsequently, soft pointing of the needle is done to give the point its initial shape (Figure 5). Thorough perfect pointing of the needle in to round, ball or cutting point is done after hardening (heat treatment process).

Fig. 5 Barb grinding stage of needle

2.1.7 Hardening

It is the process where the needle, in order to give strength and elastic characteristics for excellent performance, is treated in a special furnace protected by creating a special oxygen-free atmosphere to prevent oxidation of the surface and it is also ensured that there is no loss of carbon from the steel. After taking out of the furnace the needle are quenched in an oil bath and are kept for a pre-determined period in a deep cooler at a temperature below -70°C in order to transform the remaining austenite and to increase toughness of the needle.

2.1.8 Chemical De-burring

In this process, the surface of the needle is made silky smooth. Subsequently, the needles that have become bent during the previous stages are straightened.

2.1.9 Plating

It is done to provide smoothness to the surface of the needle. Plating provides glossy appearance, protects the needle against wear and tear. Some of the common surface finishes such as nickel plating, chrome plating, super-finishing, titanium coating, fluoro-carbon coating are also done as discussed below.

- Nickel plating is given to improve corrosion resistance of the needle.
- Chrome plating helps to reduce friction between the needle and fabric and hence the generation of heat.
- Super-finishing is imparted to needles, which are used for manufacturing synthetic apparel. It results in reduced quantity of heat generation due to less friction between the needle and the fabric.
- Titanium coating is useful for needles used in heavy fabric sewing. Basically, the needle coated with titanium coating will have higher level of hardness and wear resistance.

2.1.10 Final Pointing and Polishing

In this process, precise pointing, like round ball or cutting points are done and finally needles are polished (Figure 6).

Fig. 6 Needle pointing and polishing

3. ANATOMY OF NEEDLE

Needle is a slender strand of wire, shaped to precision that delivers thread to the machine to create a stitch. Due to the development of new sewing threads and novel fabrics, new model and high-performing needles are manufactured. The needle's configuration is engineered to manage thread and fabric to reduce the likelihood of skipped or flawed stitches. The configuration varies from needle type to type; needles are found in various sizes, with different shapes; and with more than one needle on a single crossbar. In this context, the anatomy of needle (Figure 7) plays a major role in determining its structure [4]. The configuration of the needle includes the following in its structure.

3.1 Shank

It is top of the needle that inserts into machine; most often has round front and flat back, which seats needle in right position.

3.2 Shaft

It is the body of the needle below the shank. Shaft thickness determines the needle size.

3.3 Front groove

It is a slit above needle eye, should be large enough to "cradle" thread for smooth stitches.

3.4 Point

It is a needle tip that penetrates fabric to pass thread to bobbin-hook and form stitch. The shape of point varies among needle types.

3.5 Scarf

It is the indentation at back of needle. A long scarf helps to eliminate skipped stitches by allowing bobbin hook to loop thread more easily. A shorter scarf requires a more perfectly timed machine.

3.6 Eye

It is a hole at the end of the needle through which thread passes. Needle size and type determine the size and shape of eye.

4. NEEDLE AND ITS BASIC ACTION

A sewing needle has the following three basic action cycles:

- Oscillation
- Vibration
- Paddle Stroke

Oscillation may be vertical, oblique or curved in nature. Vibration is a reciprocating action made by needle as it passes in and out of the throat plate. Paddle stroke is the unilateral stroke action from 12 'o' clock to 6 'o' clock made by a needle in the throat plate needle hole. The paddle stroke needle action includes feed as well as stitching.

5. POSITIONING OF THE NEEDLE

Correct positioning of the needle's eye with respect to the operator on the machine will depend upon the cycle of the coordinating stitch mechanism, which is supposed to take the thread from the needle's eye. There are three basic elements of these stitch mechanism namely looper, bobbin hooks, and shuttle hooks. Needle position in the needle bar is specified best by referring to the clock position of the needle scarf. The needle hole in the throat plate is the center of an imaginary clock face as shown in Figure 8 [3]. The 6 'o' clock position on this clock face is the one at the beginning and end of the sewing feed line and the 12 'o' clock position is the spot at finishing end of the feed line. The 6 'o' clock spot on most machines is directly in front of the operator. In such cases, the 3 'o' clock position is at the operator's right – hand side and 9 'o' clock is at the operator's left-hand side.

The needle scarf must be positioned with the needle eye length perpendicular to the positive thrust of its complementary looper bobbin hook, or shuttle hook. The positive thrust of the needle's complementary stitch mechanism is the thrust line made by the looper point as it passes the needle when withdrawn from the throat plate. Needle surface thrust is the distance from the upper most position of the needle point end to the bed surface of the throat late. This distance limits the operation thickness the machine can sew.

The yarn severance potential or patterning power of a needle is the impact momentum with which the needle contacts the fabric.

This can be computed as follows:
Needle Impact Energy = (Needle Velocity) 2 X (Total mass of needle, needle bar, and The link driving the needle bar)

Needle velocity, and not needle acceleration, is an important factor in impact momentum. The relative impact momentum between two needles can be estimated quickly (if the needle linkage masses are assumed to be equal) by measuring the distance the drive pulley rotates when it propels the needle through the depth of the presser foot sole at the needle line. Assuming this distance to be equal for two machines, the needle with lesser impact momentum requires more pulley rotation distance to pass the presser-foot sole thickness distance.

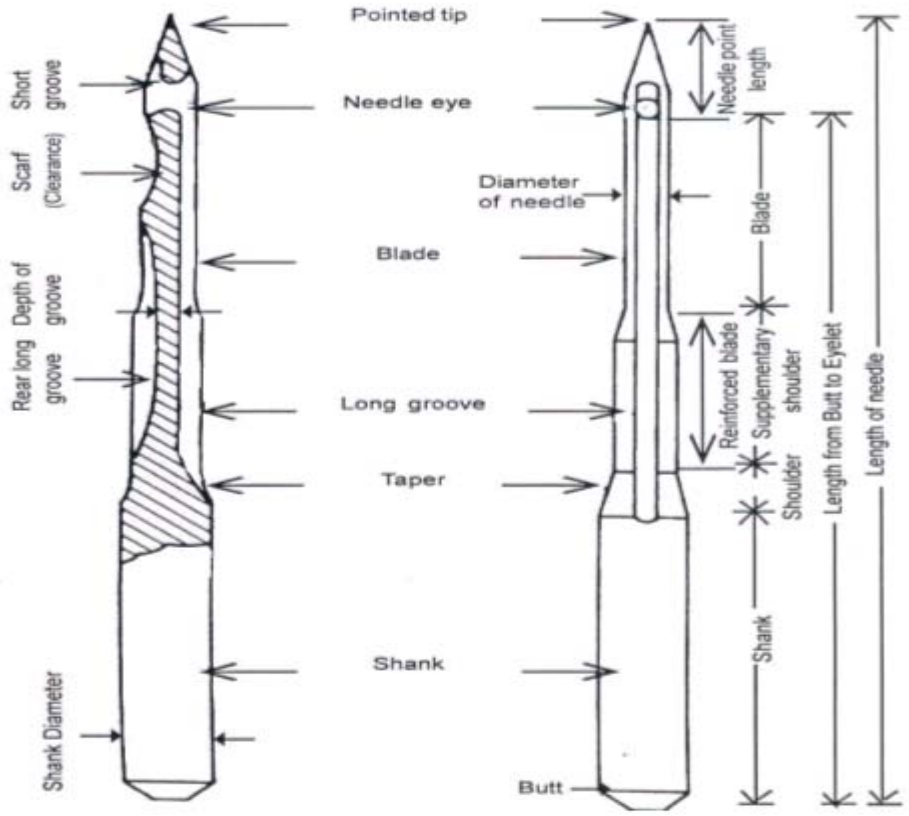

Fig. 7 Anatomy of sewing needle

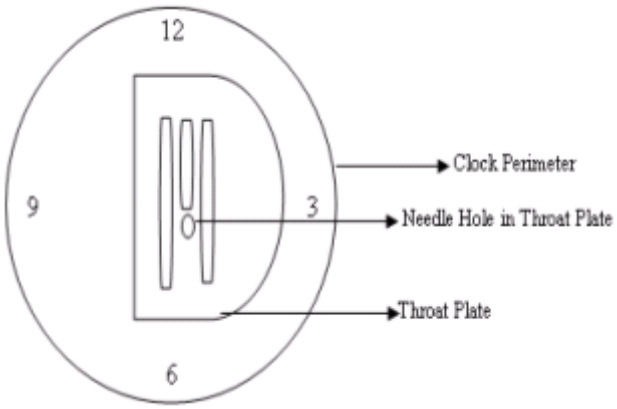

Fig. 8 Clock concept for needle cyclic operation

6. NEEDLE BAR

The function of the needle, which is fixed to the needle bar, is to penetrate the fabric and carry the thread under the stitch plate where the loop is formed. Transformation of the main shaft rotation into the translation of the needle bar is done us-ing the slider-crank mechanism, which is connected to the main shaft bolt at one end and to the slider block and needle bar at the other. The needle bar is guided in linear bearings. The displacement of the needle bar is as-signed as Si and depends on the rotation of the main shaft from 0° to 360°. This movement rises to its maximum value at Ø=180°. The value of the movement Si decreases during the rotation of the main shaft from 180° to 360°, and at 360° reaches its minimal value. The movement of needle bar Si is a function of length of the driven link, the main shaft's rotation angle and the coupler link's length. The displacement of the needle bar is highly non-linear. Velocity and accelera-tion of the needle bar are functions of the driven link's length, the main shaft's ro-tation angle, the coupler link's length and the link's angular velocity.

7. NEEDLES FOR DIFFERENT APPLICATIONS

The configuration of the needle is based on a particular fabric to be sewn and the surface embellishments to be done. According to the configuration requirement the needles can be classified in to standard, decorative, and special type needles [5]. They can also be classified with the cutting style of the fabric being sewn. The details of different kinds of needles used in apparel industry are given below:

7.1 Ballpoint Needle

This needle has a medium, slightly rounded tip that goes between the threads of a knit fabric, rather than piercing them like a sharp-point needle.

7.2 Sharp Needle

This needle has a sharp point to pierce the threads of woven fabrics. These needles are an especially good choice for heirloom sewing and when perfectly straight stitching is desired such as for topstitching or making pin-tucks.

7.3 Universal Needle

Most woven and knit fabrics can be sewn with a universal-point needle. The point is slightly rounded for use with knit fabrics, yet sharp enough to pierce woven fabrics. A universal needle can be used in all household sewing machines that accept a flat shank.

7.4 Needles for Denim/Jeans

This needle is used for stitching denim, heavy faux leather or other densely woven fabrics. It is also suitable for stitching through multiple fabric layers. The extra-sharp point and stiff shank can pierce through the weave with less likelihood of breaking.

7.5 Needles for Leather

The leather needle's point is cut in a wedge so that it easily penetrates leather, heavy faux leather, suede and other heavy, nonwoven fabrics.

7.6 Needle for Machine Embroidery

This needle is specially designed with scarf and large eye to prevent shredding and breakage when sewing dense embroidery designs with rayon, metallic and other machine embroidery threads.

7.7 Needle for Metallic Threads

Constructed specifically for use with metallic threads, this needle features a fine shaft and sharp point to eliminate thread breakage, an elongated eye to accommodate the thread and make threading easier. It has a large groove to prevent the delicate threads from shredding and a specially designed scarf to prevent skipped stitches. This needle also works well with monofilament threads.

7.8 Quilting Needle

This needle has point tapered to successfully sew through thick layers and crossed seams when piercing a quilt and machine quilting the layers together.

7.9 Stretch Needle

While sewing knit fabrics using a ballpoint needle, one experiences skipped stitches, and hence it is better to use stretch needle. The deeper scarf prevents the said problem on knits, including synthetic suede.

7.10 Top-stitch Needle

Topstitch needle has an extra-sharp point, an extra-large eye and a larger groove to accommodate top-stitching thread or two strands of all-purpose thread.

7.11 Wing/Hemstitch

The sides of this needle's shank are flared and look like wings. It is used to create decorative open-work stitching on tightly woven fabrics such as linen and fine batiste.

8. SELECTING THE CORRECT NEEDLE FOR GIVEN FABRIC

The fabric and the needle work together in stitch formation, so all must be considered before taking the

first stitch. Table 1 provides the information for selecting a needle point based on the fabric type, woven or knit and fabric weight. This results in quality garments which are produced from these needles.

The right type of needle offers greater level of production and avoids production of garment with needle hole and thread melting. The general rule for needle size is that finer the fabric, the finer is the needle. For example, when making a dress from a lightweight wool jersey, a 90/14 ballpoint needle would be appropriate. But a heavier, woven wool coat may require a sharp-point needle, size 100/16 or 110/18. Just because both garments are made from a wool fibre are should not use same needle [2]. Hence the garment manufacturers need to find the right fabric and needle combination for the best results. This is made the apparel manufacturer to understand the importance of various types of needle and their selection.

Many factors influence the needle selection However, the following factors are considered to be major that determines the sewing performance.

Table 1 Needle Point and Size in Relation to Fabric Type [6]

Sl.No	Fabric type and Weight	Machine Needle Type	Machine Needle Size
1	**Sheer to lightweight** (Batiste, Chiffon, Georgette, Organza, Voile and all microfiber or microdenier fabrics).	Regular Point	9/70 or 11/80
2	**Lightweight** (Challis, Chambray, Charmeuse, Crepe de Chine, Guaze, Handkerchief Linen, Silk, Taffeta, Tissue Faille).	Regular Point	11/80
3	**Medium-weight:** (Broadcloth, Brocade, Chino, Chintz, Corduroy, Flannel, Linen, Poplin, Satin, Synthetic Suedes, Taffeta, Terry, Velvet).	Regular Point	14/90
4	**Medium to Heavy-weight** (Coating, Damask, Drapery Fabric, Fake Fur, Gabardine, Ticking, Woolens)	Regular Point	16/100 or 18/110
5	**Denim and Canvas**	Denim/ Jeans	16/100
6	**Sheer to Lightweight Knits** (Jersey, Single Knit, Spandex, Tricot)	Ball Point	10/70 or 12/80
7	**Medium to Heavy-weight Knits** (Double Knit, Sweatshirt, Sweater Knit)	Ball Point	14/90
8	**Specialty Fabrics** (Leather, Suede, Buckskin)	Wedge Point	14/90 or 16/100

8.1 Size of Thread

The size of the thread, to be used, determines the size of the needle. Stitching and seam requirement (durability, utility, and style factors) determine the size and type of thread to be used. This must be decided before the needle is chosen. A needle that is too small or too large for the thread will lead to thread breakage and / or lack of stitch uniformity.

8.2 Needle Finish

Needle finishes can be regular or plain, extra buff, nickel, titanium and chromium plated. These finishes are listed in sequence of their degrees of surface smoothness with chromium-finished needles having the highest degree of smoothness [8]. The type of fabric, the operation, and its speed determine the finish to be used. Tough fabrics (tough with respect to needle penetration) and high speeds

require exceptionally smooth needles to reduce heat generated by friction to minimum. Similarly, the needle which is coated with titanium coating will have greater hardness level compared to the other needles. The hardness of the needle is measured at the stem part and it should have the range from 650Hv or more based on the coating given to the surface of the needle (Table 2). The needle finish also helps to reduce the temperature level and heat generated by the needle during its frictional contact with the fabric surface [10]. Hence one should analyse the needle coated with ceramic and any other coating which may have coolant behaviour, that reduce the temperature level. This decreases sewing thread breakage, leading to less puckered stitches, less downtime, fewer defects, and increased productivity.

Table 2 Type of Finish and Hardness Value [8]

S.No.	Type of Finish	Hardness Value
1	Diamond	Above 3000
2	Titanium Nitride	2600
3	Tungsten Carbide	2000
4	Chromium	1000
5	Hardened Steel	Around 2000
6	Iron	500

8.3 Needle Size

Sewing machine needle uses a dual designation to represent its size. There are two numbering systems the European (based on metric) and the American. Most needle packages list both sizes. The first number is the Number Metric (NM) and is simply a measurement of the diameter of the needle shaft in millimeters multiplied by 100 to remove the decimal reference. To combine two commonly used measurement systems, the number metric is used with the corresponding needle number. Thus always the NM 120 is used in conjunction with the number 19, or 70/102, 100/164 and so forth. Always the needle size is selected to accommodate the thickness of the thread being used and the needle point style to accommodate the type of fabric sewn.

The needle size is one can be converted from one system to the other system using the following formula.

American Needle Size = ((European Needle Size – 20) / 5)

Table 3 American and European Systems Needle Sizes [7]

American	European
Size 8	60
Size 9	65
Size 10	70
Size 11	75
Size 12	80
Size 14	90
Size 16	100
Size 18	110
Size 19	120

8.4 Needle Type

Choosing the correct needle point and size in combination with the fabric and thread to be used is essential to obtaining desired results. The shape of scarf also determines the quality of needle as longer scarf produces longer loop length. Hence, appropriate needle may be selected according to fabric materials. For every sewing application there is always a 'best' needle to be use. Devoting time to identify the needle can produce a truly satisfying sewing experience.

8.5 Stability of the Needle

The selected needle with its special blade and scarf geometry shall have an extreme bending resistance, ensuring the highest possible stability in the whole working part of the sewing operation. A very deep scarf makes an extremely tight adjustment of the hook to the needle possible [8].

The major advantages of needles with proper geometry of blade and scarf geometry (Figures 9 and 10) are:

- Less needle deflection
- Less needle breakage
- Less skip stitches
- Less thread breakage

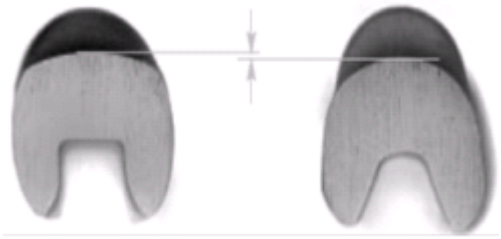

Fig. 9 Blade cross-section [5]

Fig. 10 Scarf cross-section [5]

8.6 Fabric Weight

The friction between the needle blade and the fabric creates needle heat. Needle heat is usually more of a problem when sewing either with synthetic threads and / or synthetic fabrics and can cause excessive thread breakage and / or damage to the fabric being sewn. The following factors greatly influence the amount of heat generated during sewing:

- Fabric thickness
- Fabric finish or density
- Fabric colour or density (darker colours normally are worse than lighter ones)
- Sewing machine speed
- Needle contact surface
  - Needle size or diameter
  - Needle length
  - Needle blade
  - Needle finish

Machine needles vary according to the type of point and size or thickness of needle. One can select the needle for the type of fabric and then choose the size of needle as per weight of fabric and type of thread. Lighter fabrics, requires smaller needle size.

9. NEEDLE QUALITY CONTROL

There are certain quality parameters that the needle manufacturers have been using [9]:

- Measurement of shank and blade diameter distance between butt to top of the eye, length of point etc.
- Determination of Shape and finish of the shank and butt
- Inspection of tip and point shape
- Testing of elastic limit, breaking angle, breaking force, dye (free of fins), hardness and thickness of the surface layer, torque, loop formation, needle heating, etc.
- Measurement of long and short groove levels.
- Measurement needle shape and diameter.
- Measurement of scarf geometry.

Some important tests involved in maintaining the quality of needles and also helpful in selecting the right needles for right application are:

- Breaking test
- Elasticity test
- Eye test
- Torque test
- Gun Shot test
- Mechanical stress to the sewing Needle during sewing
- Hardness of the needle
- Loop formation.

Table 4 Fabric Type and Needle Size [9]

S.No.	Fabric	Needle Size
1	Very Light weight	8 or 9
2	Light weight	9,10 or 11
3	Medium weight	12 or 14
4	Heavy weight	14 or 16
5	Very Heavy weight	16 0r 18

10. CONCLUSIONS

Sewing needle is one of the basic elements that directly contribute to seam formation. Its role is to penetrate through the textile material with the point, push away the threads and transmit the sewing thread under the throat plate. Needle thickness is an important parameter and should correspond to thickness of a fabric sewn, and the sewing thread. Proper understanding of needle parameters is essential to achieve good seam quality. Good knowledge of kinds and properties of processed textile materials as well as of types of sewing needles is essential for selecting the appropriate sewing needle for a given material. It is may be very important to understand the complex sewing process through research and practice. The problem of material damages as a consequence of unsuitable sewing needle is very critical during sewing of knitwear. Because of specific positions of yarns, built in the knit fabric mechanical and thermal damages may occur during the sewing process. A woven fabric is composed of two rectangular thread systems and when needle penetrates the fabric, yarns are pushed aside. Even if the yarn is damaged, the consequences are not severe

and the damaged spots extend only a little. On the other hand in knitwear, the yarns are connected with loops. The needlepoint pushes away loops during needle penetration. While the penetration force during sewing of a woven fabric is distributed on four yarns, it is concentrated only on one yarn in case of sewing the knit fabric. Hence, different shapes of needlepoints are used in sewing. First of all the shape of a needlepoint depends on the processed material.

The needle with a normal needlepoint (notation R or without notation) can be used for sewing of a majority of textile materials. The needle point is lightly rounded and during penetration through the material pushes away the threads without damaging the material. Needles with rounded or ballpoints are used for knitwear processing. The needle point pushes the thread loops away effectively since no thread damages are allowed because of possibility of loop bursting [4]. Elastic materials with built-in elastic threads require special heavy ballpoints. Damage of material appears when the needle penetrates into the layer(s) and hits the thread. The thread can be damaged or even broken if the needle is too thick. Damage can be seen in materials produced from natural or synthetic fibres as holes that spread across the elastic thread system. Damage can have different forms and can be clearly visible under the microscope.

Bursting of fibres mostly appears in materials made from cotton while thermal damages are characteristic of synthetic fibres. Friction between the sewing needle and textile material that acts at high sewing speeds causes heating of the needle. If the needle temperature exceeds the fibre's melting point, it results in material damage. Needle size has a decisive role on the appearance of material damage. An oversized needle can cause bursting of threads or tension around the stitch area, which results in too large holes. For that reason as fine a needle as possible should be used. However, one must pay regard also to considerable vibrations of finer needles at high sewing speeds, which can result in frequent needle fractures. Type and fineness of a sewing thread also influences the size of a sewing needle. Hence this paper provides the detailed knowledge to the garment manufacturer on selecting a proper needle for right application in the process of garment production.

REFERENCES

[1] Zoran Stjepanovic and Helena Strah, "Selection of Suitable Sewing Needle Using Machine Learning Techniques", International Journal of Clothing Science and Technology, Vol.10, 1998, pp.209 – 218.

[2] Darja Zunic-Lojen and Karl Gotlih, "Computer Simulation of Needle and Take-up Lever Mechanism Using the ADAMS Software Package", Fibres & Textiles in Eastern Europe, Vol.11, No.4 (43), October / December 2003, pp. 39-44.

[3] Jacob Solinger, "Apparel Manufacturing Analysis", 1961, pp 244-246.

[4] J.V.Rao, "Sewing Needle", Northern India Textile Research Association, 2006, pp.7-11.

[5] www.schmetzneedles.com

[6] http://www.singerco.com/resources/needles.html

[7] http://www.sewnews.com/library/sewnews/library/aamach21c.html.

[8] www.groz-beckert.com.

[9] www.prymdritzcorporation.net/tips/images/machine_needles.pdf

[10] http://www.wireworld.com/amefird/minimizing_needle_heat.html

Indian Journal of Engineering, Science, and Technology (IJEST)

(ISSN: 0973-6255)
(A half-yearly refereed research journal)

Information for Authors

1. All papers should be addressed to The Editor-in-Chief, Indian Journal of Engineering, Science, and Technology (IJEST), Bannari Amman Institute of Technology, Sathyamangalam - 638 401, Erode District, Tamil Nadu, India.
2. Two copies of manuscript along with soft copy are to be sent.
3. A CD-ROM containing the text, figures and tables should separately be sent along with the hard copies.
4. Submission of a manuscript implies that : (i) The work described has not been published before; (ii) It is not under consideration for publication elsewhere.
5. Manuscript will be reviewed by experts in the corresponding research area, and their recommendations will be communicated to the authors.

Guidelines for submission

Manuscript Formats

The manuscript should be about 8 pages in length, typed in double space with Times New Roman font, size 12, Double column on A4 size paper with one inch margin on all sides and should include 75-200 words abstract, 5-10 relevant key words, and a short (50-100 words) biography statement. The pages should be consecutively numbered, starting with the title page and through the text, references, tables, figure and legends. The title should be brief, specific and amenable to indexing. The article should include an abstract, introduction, body of paper containing headings, sub-headings, illustrations and conclusions.

References

A numbered list of references must be provided at the end of the paper. The list should be arranged in the order of citation in text, not in alphabetical order. List only one reference per reference number. Each reference number should be enclosed by square brackets.

In text, citations of references may be given simply as "[1]". Similarly, it is not necessary to mention the authors of a reference unless the mention is relevant to the text.

Example

[1] M.Demic, "Optimization of Characteristics of the Elasto-Damping Elements of Cars from the Aspect of Comfort and Handling", International Journal of Vehicle Design, Vol.13, No.1, 1992, pp. 29-46.

[2] S.A.Austin, "The Vibration Damping Effect of an Electro-Rheological Fluid", ASME Journal of Vibration and Acoustics, Vol.115, No.1, 1993, pp. 136-140.

SUBSCRIPTION

The annual subscription for IJEST is Rs.600/- which includes postal charges. To subscribe for IJEST a Demand Draft may be sent in favour of IJEST, payable at Sathyamangalam and addressed to IJEST. Subscription order form can be downloaded from the following link http:// www.bitsathy.ac.in./ ijest.html.

For subscription / further details please contact:

IJEST
Bannari Amman Institute of Technology
Sathyamangalam - 638 401, Erode District, Tamil Nadu Ph: 04295 - 221289
Fax: 04295 - 223775 E-mail: ijest@bitsathy.ac.in Web:www.bitsathy.ac.in/ijest.html

Published by

BANNARI AMMAN INSTITUTE OF TECHNOLOGY
Sathyamangalam - 638 401 Erode District Tamil Nadu India
Ph: 04295-221289 Fax: 04295-223775
www.bitsathy.ac.in E-mail: ijest@bitsathy.ac.in

BANNARI AMMAN INSTITUTE OF TECHNOLOGY
Stay Ahead

TÜV CERT EN ISO 9001 Certificate : 3410021309
RWTÜV